SOLAR AND GALACTIC COSMIC RAY STUDIES IN MOON AND METEORITE SAMPLES USING NOBLE GAS MASS SPECTROMETRIC METHODS

BY

CHANDRA MOHAN NAUTIYAL

A THESIS

SUBMITTED FOR THE DEGREE OF

DOCTOR OF PHILOSOPHY

OF THE

GUJARAT UNIVERSITY

AHMEDABAD

OCTOBER 1983

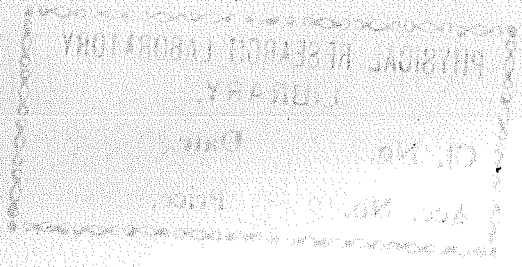

PHYSICAL RESEARCH LABORATORY

AHMEDABAD - 380 009 (INDIA)

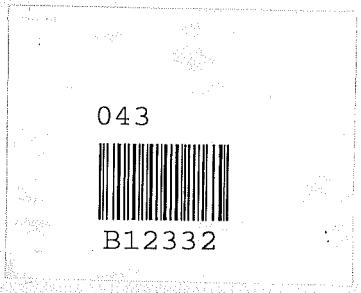

CERTIFICATE

I hereby declare that the work presented in this thesis is original and has not formed basis for the award of any degree or diploma by any university or institution.

C M Nautiyal

CHANDRA MOHAN NAUTIYAL
(AUTHOR)

Certified by:

Rao M.N.

Prof. M. N. Rao

Oct., 1983

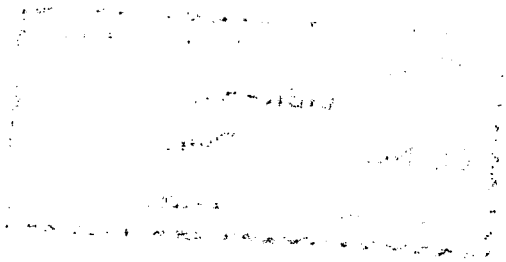

TABLE OF CONTENTS

ABSTRACT

The main problems addressed to in this thesis are centered around the identification and characterization of the implanted component of the noble gases due to solar energetic particles (SEP); the solar cosmic ray (SCR) proton-induced neon composition in lunar and meteoritic samples and the resolution of the cosmogenic effects of the SCR and GCR protons in them. Several interrelated problems have been dealt with in the thesis though all pertain to the irradiation effects of solar and galactic cosmic rays.

In this study, a systematic analysis of lunar soils which accumulate solar flare gases over several millions of years has been carried out. The results based on etched feldspars and etched pyroxene mineral residues suggest that the Ne isotopic composition of the solar flares is not planetary and is different from but closer to the solar wind value. The conclusion is further strengthened by the fact that noble gas elemental composition in these etched samples compares well with the solar composition rather than with the planetary composition.

A procedure making use of the characteristic Ne-isotopic compositions of different reservoirs has been developed. This procedure allows an estimation of the surface exposure ages (integrated residence time in top one cm of the regolith) for the soil samples.

An attempt has been made to understand the observed trend of Ne isotopic compositions of the gas-rich meteorites in the frame-work of the known reservoirs viz. implanted SEP and SW as well as spallation (SCR-and GCR-proton produced) components. The results suggest necessity for invoking a higher proton flux with a pulse-like spectral shape during the early history of the Sun. A qualitative explanation is offered for this observation considering possible physical conditions in the early solar system when interplanetary medium was denser and (young) Sun was presumably much more active than at present.

During the course of this study, two meteorites were found to be interesting viz. Isna (C3-O) and AH 77216, 18 (L-3) as they showed the presence of Ne of planetary and solar compositions respectively in appreciable quantities which is not common for their respective groups. Results of noble gas study of these meteorites have also been presented.

Further, some relevant experimental studies are proposed to improve the findings of this study in future.

ACKNOWLEDGEMENTS

I am greatly indebted to Prof. M. N. Rao for exposing me to this exciting field and for his inspiring guidance throughout the course of this study.

I express my gratitude to Dr. T. R. Venkatesan whose help in every phase of the work has helped me in accomplishing the task. The interest shown by Prof. D. Lal in many a phase of this study has been a source of constant inspiration. I record my sincere thanks to him. I have also been benefitted by the suggestions and advice of Prof. K. Gopalan especially in the experimental aspect of the work. The track results were provided by Dr. J. N. Goswami and I owe him special thanks for this.

I gratefully acknowledge the help rendered by Mr.J.T. Padia in the experimental work especially during the analysis of the lunar samples. The job of data-reduction was made considerably easier with the assistance from Mrs. Rashmi Jadeja.

The Bruderheim international standard was kindly provided by Prof. J. H. Reynolds (University of California, Berkeley) and the UHV- valves by Dr. T. Kirsten (Max Planck Institute.Heidelberg). I express my sincere thanks to them. I also thank NASA and the USSR Academy of Sciences for providing the precious lunar samples used in this study.

A special word of thanks is due to Dinesh bhai Ranpura whose excellent photography skill (blended with his typical sense of humour) has been always available. I also thank all other members of the Photography-Documentation Section especially Mr. H. S. Panchal whose co-operation was crucial in expediting the thesis in the last phases. M/s. M.M. Sarin and V. G. Shah made the atomic absortion spectrophotometry and SEM study of the lunar soil grains possible. I express my thanks to them. The expertise of M/s. Sivasankaran and Kurup was available as and when glass-blowing need arose. The Electronics lab of the group, the Liquid Nitrogen facility and the Air conditioning section, all contributed to the smooth functioning of the mass spectrometry lab. I wish to record my sincere thanks to them all.

The ever cheerful library staff has always been co-operative. I thank Mrs. R. R. Bharucha and her staff for their valuable help.

I wish to thank all the members of the Geo CP and ARC-HD groups - especially Prof. B.L.K. Somayajulu, whose co-operation and good-will made the task easier.

I thank all my friends, too numerous to mention individually, who made this journey pleasant by their company.

The arduous job of typing was cheerfully carried out by M/s. M. Sourabhan and P. C. Abraham and I extend them my warmest appreciation.

x - x

LIST OF FIGURES

LIST OF TABLES

CHAPTER I

INTRODUCTION

Interplanetary space is a huge showroom of the charged particles. In this thesis, noble gas mass-spectrometry has been employed to study the characterstics and effects of these particles. These particles differ in their energies, in their charge, in the way they interact and also in their origins (Fig. I.1). The extremely high energy particles ($\sim$1 GeV nucleon^{-1}) are mainly due to the galactic cosmic rays (GCR) which originate most probably from supernova-explosions and also probably in pulsars. But in the low energy region, it is particles of the solar origin which dominate. Solar wind (SW) is a result of continuous expansion of the solar corona. First predicted by Parker (1958) on considerations of gravitational and kinetic pressures in the corona, it received experimental confirmation one year later by Luna-3 and then by Explorer-10. The SW- particles have mean velocity of about 400 km sec^{-1} which corresponds to an energy of $\sim$ keV/nucleon. The solar cosmic ray (SCR) particles, in contrast, have higher energy ($\sim$ MeV/nucleon). These particles originate in the solar flares. The charged particles mentioned above are accompanied by a host of electromagnetic radiations such as X-rays and γ -rays but it is the charged particle component (protons, alphas and heavier particles) which is capable of bringing about observable changes in the isotopic and elemental composition of the solar system material either by inducing nuclear

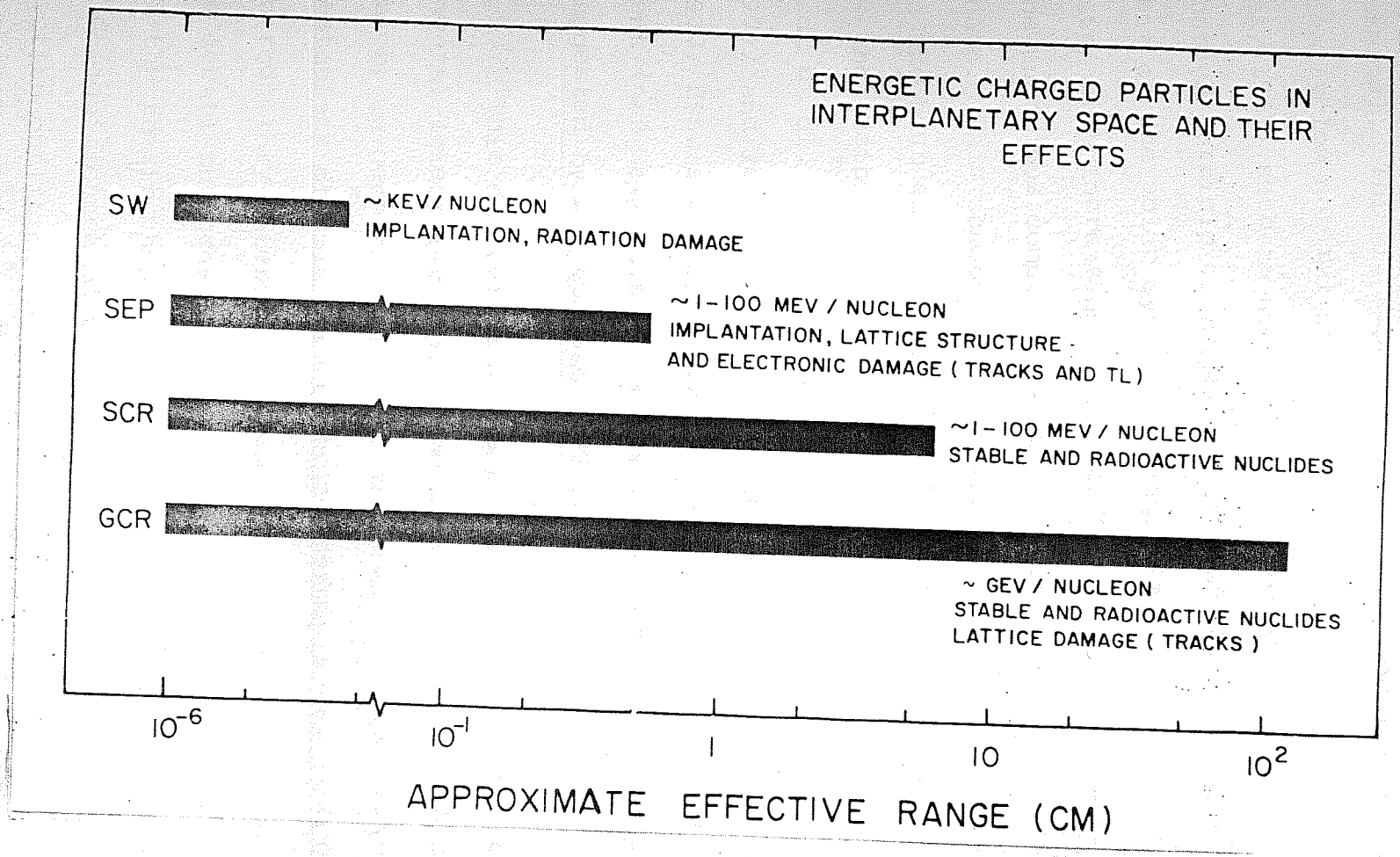

Fig. I.1 A schematic representation of the ranges and some effects of the charged particles permeating the interplanetary space.

reactions or by simply getting implanted into the target material. This is especially true for elements with intrinsically low natural abundance (e.g. see Geiss et al., 1961; Lal, 1965) such as noble gases. However the picture of the charged particle distribution in the interplanetary environment of the solar system is getting more complicated, of late, with increasing influx of information. The origin of the anomalous component of the cosmic rays is not yet well known. This component shows enhanced O, N and Ne abundances. In the high energy region ($\geq$15 MeV/nucleon), it is found to be increasing with increasing distance from the Sun (Hovestadt et al., 1973; Mckibben et al., 1975; Mckibben et al., 1979) and is possibly due to some steller source (Durgaprasad, 1977, Biswas and Durgaprasad, 1977). The low energy component ($\sim$ 2 MeV/nucleon), however, may be solar in origin as suggested by Durgaprasad (1977).

This chapter provides a general background to the several interrelated problems investigated in this thesis which, in general, relate to the characterstics and manifestations of solar and galactic cosmic rays. The specific introductory material is presented in the individual chapters in detail but general ideas not appearing in the main body of the thesis though vital for understanding the motivation and significance of the work, are briefly reviewed here. A section outlining the scope of the thesis also follows.

A. ISOTOPIC STUDIES AND THE SOLAR SYSTEM

The isotopic structures of elements especially the noble gases have received much attention in the last several years. The noble gases, especially neon, are effective monitors of the isotopic anomalies because of their chemical inertness and high volatility which ensure a low natural background in the samples. Thus it is easier to attribute the observed isotopic and elemental anomalies in noble gases to nuclear process, implantation or trapping mechanism. As a result of improved techniques, the samples of extra terrestrial material have been subjected to sophisticated experimentation resulting in the unravelling of hitherto unknown features of isotopic structures and providing new clues to the solar system-processes. Kuroda's assertion of r-process ^{244}Pu yielding fission-Xe (Kuroda, 1960) was experimentally verified by Rowe and Kuroda (1965) and Alexander et al. (1971) marking the importance of noble gases in delineating the early nucleosynthesis-process. Many a concept has been confirmed, revised or completely abandoned following such discoveries. Reynolds' discovery of excess ^{129}Xe (due to the decay of ^{129}I) in the Richardton chondrite gave the first estimate of the time interval between the cessation of nucleosynthesis and solidification of the bodies in the solar system (Reynolds, 1960). This presence of ^{129}Xe-excess indicates the presence of live ^{129}I

when the body solidified. This is possible only if the time elapsed since the end of nucleosynthesis was less than a few half lives of ^{129}I ($T_{\frac{1}{2}}$ = 15.7 Myr). Another breakthrough which led to the abandonment of the earlier belief regarding isotopic homogeneity in the solar system is study of oxygen and magnesium isotopes in Ca-Al rich inclusions in Allende and other carbonaceous chondrite. The observation of excess ^{16}O and ^{26}Mg established the inhomogeneity of the solar nebula (Clayton et al., 1973; Lee et al., 1976). These results and several others (e.g. reviews by Podosek, 1978; Clayton, 1978; Lee, 1979; Grossman, 1980; Wasserb rg et al., 1980) showed the potential of isotope-studies of solar system-material. The knowledge of isotopic structures clearly provide clues to many unsolved problems of solar system-processes.

Identification of various components in the meteorites based on elemental and isotopic composition of noble gases was a crucial achievement (Signer and Suess, 1963; Pepin and Signer, 1965; Pepin, 1967; Black 1972 a, 1972 b). It was shown that the solar component is enriched in the light noble gases compared to the planetary components. The question whether the Sun and the planets were cogenetic or not could also probably be investigated using the isotopic criteria. If the Sun and the planets represent material from the same reservoir, then the isotopic composition (not being subject

to the chemical fractionation) should provide the clue. There is at least one such element, neon, which shows appreciable difference in isotopic composition for planetary and solar components and which is unaffected by fission. A simple way to trace origin of certain material, therefore, is to compare its isotopic composition (e.g. $^{20}Ne/^{22}Ne$ and $^{21}Ne/^{22}Ne$) with that of the probable source established from some independent studies.

B. SUN AND THE SOLAR FLARES :

Sun is a normal star (G type). Though it is the nearest star to us, its behavior remains enigmatic in several respects. There are a number of observational data and as a result too many constraints to permit a simple-minded picture. Even the basic processes operative on the Sun are not well-understood. About a factor of three lower neutrino-flux from the Sun, for instance, is still unexplained (Davis, 1955; Davis, 1978). A number of possibilities have been suggested such as its core being depleted in the heavy elements like ^{8}B which is mainly responsible for the neutrinos (Bachall and Ulrich, 1971) and the possibility of neutrino-oscillations between mu-neutrino and electron-neutrino state (e.g. see Davis and Evans, 1978). But the diversity of opinions and lack of agreement suggest that the classical model of thermonuclear processes for energy generation on the Sun, may not be an adequate account of what is actually occuring inside the Sun.

Solar flare is a high energy phenomenon on the Sun normally occuring during its active phase. The flare-occurance follows an eleven year cycle, the maximum flare occurance being in the middle of the cycle i.e. 'around' the time of the Sun spot maximum. As the time scales dealt with in this thesis are of the order of million years (Myr)*, these short term variations are averaged out. A good amount of information exists on the observational aspect of the solar flares but opinions are divided over origin of the solar flares. However, it is generally believed that the tremendous amount of energy (upto $\sim 10^{32}$ ergs) associated with the flares is derived from the magnetic field in the Sun though the mechanism is far from clear. Sweet (1958), Petschek (1964) and Sonnerup (1970) had demonstrated how reconnection of the magnetic lines of force can accelerate the material as opposite polarity tubes meet. Newkirk (1973) reported having observed more of open field lines emerging from the flare region into interplanetary space suggesting a close relation between the particle-escape and the solar magnetic field.

---

* Hereafter, the abbreviations Myr and Gyr will be used for million year(s) and billion (giga) year(s) respectively.

As a consequence of magnetic fields on the solar surface and in the interplanetary medium, the characteristics of the flare particles are considerably modified between generation on Sun and detection on earth or in space. The acceleration of particles on the Sun, their escape from there and the propagation, all influence the energies and the energy spectra of these particles. The observed variability of the solar emissions is a natural consequence of the interplay of these complex processes. Highly unpredictable flaring, isotopic and elemental compositional variations such as in $^3He/^4He$ (Hsieh and Simpson, 1970; Ramaty et al., 1975; Kleckler, 1979) variability in the relative abundances of carbon and iron (Gloeckler et al., 1979; Dietrich and Simpson, 1979; Mason et al., 1979; and many others) indicate the complexities of the flare phenomenon. Theoretical attempts to explain the variations have met only with partial success. Several suggestions such as of heating of ambient $^3He^{++}$ in the lower corona by ion accoustic waves (Fisk, 1978) and ^3He production by spallation (Colgate et al., 1977) to explain variations in $^3He/^4He$ and rigidity-dependent entry into the acceleration zone (Price et al., 1971; Cartright and Mogro-Campero, 1973) to explain the variation in the elemental composition have been proposed. But even with the enormous amount of available information, a convincing answer to the true nature of the Sun still eludes us.

C. EVOLUTION OF SOLID BODIES AND RADIATION-RECORDS IN THEM

The results reported in this thesis make use of the information provided by the mass-spectrometric study of extra-terrestrial samples which were parts of planetary bodies such as moon and the asteroids. The process of formation and evolution of solid objects in the solar system is far from being fully understood. Gravitational instability had been suggested as a mechanism for forming planet-sized bodies (see Wetherill, 1978 for a review). Safranov (1969) and Goldreich and Ward (1973) stressed the importance of accumulation-process. The latter authors showed that kilometre-sized bodies could be formed by small scale gravitational instability and their subsequent accumulation could result in planetary bodies when the seed-planetesimal formed in this manner settle to the mid plane of the disk. The time scale for the formation of centimetre-sized bodies is short ($\sim 10^4$ years) and if sweeping-up process dominates, the process could take 10-100 Myr to grow to planet-sizes (Wetherill, 1978). Once the solid bodies are formed, regolith generation due to meteoritic bombardment on the bed-rocks can build up to considerable thickness if the bodies are large enough to gravitationally hold a sizeable fraction of the impact ejecta. Lunar regolith is essentially a result of such processes i.e. communition of the bed-rock. The life of a rock or a grain in this regolith is full of

events. The surface material is continuously bombarded and the regolith grains are in a state of continuous evolution. The top layer of the regolith is continuously churned, stirred and agglutinated until it is covered by fresh ejecta resulting from impact in the vicinity (Gault et al., 1974; Crozaz 1977). A typical rate for such deposition is a millimetre per Myr. During this process of gardening, the grains record the charged particle-signatures. The conditions in the asteroidal belt can be considered to be qualitatively similar. The intensity of SW or SCR irradiation is, however, expected to be lower by an order of magnitude at about 3 AU (Parker, 1963; Anders 1975; 1978). The nature of these records of charged particles are varied and figure I.1 summarizes some of these effects.

The possibility of the meteorites' possessing cosmogenic records was suggested by Bauer (1947) and Urey (1951). Paneth et al. (1952), however, were the first to observe excess ^{3}He in ordinary meteorites and attribute it to the GCR-spallation during space journey of the meteorite. The journey of a meteorite in space begins with a high velocity impact by an external object on its parent body resulting in its fracturing and then in hurling out of a part of the fractured material with high velocity (greater than the escape velocity) into the space. Between this ejection into the space and capture by the earth, the meteoroid spends

considerable time (typically of the order of a few Myr) in the space during which it is directly exposed to solar and galactic cosmic rays. However, as a meteoroid falls through the atmosphere, it loses its outer skin resulting in the loss of low-energy-particle-records acquired during the space-journey. However, some meteorites accumulated these records during their pre-compaction history in the regolith and they can reach earth with SW-and SCR-records intact if the brecciating event had compacted some irradiated material inside them. These meteorites, known as gas-rich meteorites, were the first to provide evidence of SW-gases (Gerling and Lev'skii, 1956; Manuel and Kuroda, 1964; Signer and Suess, 1963; Marti, 1969) and later the records of heavy solar energetic particles were also found in them (Lal and Rajan, 1969; Pellas et al., 1969) which they had acquired during their residence in the parent-body-regoliths.

Meteorites are interesting otherwise also. Having been derived presumably from small parent bodies, most of them (chondrites) have chemical composition resembling the solar composition for non-volatile elements. Being small, many of these parent bodies had no significant internal heat sources. As a result they escaped process of extensive melting and chemical rearrangement though some of them underwent melting due to ^{26}Al or other radionuclides. Moon, in contrast, underwent these differentiation processes

resulting in the obliteration of its embryonic features. Thus meteorites are considered to be relatively primitive objects. The idea that meteorites came from smaller parent bodies is partly based on dynamical consideration, knowledge about asteroids and the chemical and mineralogical properties of meteorites (Wetherill, 1971; Anders, 1975; Anders, 1978; Wetherill, 1978). Eventhough evidence for carbonaceous-like material on asteroids has been found (Chapman et al., 1975), considering the fragility, richness in volatiles and short GCR-exposure age, the cometary origin for atleast some of the carbonaceous chondrites can not be ruled out.

D. SOLAR SYSTEM-BODIES AND THE CHRONOMETERS

Time is the most important parameter while narrating the evolutionary history of the solar system and solar system-bodies (e.g. Wetherill, 1975; Kirsten, 1978). A number of indices have been evolved for dating different events and durations of certain processes. No two such indices mean exactly the same but a multi-pronged approach helps in putting constraints on the evolutionary process of a sample under study. Different ages can be defined for a sample. The galactic cosmic ray (or GCR)exposure age denotes the time elapsed since break-up from the parent body marking the fragmentation event. Precisely speaking, the exposure age so deduced is the sum of the durations of the cosmic ray exposure in space and on the parent body. Comparison with

the age deduced by some radionuclide technique alone can help to resolve these difficulties in favourable cases. The surface exposure age is a less precise term in the sense that it is also defined by the technique used (range of effect e.g. time of residence in top one cm of the regolith or in top one mm of the regolith). Normally the SCR-exposure age and the surface exposure age are meant to convey residence duration at ~ one cm shielding depth in the regolith. Principles of three commonly used dating techniques are given below :

1. Noble Gases : Following the demonstration that excess ^{3}He observed in meteorites was due to cosmic ray interaction, several noble gas isotopes e.g. ^{21}Ne, ^{38}Ar and ^{126}Xe were found useful and came to be used for cosmic ray exposure age determinations (Paneth et al., 1952). With improvements in mass-spectrometric techniques (Reynolds, 1956) as well as a better understanding of the noble gas compositions (Eberhardt et al., 1970; Geiss et al., 1972; Reynolds et al., 1978) and the systematics of cosmic ray production of noble gases (Reedy and Arnold 1972; Hohenberg et al., 1978) versatility of this technique has increased. New dating method based on ^{81}Kr-^{83}Kr (Marti, 1967) provided opportunity to determine exposure ages independent of flux, as the method makes use of the ratio of the two production rates rather than absolute amounts. The basic principle

of noble gas dating is that other parameters being constant, in the simplest case, the amount of noble gas produced is directly proportional to the duration of exposure. Therefore, the exposure age is obtained by dividing the measured cosmogenic noble gas amount by the production rate. However, the production rate is a function of several parameters viz. flux and energy spectrum of protons, excitation functions, target composition as well as depth and geometry of irradiation among other things. Thus the method requires several input parameters. Nyquist et al. (1973), Cressy and Bogard (1976), Hohenberg et al. (1978) and Nishiijumi et al. (1980) estimated the noble gas production rates considering the depth and composition parameters in case of several meteorites. By virtue of their stable and inert nature, noble gases are useful for dating where track and radio nuclide methods can not be employed due to the limitation of resolution and saturation respectively.

2. Particle Tracks : This simple yet powerful technique had added much to our understanding of the charged particle environment in our solar system. Tracks are results of radiation damage caused by the energetic charged particles as they traverse through matter. An etchable radiation damage is created in the dielectric medium (for example silicate crystals) when the damage exceeds certain threshold (Fleicher et al., 1975). The latent track formed

is about 100 Å in diameter but etching treatment with appropriate chemical, results in enlargement of the track so that it can be viewed even with an optical microscope.

Lunar samples and meteorites accumulate tracks during their exposure to the heavy component ($Z \geqslant 18$) of the solar and galactic cosmic rays. The track density in a sample is linearly proportional to the flux and the duration of exposure. That is why one finds extremely high track densities in lunar regolith grains. However, the maximum age which can be measured by this technique is limited by the highest track-density that can be measured. The highest measurable track density is $\sim 10^8$ tracks cm^{-2} for the optical microscope and about 10^{11} tracks cm^{-2} for the transmission electron microscope. Knowing the flux of the incident track-producing particles and registration efficiency of the detector, one can use the track-results for finding the exposure ages of the samples. Several other variations of the track-method for surface-exposure determination are available. They are methods making use of the quartile track-density (density above which 75% of the grains lie), lowest track density and the average track-density as given by Arrhenius et al. (1971), Fleicher et al. (1973) and Fleicher and Hart (1973). Study of track features can yield clues to the history of the samples also. Anisotropy in the track density, for instance, indicates asymmetric irradiation such as on a

planetary regolith and observation of track gradients on all sides of a rock would indicate tumbling during the exposure history.

Track-information has often been used as complementary to the noble gas based results in this work as both are basically manifestations of particles constituting two components (protons and the heavier nuclei) of the solar and galactic cosmic rays.

3. Radionuclides : The cosmogenic radionuclides are those produced as a result of spallation by cosmic rays. These radionuclides have been subject of extensive studies and have been widely used as potential chronometers and also monitors of flux and spectrum of solar protons (Arnold et al. 1961; Reedy and Arnold, 1972; Lal, 1972; Kohl et al., 1977). The application of radionuclides for dating is based on the general principle that a [illegible] radionuclide decays to daughter nuclide with a characteristic half life ($T_{\frac{1}{2}}$) or decay constant (λ). In the case of cosmogenic radionuclides, the production and decay occur together and for a meaningful determination of the exposure age, the duration must not have been more than a few half lives of the radionuclide. The most commonly studied cosmogenic radionuclides are ^{26}Al and ^{53}Mn with half lives of 0.73 and 3.7 Myr respectively. All these methods face some problems or the other.

The track and radionuclide-based methods suffer from saturation and hence can not be applied beyond a certain exposure duration defined by the resolution in measurement for tracks and half life in the case of radionuclides. The noble gases are cumulative in nature and deciphering the contributions from different sources is not a straightforward affair. Besides this, radionuclides give information about the recent exposure while noble gases give information about the integrated exposure. However, the results derived from these different indices for exposure age based on the above three techniques normally show good correlation and are also consistent with the other maturity indices such as Ferromagnetic resonance (Morris, 1978), agglutinate content (Heiken, 1975; Kerridge and Kieffer, 1977) and the grain-size (e.g. Bhattacharya et al., 1975).

E. SCOPE OF THE THESIS

The thesis primarily aims at investigating the following problems : (i) The long term isotopic composition of SEP*-Ne is planetary or solar. (ii) Demonstration of the SCR-proton produced neon and determination of the surface-exposure ages of lunar soils. (iii) Whether the sun was more active during the early phase of its evolution (i.e. 4.6 Gyr ago).

*Solar energetic particles.

1. SEP-Ne Composition : Whether it is solar wind or SEP which represents bulk solar composition may be debatable (Meyer, 1983). Some believe the SW to be representative of the solar composition (Anders and Ebihara, 1982) while some take SEP to be representing the solar composition (Cameron, 1973; Cameron, 1982). The SW elemental composition is constant and the variations are normally reproducible. The SEP Mg-isotopic composition and the C1*-meteorite based cameron's 'solar-system' value have been shown to be similar by Dietrich and Simpson (1979). What prompted the present investigation of the SEP-composition was the suggestion that the SEP-Ne has planetary composition (Dietrich and Simpson, 1979; Mewaldt et al., 1979). After the measurements of Webber et al. (1973), these were the only measurements of SEP Ne-isotopic composition.

Even though the direct measurements of solar abundances were made as early as 1929 (Russel, 1929), the noble gases could not be measured in the Sun because of their higher ionization potential and the low abundance in the corona. Isotopic composition in Sun, to date, have not been possible, to make by spectrographic methods.

The biggest drawback of direct SEP-measurements is their vulnurability to the large variation. But lunar soils record the solar corpuscular radiation over long time

*Carbonaceous chondrite of type 1.

periods, so they can provide a value which is unaffected by the short term variations and is a result of integration over the entire energy range. The accumulation of noble gases in lunar soils is over tens of Myr as judged from their exposure ages. Thus lunar soils are expected to give long term value in contrast with the rocket borne detectors which typically make observations for a few minutes and satellites for which typical duration is a few years. In this thesis are reported the long term SEP-Ne and noble gas elemental ratios as deduced from the analyses of etched mineral suites (grain size fractions) from lunar soils.

Particle-tracks and radio nuclides are conventional methods for the estimation of the surface exposure ages of the lunar samples. But the track and radionuclide based techniques have an inherent limitation due to the limitation on maximum measurable track density and the saturation. ^{21}Ne based method is developed for the purpose of the determination of lunar soil surface exposure ages. The available knowledge of regolith dynamics (Arnold, 1975; Duraud, 1975) and improved experimental approach have been combined to quantitatively decipher the SCR-proton-produced neon in lunar soil. Based on this, model surface-exposure ages have been calculated and shown to be qualitatively agreeing with the other parameters of maturity.

The more interesting phase of the solar history of the Sun is its early phase before it joined the main sequence. Drawing parallels from the history of the other young stars, one expects a highly active sun 4.6 Gyr ago. For Sun such evidence can only be fossil. In this study, signatures of such an active Sun are sought in the dark parts of the gas-rich meteorites which were exposed to the solar radiation during their pre-compaction history on the parent-body. Since solar cosmic ray protons are energetic enough to induce nuclear reactions, these effects are looked for in the neon isotopic ratios.

In brief, the scope of this thesis is the investigation of the SEP-noble gas composition, demonstration of the SCR-proton produced neon in the lunar samples and the identification and resolution of the SCR-proton effect in the gas-rich meteorite-samples to estimate the SCR-proton flux during the very early history of the solar system.

CHAPTER - II

EQUIPMENT AND EXPERIMENTAL TECHNIQUES

The noble gas mass spectrometer used in this study was an indigenously built Ultra High Vacuum (UHV) glass mass-spectrometer. This is of conventional Nier design with 60° sector magnet and 11.4 cm radius of curvature. The mass-spectrometer is similar to the one designed by Prof. John Reynolds at Berkeley (Reynolds, 1956). The technical details of the mass spectrometer are given in a technical report by Gopalan et al. (1973).

In this chapter a description of the mass spectrometer and its performance are given along with the details of the samples and the relevant experimental techniques.

A. THE MASS-SPECTROMETER

This is an all-glass mass-spectrometer (shown in figs. II.1,2) which is mainly intended for noble gas studies. The metal parts are kept to a minimum to minimise outgassing problem. Pyrex glass 7740 was used in the construction of analyser and extraction section and some parts are made of He-leak proof Pyrex glass 1720.

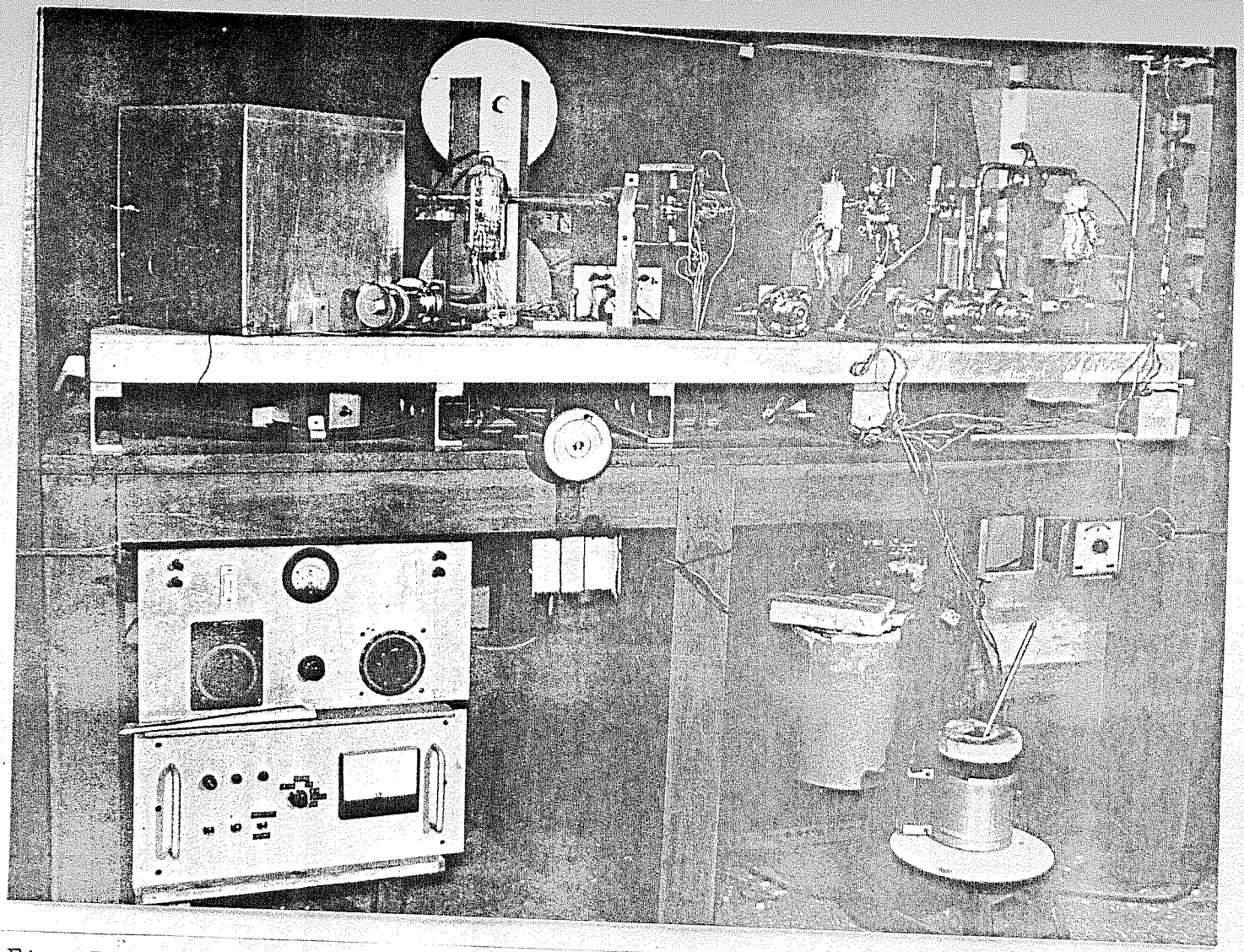

Fig. II.1 The Reynolds-type glass mass-spectrometer used for the noble gas analysis.

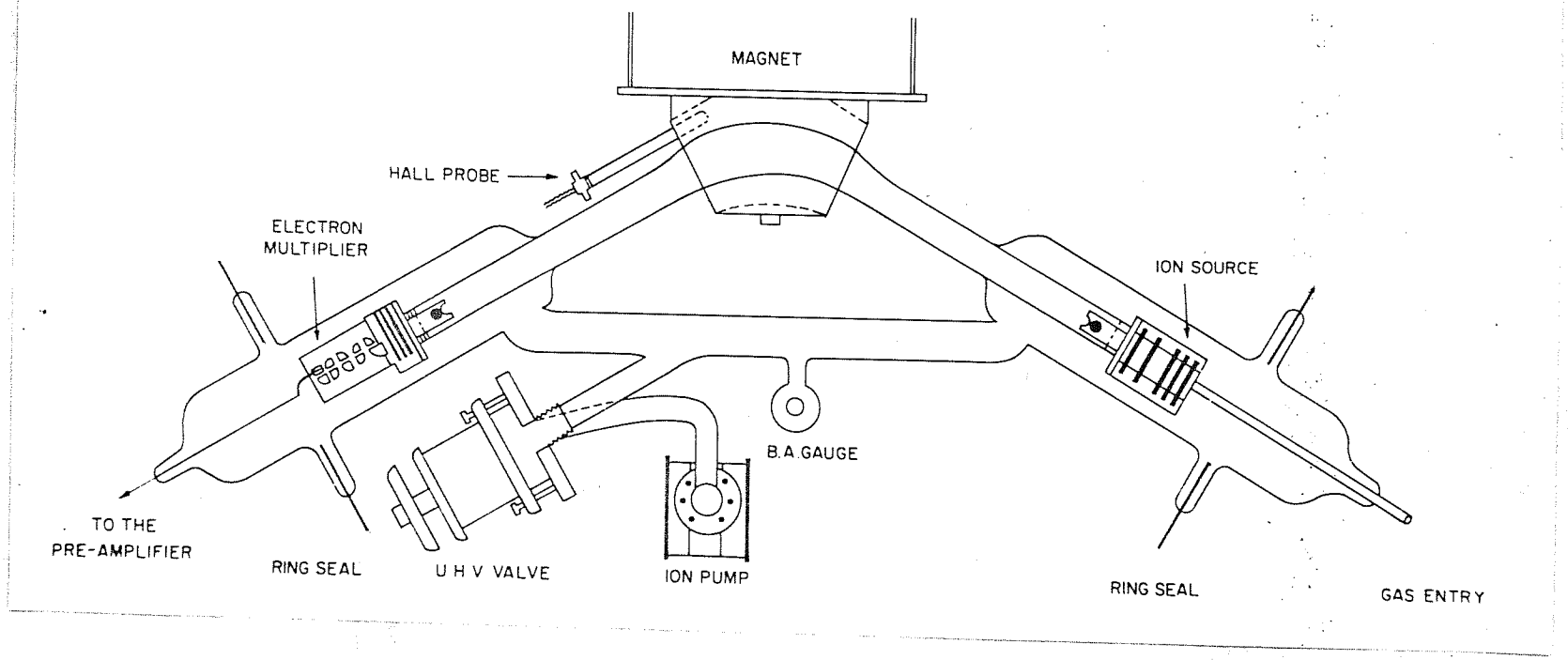

Fig. II.2 The top view of the mass-spectrometer.

1. Analyser Tube : The 11.4 cm radius of curvature of the analyser tube and the associated ion optics, in principle, permit sufficient resolution to analyze the heaviest noble gas isotopes of interest i.e. of xenon. The inner surface of the analyser is coated with Sn Cl4 to make it electrically conducting. This is to avoid the charging of the inner surface which could result in beam defocussing. Figure II.2 shows the schematic view of the mass spectrometer.

2. Ion source : An electron impact ion source has been employed in the mass spectrometer as it is known to produce efficient ionization and ion beam characterstics with low energy spread. The ion optics-design is based on the design by Nier (1947) and Reynolds (1956). A ribbon filament of tungsten has been used in this machine. The ultrahigh vacuum at which the system was maintained, allowed a filament life of about 10 years.

Figure II.3 shows construction of the ion source assembly. The gas atoms, ionized by electrons, are accelerated to 50 to 70 eV by keeping the slit just in front of the filament at + 50 to + 70 V. The trap is kept at + 60 V with respect to the slit plate. The first slit plate J_1 is kept at + 35 to + 105 V with respect to the filament while J_3 is kept at higher potential (+ 500 V) with respect

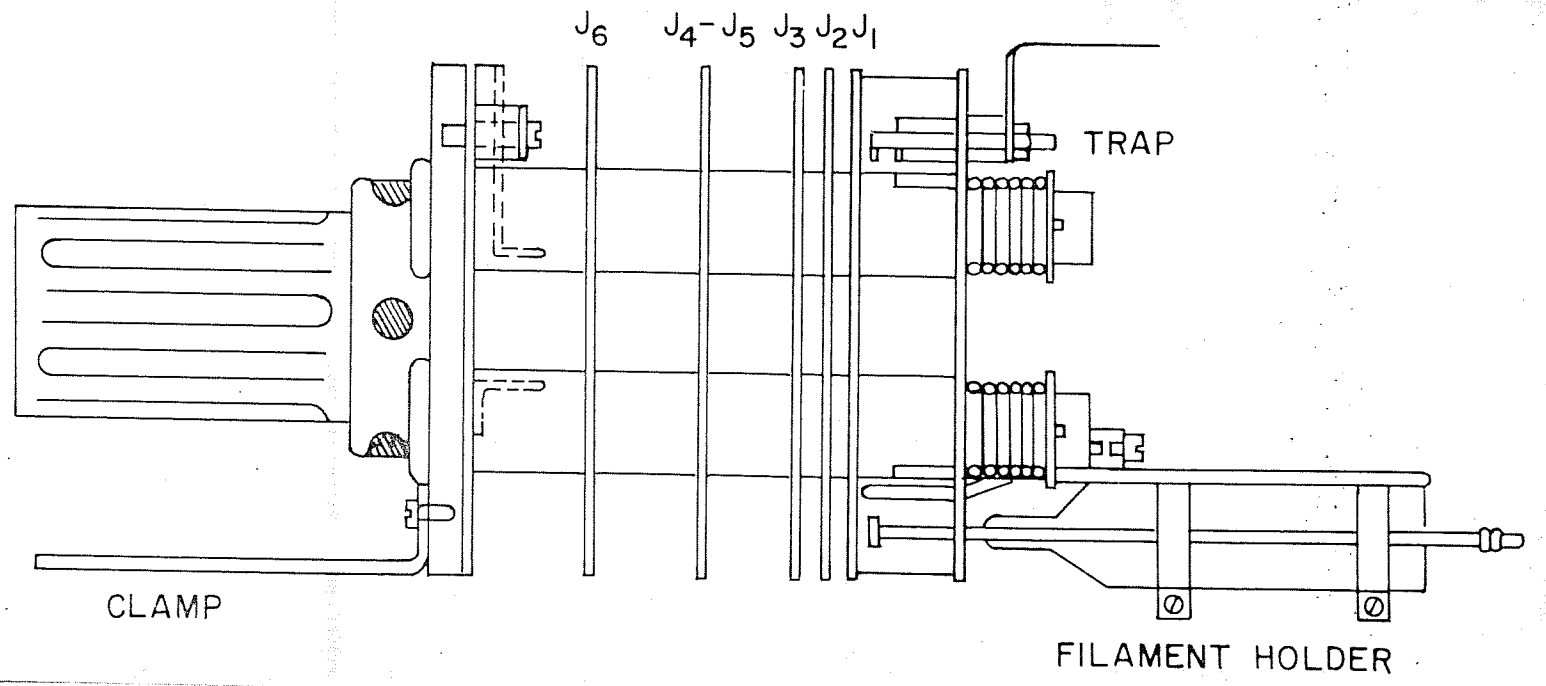

Fig. II.3 The ion source assembly.

to J_1 and J_2 for acceleration of ions. The potential on J_2, J_3, J_4 and J_5 can be varied by amounts ranging from 50% to 100% of that on J_1. The split half plates J_4 and J_5 are meant for horizontal deflection of the beam. However, in practice, once a good beam is obtained,, only small adjustments are needed.

Filament current is regulated by shield current. A typical value for the trap current was 0.14 mA when shield current was 0.7 mA.

3. Ion Collector Assembly and Electron Multiplier :

The ion collector assembly resembles to some extent the source assembly. The design (Fig. II.4) is based on Nier's (1947). It has a collector plate with a slit width of 0.018" and is followed by a pair of split half plates used for horizontally deflecting the beam by adjustment of the potential as in the case of ion source. These half plates are grounded as in the case of collector electrode. The plate C3 is used for pre-acceleration of the ion beam to a few hundred electron volts before it impinges on the first dynode of the multiplier. The multiplier is a ten stage-SPM-103 Dumont electron multiplier with beryllium copper dynodes. The high voltage for the ion collector and multiplier is supplied from a stablised high voltage D.C. distribution network. A high voltage of 260 V per stage is

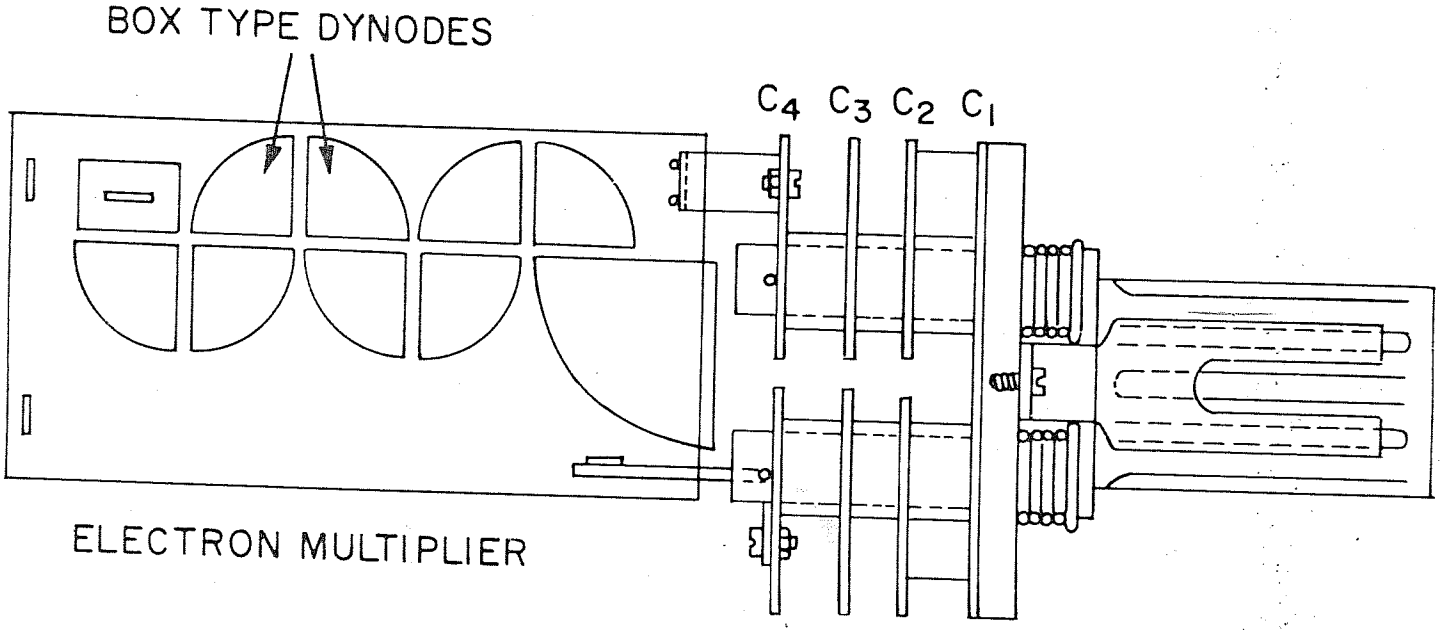

Fig. II.4 The ion collector assembly.

used for Kr and Xe compared to 125 V per stage used for He, Ne and Ar improved the sensitivity for Kr and Xe significantly.

The part of the analyser section housing the collector and multiplier is wrapped with a mu-metal foil to shield it from stray magnetic fields.

4. Main Magnet and Source Magnet : The magnet used in this study is a 60° sector type electromagnet which combines the dispersion and focussing action. The resulting magentic field, with field-current linearity being maintained upto 8000 gauss (corresponding to $\sim$ 250 mA), sufficed for Xe-isotope study. The pole gap of 7/16" allows free movement of the magnet. The magnet can be moved back and forth with reference to the analyser tube (thickness 3/8") in the horizontal plane over (non-magnetic) rails by a screw-drive mechanism. Vertical and lateral adjustments are made possible by use of four screws at the four corners of the magnet carriage. Repeated air spike (air standards) measurements accompanied by incremental changes in the magnet position are used to fix the magnet in the best position with respect to analyser tube to achieve the best peak shape and resolution. The current for the magnet coil is supplied by a Kepco HV regulated supply unit HB4A(M) capable of giving DC output of 0 to 325 V and 0 to 400 mA

with less than 0.01% variation. The magnetic field is sensed by means of a Hall probe. A small permanent magnet with nearly 100 gauss magnetic field is used at the source to collimate the electron beam and to increase the electron path length. This resulted in a 10-fold improvement in the sensitivity of the instrument.

5. Extraction System : The extraction system is shown in Fig. II.5. The double walled quartz bottle encloses the molybdenum crucible attached to the base of a quartz funnel. The samples are stored in the side arms and can be dropped into the crucible through a quartz funnel. Sample-melting for gas-release is performed by means of a 12 KW RF induction heater. A water-cooled copper coil encloses the section of the bottle which contains the crucible. Temperature as high as 1700^{o}C are achieved with this system. The temperature is sensed with an optical pyrometer with the reproducibility of $\pm$ 25^{o}C for a given voltage. Cleaning of the released gases is performed by Ti-Zr getter and two VAC sorb pumps (VAC).

B. DATA ACQUISITION

The data-acquisition system consists of a vibrating reed electrometer (VRE) of Cary 401 model and a chart recorder. The electron-multiplier output is fed to a pre-amplifier which in turn feeds the VRE. Its output activates

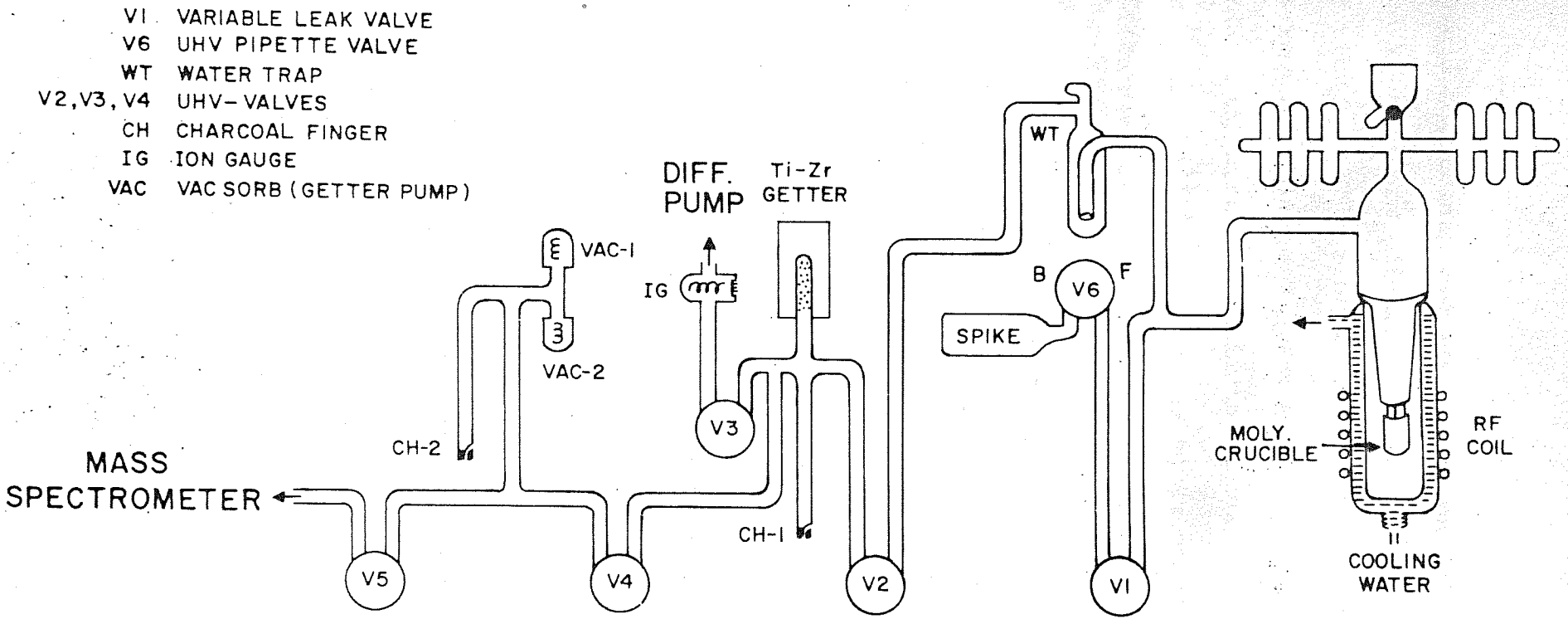

Fig. II.5 The noble gas-extraction and purification system.

a Honeywell Electronik 194 Lab. recorder. The data are acquired in the form of peaks on a strip chart as a function of time. Peak height is linearly proportional to the gas isotope abundance. The multiple choice range switch of VRE along with the facility of choosing input resistance (10^9, 10^{10} and 10^{12} Ω) allows measurement of signals of widely differing strengths as very often encountered while analysing the extraterrestrial samples.

C. SYSTEM VACUUM

Study of the structures in the isotopic composition and detection of small contributions from a source against a dominating background from other source demands high degree of precision and reproducibility in measurements with the mass spectrometer - a requirement which, along with several other factors, relies heavily on the level of the achievable vacuum in the system. During the course of the present study, ultra high vacuum has been maintained all through. Extraction side was usually maintained at 10^{-8} torr and analyser side at 10^{-9} torr to 10^{-10} torr. This was achieved by the combined use of rotary, diffusion and getter ion-pumps. Liquid nitrogen traps are used between rotary pump and diffusion pump and between diffusion pump and the extraction system. Welsch-Duo seal rotary pump, an indigenously built three stage glass mercury diffusion pump and a getter ion pump are the major components used for generating

ultra high vacuum. After initial pumping down to 10^{-7} torr level, the analyser side is isolated from the diffusion and rotary pumps. Thereafter, pumping is carried on only with the getter ion pump thus avoiding any possibility of oil or mercury contamination which can result in undesirable background effects.

2. Baking : Two cycles of baking for twelve hours each at 300-350^{o}C are carried out following any exposure of the system to the atmosphere. Every twelve-hour-baking is followed by an equal duration of pumping at room temperature. This helps in realizing the desired vacuum quickly. However, in the case of short-term shut-down of the system; the extraction side is vented to nitrogen thus enabling us to recover the vacuum easily. Two ovens, one each for the analyser and extraction section, are provided and can be lowered over these sections for baking. Heating tapes can be wrapped around all those parts not enclosed by the ovens. However, as the system was not exposed to atmosphere for long durations, only rarely was baking resorted to.

3. Invertor : As a protection against power failure, the system is backed by an invertor (1 KW). This automatically takes over in case of power failure and is capable of running the rotary pump and diffusion pump for two hours.

4. Valves : All the valves used are ultra-high vacuum metal valves based on Alpert's design. V-1 is a variable leak valve (Granville-Phillips valve); V-2, V-3, V-4 and V-5 are C-type UHV valves (see Fig. II.5) and V-7 is a low torque valve of similar type connecting the analyser section to the getter ion pump. (These valves were kindly made available by Dr.T.Kirsten, Max Planck Institut fur Kern Physik, Heidelberg). A pipette valve V-6 is provided to draw air samples from the pipette. The valve V-3 joins the extraction side to diffusion pump while V-5 connects the analyser and extraction systems.

D. Measurement Details : The analyses are carried out in static mode. For calculating the mass-discrimination, gas samples of known composition are drawn from a gas reservoir made of 1710 glass containing air sample with ^{3}He enrichment. The valve V-6 allows a constant volume of 0.098 cc STP to be taken from the pipette for the analysis. Air spikes provide periodic checks on the consistency of the instrument behavior.

1. Extraction and Purification : The extraction and purification system consists of the RF-furnace, sample bottle and crucible, water trap, charcoal fingers, VAC sorbs, Ti-Zr getter and the standard air pipette (Spike). The pumps, valves and the furnace have already

been described. The water trap is maintained at - 50°C (using an acetone and dry ice slurry) when the gases are being evolved from the sample (or being drawn from the spike). This prevents the water vapour from getting into the system. The charcoal fingers Ch-1 and Ch-2 contain activated charcoal powder which can adsorb large amount of heavy (Ar, Kr and Xe) gases when maintained at about - 180°C (liquid nitrogen temperature). Cleaning of the gases is performed by means of a Ti-Zr getter which is heated to 850°C and then allowed to cool for 30 minutes. This removes the chemically active gases. Two VAC sorbs are used to crack and pump the residual hydrocarbons and hydrogen.

2. Analysis Procedure : The flow chart (Fig. II.6) outlines the general procedure. The samples are dropped in the crucible by moving them from outside with the help of a nickle-wire (kept inside the sample arm) and a magnet. The sample is melted by means of an RF-induction heater. Normally reached in 20 minutes in three steps. In the case of low temperature heating, the desired voltage can be reached directly. Heating is carried out for an hour with bottle isolated from rest of the system. Also, V-1, V-3, V-4 and V-5 were closed thus disconnecting the extraction system from the pumping. During heating (of the sample) or adsorption (of the air spike), the water trap is maintained at - 50°C and Ch-1 at - 180°C. In the case of

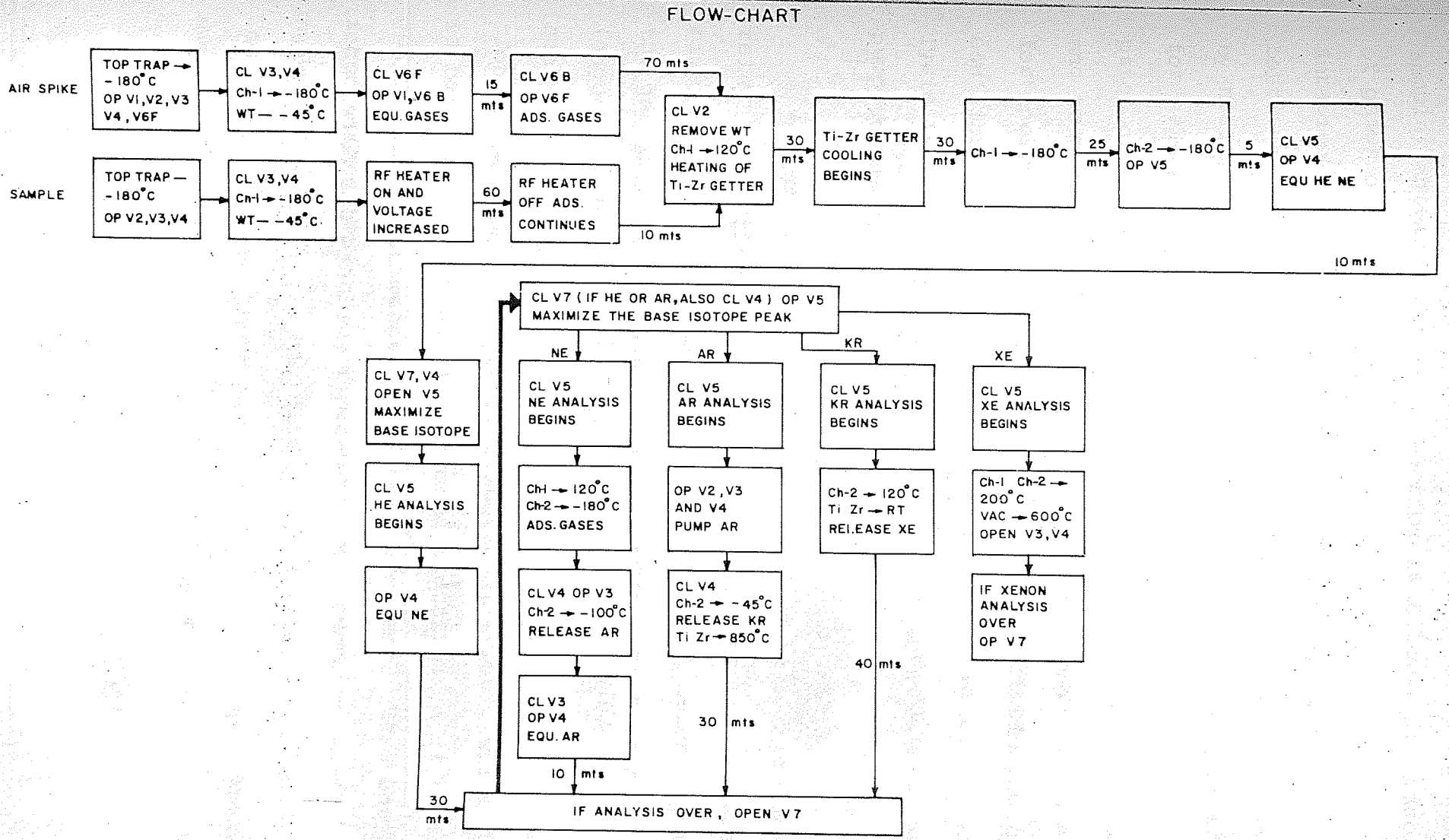

Fig. II.6 The noble extraction and purification procedure. The initial steps for the sample and the airspike are different.

12332.

sample, an extra ten minute-period is allowed for adsorption of gases on Ch-1. For airspikes, instead, the adsorption duration is 70 minutes. Now by closing V-2, extraction bottle is separated and evolved gases subjected to cleaning by heating the Ti-Zr getter to 850°C and allowing it to cool for half an hour. This is followed by half an hour of adsorption of cleaned gases on Ch-1 (He and Ne remain floating) and then the gases can be let into the mass-spectrometer for analysis. The intermediate steps of partitioning and equilibration are given in the flow chart. After the analysis is over, gases in the analyser are pumped by an ion pump through the valve V7.

As the source filament is provided with a protection relay in the circuit to guard against any spurious pressure-rise, the analyser side ion guage is floated before letting the gas into the analyser. Thus pumping action of the ionguage is temporarily suspended. Helium and neon are analysed separately by letting them into the analyser section in two steps. Argon is released at - 100°C while Ne is being analysed. Due to enormous contribution of radiogenic ^{40}Ar, argon measurements pose problems. Here one is faced with the problem of measuring two isotopes whose amounts in the sample may differ by very large factors. The difficulty was circumvented, by first letting a small amount of the total gas into the analyser recording all the

3 isotopes. Then valve V-5 was opened fully and all of the argon allowed to equilibriate with the analyser section for a short time and only ^{36}Ar and ^{38}Ar were measured in case ^{40}Ar is out of scale during the full entry. Later, using ratios measured in the partial entry, amount of total ^{40}Ar was determined. Krypton is released at - 45°C while Xe is released by raising the temperature of the charcoal Ch-2 to 120°C to desorb all the xenon.

The peaks are scanned by sweeping the magnetic field continuously. It is possible to scan over the mass range of interest (in automatic or manuel mode) and then switch back to initial point to resume scanning. Normally 10 peaks are recorded for each isotope. In addition, contamination peaks for example at mass 2 in He-run, masses 40 and 44 in Ne-run are also recorded because doubly charged ions e.g. 40^{++}, 44^{++} are observed as 20^{+} and 22^{+}. Since ^{40}Ar abundance is normally high, doubly charged ions may interfere with Ne- measurements and have to be corrected for as described later.

Time duration between successive steps, equilibration time; gas release time and Ar pumping time etc. are kept fixed to maintain identical conditions and to ensure reproducibility. Similarly the energy of ionizing electrons (governed by the accelerating potential), multiplier voltage,

filament current etc. are all kept constant. The ionization energy was chosen by trial and error. While electrons should be given sufficient energy to create enough ions, they should not create too many doubly charged ions either as the ionization efficiency peaks much above the (first) ionization potential. In order to suppress the doubly ionized species and still attain a reasonably good sensitivity, different ionization voltages were employed for He, Ne, Ar (50V) and Kr, Xe (70V). This helped to a large extent in reducing ^{40}Ar and $^{44}(CO_2)$ interferences.

E. DATA REDUCTION

The data reduction was off line. The peak heights (signal strengths) are manually read from the strip chart and reduced using IBM-360 computer.

1. Algorithm : The values of isotopic ratios and abundances have been back extrapolated to time t_o of gas entry into the analyser to find the true values. Linear, exponential and quardratic fits were obtained for the signal versus time data. The computer programme (to find the value of the ratios and gas - amounts)fits a straight line, exponential curve and a quadratic fit to the data. This programme enables the calculation of the coefficients for three fits yielding minimum value of χ^2 (Chi-square)

defined as

$$\chi^2 = \sum_i \left[\frac{1}{\sigma_i^2} \{ y_i - y(x_i) \}^2 \right]$$

where σ_i is the variance in the data points. In mass-spectrometry it is not possible to find y as heights of different peaks are not measured under identical conditions. Hence two ways of weighting the expression were used :

i) Equal weight to all data points ($\chi^2 = 1$)

ii) Statistical weight i.e. $\sigma^2 \propto 1/$ peak height.

The value of Chi-square can be determined by analytical method which involves linearization of the fitting function. However, convergence is slow for analytical solution method unless it is in the close vicinity of the solution (i.e. minimum Chi square - value). Therefore, gradient-search method is combined with the analytical solution approach. In the gradient search method, the coefficients of the function are varied to obtain the lowest Chi-square value.

In the present study the algorithm includes combination of the two methods as discussed by Marquardt (1963) and Bevington (1969). First the gradient-search method is followed and on nearing the solution, algorithm approaches the analytical solution method thus improving the precision.

For gases released from the samples and for air spike-analyses the t_o- values are obtained by curve fitting as described above. However, for obtaining t_o- values in the case of blank-runs, the hand-extrapolated t_o - values are used. As blanks in general are very low, this does not introduce any significant error as deduced by comparing a few sets of blank-values obtained by these two methods.

The choice of a particular fit (linear, exponential or quardratic) is governed by Chi-square test. The data thus obtained is further subject to corrections which are dependent on the mass spectrometer performance (see sub-sections 3 and 4 below) and are incorporated wherever necessary.

2. Sensitivity : The typical values for mass spectrometer-sensitivity are given in Table II.1. The sensitivity remained constant throughout a set of measurements for a given sample and variation over longer time periods were also small. The values given in the table are typical of one such set. The sensitivity variation in Ne and Xe over the last five years have been within $\pm$ 10% and $\pm$ 20% respectively.

Source magnet is usually not disturbed. However, in case of readjustment of the source magnet or in case of

TABLE II.1

SENSITIVITY OF THE MASS-SPECTROMETER FOR NOBLE GASES*

Isotope	Sensitivity (10^{-10} cc STP per mV)
^{4}He	0.40
^{22}Ne	0.15
^{36}Ar	0.026
^{132}Xe**	0.0016

* Normally 0.15 mV signal could be conveniently measured.

** The higher sensitivity is with the use of higher voltage for the multiplier (See section D).

TABLE II.2

BLANKS OF THE MASS SPECTROMETER

	600°C	1000°C	1200°C	1600°C
^{4}He (10^{-8} cc STP)	10.0	11.0	12.0	9.0
^{22}Ne (10^{-11} cc STP)	5.6	4.1	4.1	9.9
^{36}Ar (10^{-11} cc STP)	1.0	1.48	1.9	31.7
^{132}Xe (10^{-13} cc STP)	0.4	0.6	0.6	0.45

measurement after a long lapse of time, recalibration is carried out using Bruderheim international standard (kindly provided by Prof.J.H.Reynolds, University of California, Berkeley). A continuous monitoring on the instrument sensitivity is provided by measuring air spikes of known amounts before and after each sample run. Use of a source magnet effectively increases the sensitivity manifold. By use of a higher dynode potential (260V/stage) for Kr and Xe, higher sensitivity is achieved. In case of very high signals, lower input resistance of the VRE can be chosen thus keeping the signal within scale as discussed in section B and in such a case sensitivity will be different. The sensitivity in Table III is expressed in cc STP/mV and the measured signal (after proper blank and m.d. corrections) are converted into cc STP per g of sample by multiplying the sensitivity and dividing by the sample mass.

3. Blank Corrections : When sample is heated in the crucible, gases are released from the crucible also. In addition some residual gases are always present in the analyser. Therefore, the observed signals should be corrected for the crucible-contribution and for the background due to the residual gases. These contributions are estimated by heating the crucible to the same temperature to which the sample was heated and then measuring the released gases. In case the sample is heated in steps, blanks are also determined in steps. Normally blank corrections are small.

Actual signal is obtained by subtracting the blank correction from the observed signal. Table II.2 gives typical values of blanks for noble gases during this study.

4. Mass Discrimination and Its Correction :

Deviation of the measured abundances from the true abundance due to mass difference is termed mass-discrimination (m.d.). It is a cumulative result of several factors. Among factors contributing to mass-discrimination are differential response of the multiplier to different masses and fractionation in the ionsource chamber. The mass-discrimination (m.d.) can be defined as : $m.d. = \frac{R_T}{R_{obs}}$

where R_T is the true ratio and R_{Obs} is the observed ratio. Multiplication of m.d. with the observed value gives the true ratio. The true values for air-composition are taken from Neir (1950). The value of mass-discrimination factor is calculated by repeated measurements of the air spikes. Nearly 200 such measurements were made over last five years and the measured m.d.-values have shown remarkable consistency for any given set. Over this whole period also, m.d. for neon has been about 0.4% per mass unit and for Xe about 0.5% per mass unit. The linearity in m.d. versus mass is maintained when the m.d. was high. A set of typical values for mass-discrimination is plotted in Fig.II.7 and II.8 for neon and xenon.

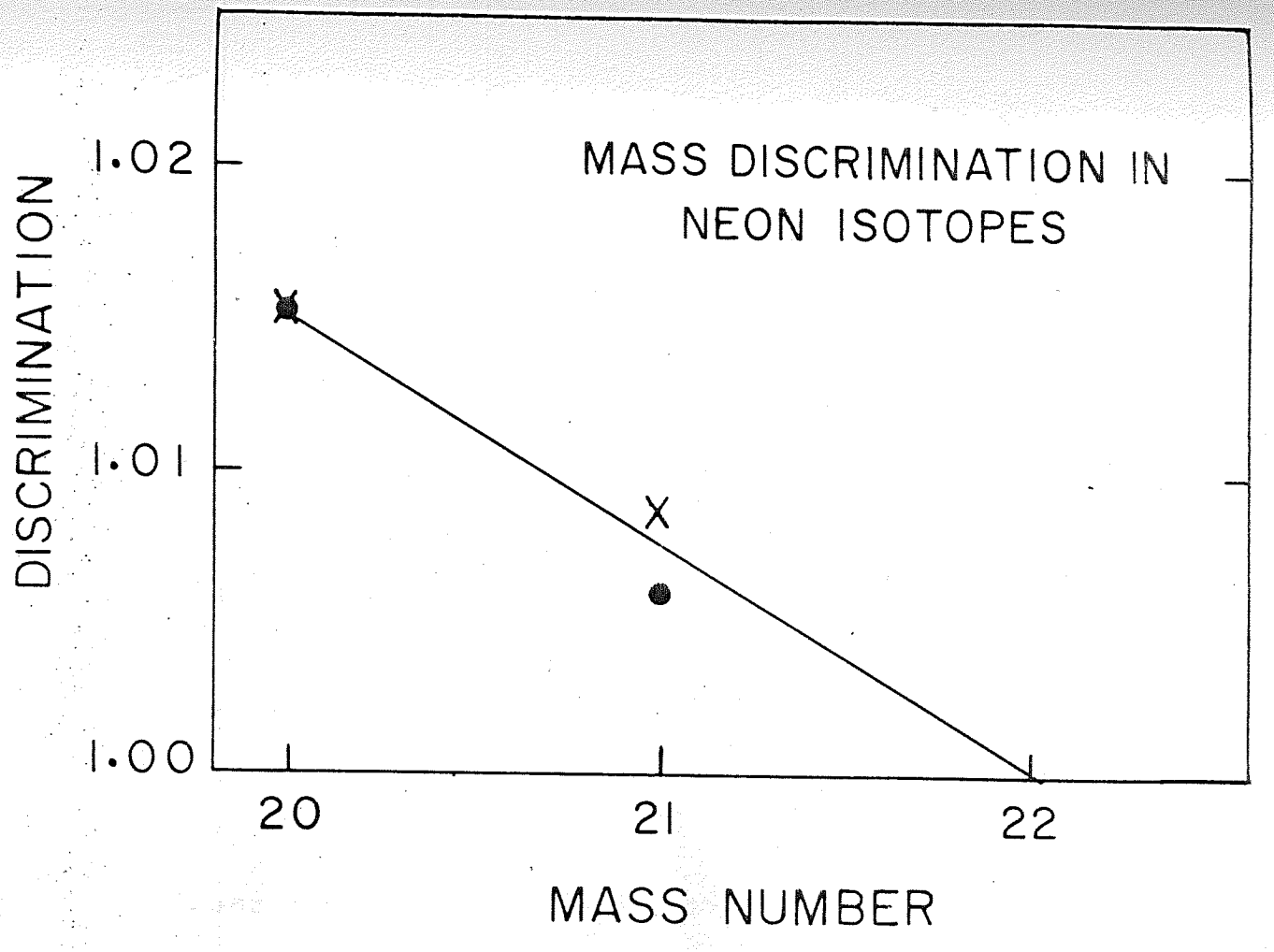

Fig. II.7 Mass-discrimination (m.d) in neon. The filled circle and the crosses represent two typical sets of m.d. values. The normalization is at ^{22}Ne.

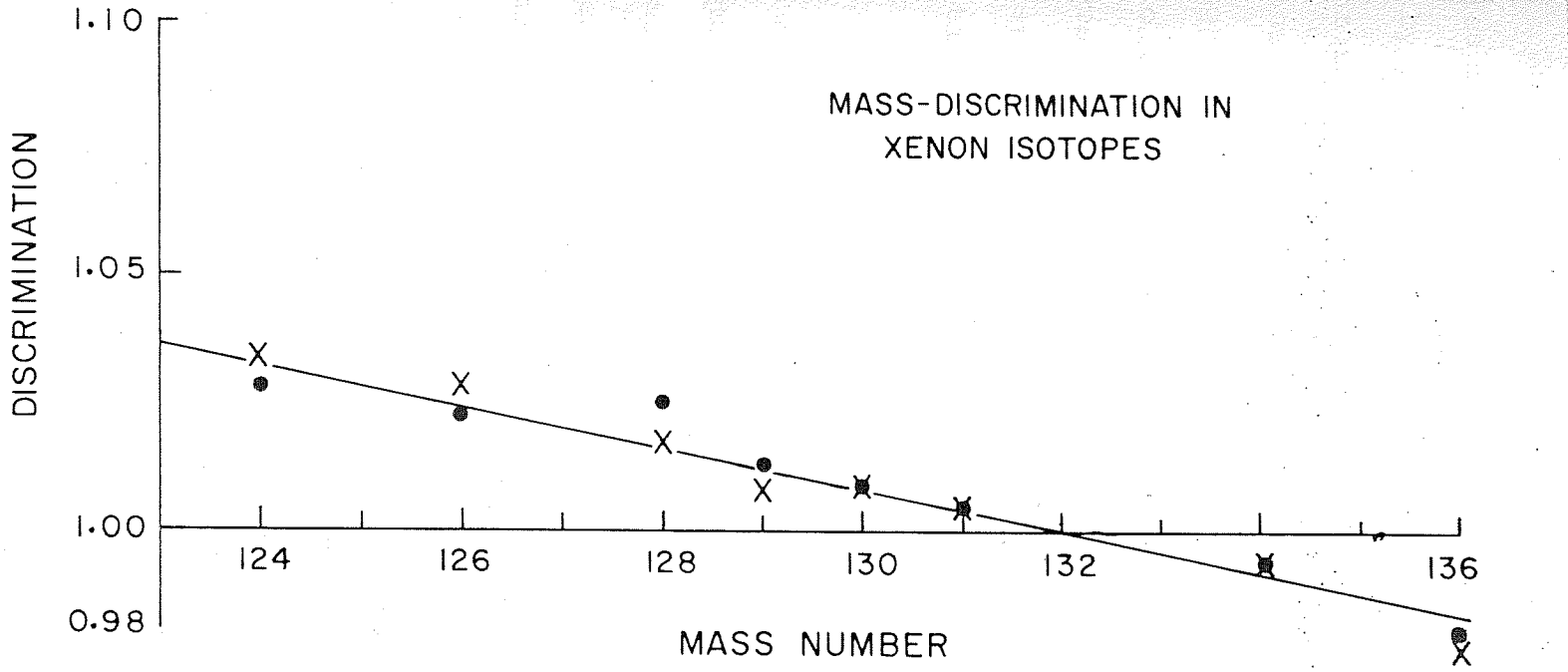

Fig. II.8 Mass-discrimination (m.d.) in xenon. The filled circles and the crosses represent two typical sets of m.d. values. The normalization is at ^{132}Xe.

F. SELECTION, DESCRIPTION AND PREPARATION OF SAMPLES

The noble gases observed in an extraterrestrial samples result from several processes such as in-situ production by protons (spallation) and implantation of SW or SEP and/or from trapping. The SCR-proton produced noble gas component is strongly depth and composition-dependent thus making the sample selection important. Also masking effects due to large GCR production as well as large implanted SW, if present, should be taken into consideration. Target chemistry and sample-depth are also important criteria for selecting the samples.

1. Samples : Lunar soils remain exposed to solar corpuscular radiations on the lunar surface for long time-periods and therefore provide natural choice as detectors for studying long term SCR-proton flux which are of present interest. Gas-rich meteorites are selected to deduce similar information for the early period ($\sim$4.6 Gyr ago) of the solar system history. The lunar rocks are studied for deducing their cosmic ray exposure ages

(1) Lunar Rocks : Three well documented lunar rocks analyzed for cosmic ray exposure ages are anorthositic breccias from lunar highland. Two rocks 61016 and 64435 were collected during Appolo-16 mission while the third rock 79215 was collected during Apollo-17 mission.

Rock 61016 was collected from a location near Flag crater. It was dated by Stettler et al. (1973) by ^{38}Ar-^{37}Ar method and an upper limit of 7 Myr was given for GCR-exposure age.

Rock 64435 is from Stone mountain which are covered by South Ray crater ejecta (Appollo-16 Preliminary Science Report, 1972). The chemical composition of this rock was determined by Laul et al. (1974) and Hubbard et al. (1974).

The third rock 79215 is a brecciated troctolite and has higher Mg-content as determined by Blanchard et al. (1977) and McGee et al. (1978). The plagioclase from this rock has very low Mg content ($\sim$ 0.06%) but the bulk sample may contain as much as 5.7% Mg (Bhandari et al., 1976).

All the three rocks are well documented as to the exposure geometry and they have recognisable top surfaces, as determined by particle track measurements. The samples were taken from interior protions of the rocks as the purpose was to find GCR-effect on feldspar targets. Samples for mass-spectrometry were selected from white portions which are nearly pure feldspar. Table II.3agives the depths of these three rock samples.

(2) Lunar Soils : Soils of differring maturity as judged from values of various available parameters such as agglutinate percentage, particle track density or

TABLE II.3 a

DESCRIPTION OF THE ROCK SAMPLES

Rock	Associated crater on moon	Depth of sample from the top surface (mm)
61016	Flag Crater	16-18
64435	Stone Mountain	7.5-9
79215	Van Serge crater	5-8

TABLE II.3 b

DESCRIPTION OF THE SOIL SAMPLES

Soil	Location on moon	Sample reference
61221	Near Flag crater	Bottom of trench (30-35 cm deep)
69921	Near Plum crater	Skim soil (top 5 mm)
14148	Station G	Top of trench (top 1 cm)
24087	Centre of the multiringed basin	From core

mean grain size, were chosen. The purpose has been two fold : to study the cosmogenic component due to SCR and GCR protons and the components of directly implanted solar energetic particles. Both these effects are recorded by lunar soil grains though they suffer from one drawback viz. uncertainty in the depth of irradiation. Only mineral separates are used for study because SCR effects are sensitive to mineral composition.

Skim soil 69921,9 is a plagioclase rich soil representing top 5 mm of the lunar regolith. It was collected by the Apollo-16 crew at station 9. It is expected to be mature as indicated by its grain size and Ferro Magnetic Resonance (FMR) studies. It has FMR-index (I_s/FeO ratio) of 90 which indicates surface maturity (Morris, 1978).

The soil 61221 is an Apollo-16 soil dug from the bottom of a trench in the rim of Plum crater at station-1 from a depth of about 30-35 cms. The colour of the soil was unusually white and it has several unusual features such as high amount of low temperature volatiles (Gibson and Moore, 1973). This soil was known to be relatively immature based on large mean grain size of 234 microns, low percentage of glassy agglutinates (Heiken et al., 1973) and low I_s/FeO ratio of 9.2) determined by FMR technique by Morris (1978). As SCR-effects are more pronounced in the mature soils, this soil was included in this study to provide a comparison.

Another feldspar rich soil 14148 was taken which is supposed to be a mature soil (I /FeO= 74, Morris, 1978). It was collected from the surface of a trench at station G. It has a median grain size of 87 microns (L S P T, 1971). It represents top one cm of the lunar regolith. ^{26}Al activity in this soil is saturated (Yokoyama et al., 1975) while in the soil 69921,9 it is not, even though 69921 is at least as much mature by other considerations.

The soil 24087 is a mature soil taken from a depth of 86 cm from 2 metre deep drill core collected during Luna-24 mission from a site just outside the innermost ring of the multi-ringed basin of Mare Crisium.

These four samples taken from several locations and varying depths show different degrees of maturity and may be representing irradiation records of same or different epochs. Table II.3 b summarizes the sample-description.

(3) Gas-rich Meteorites : Two H-chondrites, Pantar and Leighton, and one L-chondrite AH 77216,18 are analysed in course of this work. The first two meteorites belong to metamorphic grade 5 while the third meteorite is L-3 chondrite. The two other meteorites, Kapoeta and Fayetteville are achondrite and H-4 chondrite respectively whose published noble gas data (Black, 1972 a) are used for

comparison. A description of the samples analysed (Table II.4) for noble gases in the present study is given below.

Pantar is a fall and it has been classified as H-5. Pantar contains clasts which are as much equilibrated as the matrix. Wlotzka (1963), Koenig et al. (1964) and Suess et. al. (1964) have described its petrographic features. Fredriksson and Keil (1963) and Koenig et al. (1964) carried out chemical analysis. The results of Koenig et. al. (1964) showed 'virtually identical' chemical composition in the light and the dark portions for major elements. The samples for mass-spectrometric analysis were taken from both the dark and the light portions of the meteorite after examination under the stereo microscope. The light portion was quite free from contamination from the dark portion.

Leighton is a fall and Van-Schumus and Wood (1967) have classified it as H-5. However, compositional ranges of mineral grains overlap with those of unequilibrated H-chondrites. The individual dark portions can be classified as H-3,4 and the light clasts as H-5,6 but mineralogy is the same in both the portions (McSween et al., 1981). Track-study in Leighton showed that about 0.5% of the grains in the dark portion are irradiated by solar flare nuclei (Goswami and Nishiijumi, 1980). For mass spectrometric analysis, dark portion of a meteorite was examined under the stereo microscope and a piece selected for stepwise heating

TABLE II.4

DETAILS OF METEORITE SAMPLES

Meteorite sample	Type	Sample amount (mg)	Remark	
Gas-rich				
AH 77216,18	L3	238.8	Find	(1977)
Leighton (Dark)	H5	73.9	Fall	(1907)
Pantar (Dark)	H5	279.5	Fall	(1938)
Pantar (Light)		95.6		
Carbonaceous :				
Isna - I	C3-O	190.4	Find	(1970)
Isna - II		363.7		

analysis.

(4) Carbonaceous Chondrite : Isna, a carbonaceous chondrite, was found in Egypt in 1970. Based on its chemical and petrographical features (which showed a little metamorphism) Methot et al. (1972) classified it as C3 meteorite. For mass-spectrometry, two aliquots were prepared. Isna-I was selected for Ne-analysis while Isna II was exclusively for xenon analysis.

2. Sample Preparation : As different components of noble gases are sited at different locations, their resolution requires special care at sample preparation stage. Soil sample preparation involved size separation, mineral-selection and chemical etching. Rock samples were not given any pre-treatment. The rock samples for mass spectrometry were removed from the white looking parts of the rocks using stainless steel tools after noting the exact depth with reference to the top surface (0 g cm^{-2}).

(1) Size Separation : Dry seiving using nylon seives was employed and grains were separated into (40-90 microns), (90-200 microns) and (200-500 microns) fractions.

(2) Mineral Separation : The standard heavy liquid density-separation method was followed for mineral

separation. For feldspar separation, bromoform (density = 2.89 g/cc) was used. The sample was thoroughly washed in acetone and then in alcohol and allowed to dry in an oven at 60°C for 12 hours. The feldspar separate so prepared was also examined under stereo microscope to remove any undesired components such as agglutinates. For the feldspar fraction, special care was taken to remove any non-feldspathic grains. Scanning electron microscopic examination of randomly selected grains confirmed the purity of the prepared samples.

For pyroxene separate preparation, sample was 'cleaned' with a hand magnet and the remainder subjected to density separation in Methylene iodide (density 3.3. g/cc) in a manner similar to that described above.

(3) Etching : To get rid of the overwhelmingly dominating solar wind gases, diluted mixture of HF (40%) and $HClO_4$ (60%) was used (HF, $HClO_4$ and water in 1:1:10 ratio). However, for stronger etching as was done for pyroxene grains of 14148, 24087 and feldspars of 61221 and 14148, a mixture of H_2SO_4, HF and water was used in 1:1:4 ratio.

The etched grains were washed in ethyl alcohol and then left at 60°C for 12 hours for drying inside an oven.

After careful weighing, they were wrapped in thoroughly cleaned, 99.9% pure alumunium foils and stored under vacuum in the sample arm of the mass spectrometer. From the samples, a small aliquot was kept for the determination of chemical composition.

(4) Chemical Composition : An Atomic Absorption spectrophotometer (Perkin-Elmer model 3058) was used for the chemical composition determination of the sample. A weighed amount of sample from the rock and soil mineral separates were taken and digested with ultra-pure hydrochloric acid. This was diluted with double distilled water to the desired level for use in the Atomic Absorption spectrophotometer. The abundance of elements in the samples were determined by comparing them with the peak heights obtained from the standards. Abundance of Mg, Al and Na were determined in this manner. Plagoiclase showed extremely low magnesium concentration ($\simeq$ 0.05%) while pyroxenes contained appreciable (15 to 19%) magnesium. The compositions used for the end point or production rate calculations were based on these determination except when mentioned otherwise.

CHAPTER III

NEON ISOTOPIC STRUCTURES AND PROCEDURES FOR RESOLUTION OF VARIOUS COMPONENTS

The noble gas isotopic features observed in extra-terrestrial samples such as lunar and meteoritic meterial are results of various processes that have occured over long time spans. The vestegial records of these processes are retained superimposed on one another in these samples to varying degrees. What distinguishes the noble gases in different reservoirs is their characteristic isotopic signatures. The knowledge of the isotopic structures in these reservoirs permits the decomposition of the multi-component noble gas-mixtures into individual components.

In this chapter, the isotopic structures of neon are briefly reviewed and the analytical procedures, developed to resolve the observed neon mixtures into individual components, are described. Neon shows widely differring isotopic compositions in different reservoirs. The composition of the implanted components depend on their sources while those of cosmogenic components depend on the energy spectra of the incident particles as well as on the target elements present in these lunar and meteoritic samples.

A knowledge of the exact isotopic ratios of different components is an important requirement for the quantitative isolation of the components from the noble gas mixtures, observed in lunar and meteoritic samples. The noble gases are good isotopic monitors because they are not subject to chemical fractionation. High volatility, especially of He and Ne, also implies they were not condensed in the solid bodies when they formed. Of all noble gases, Ne is one element showing enormous differences among isotopic composition in different reservoirs and has three stable isotopes. Therefore isotopic composition of Ne has formed the basis of resolution of components in this study. The SCR-proton induced neon isotopes have strong dependence on depth and chemical composition. Therefore average production rates and isotopic ratios of Ne are model based estimates in the case of soils as described later. For this purpose, the knowledge of lunar regolith-dynamics and that of depth profile of Ne-production rates have been combined to obtain the resultant isotopic ratio and the average production rate for a given composition as described in section B.

A. NEON COMPONENTS

Many sources contribute to the observed Ne in a given moon - or meteorite - sample (Signer and Suess, 1963; Pepin and Signer, 1965; Manuel, 1967; Pepin, 1967; Black and Pepin, 1969; Eberhardt et al., 1970; Hohenberg et al., 1970; Pepin

et al., 1970; Black, 1972 a,b,). The observed neon can be cosmogenic in origin produced as a result of proton interactions with the target elements; implanted by solar wind or solar flare particles or it can simply be primordial. Below is given a brief account of various Ne-isotopic components of interest which one comes across in extraterrestrial samples. However, for reviews, reference is made to Bogard, 1971; Black, 1972 c; Podosek, 1978 and Srinivasan, 1981 also. The implanted SEP-Ne composition will be discussed in the Chapter IV. Fig. III.1 shows different Ne-components.

1. Implanted or Trapped Components : Some of these components have been in-situ measured (such as solar wind) while some others (such as planetary) have been inferred. The components like solar wind dominate the observed inventory of gases while components such as Ne-E are present in so small amounts that they can be directly observed only if phases bearing them are separated (and weight wise these phases constitute less than 1% of the bulk) and then analysed (Eberhardt et al., 1974; 1981; Alaerts et al., 1979). Consequently, for some of the components, compositions are reliably known but in some cases only limits can be placed on their composition. Table III.1 contains the isotopic compositions of solar wind, planetary, atmospheric and Ne-E components.

(1) Solar Wind (SW) : The solar wind particles

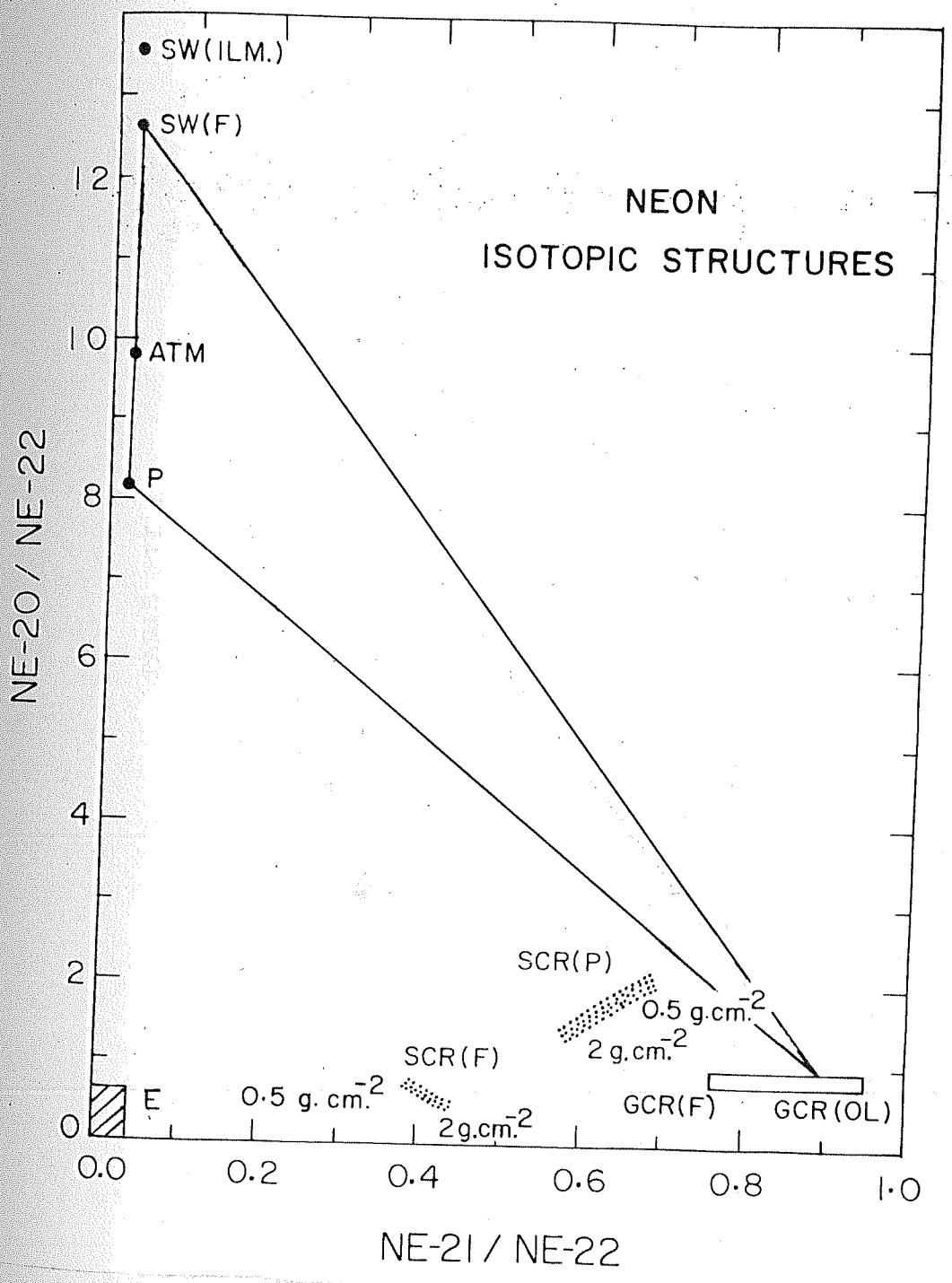

Fig. III.1 Different neon isotopic ratios in various reservoirs.

TABLE III.1

NOBLE GAS ISOTOPIC RATIOS IN VARIOUS SOLAR SYSTEM RESERVOIRS*

	$^{3}He/^{4}He$ (in 10^{-4})	$^{20}Ne/^{22}Ne$	$^{21}Ne/^{22}Ne$	$^{38}Ar/^{36}Ar$	$^{40}Ar/^{36}Ar$
Solar Wind	3.9	12.65**	0.0335	0.186	-
Planetary	1.4	8.2	0.025	0.192	-
Atmospheric	0.0139	9.8	0.029	0.188	296
Neon-E	-	< 0.15	< 0.0022	-	-

* For reference see text.

** This is the value observed in lunar samples. The direct measurements by exposing a foil, give higher value (see text).

are dominated by protons ($\sim$ 90%) and they outnumber the very heavy particle (VH, $Z \geq 18$) flux by a factor of about 10^4. Considering a proton flux of about 3×10^8 protons cm^{-2} $sec.^{-1}$ at 1 AU (Ness, 1968), the time for saturation of outer $\sim$ 300 angstroms (Å) of a grain at 1 AU is $\sim$ 100 yrs in the case of noble gases such as helium or neon. These particles have energies of a few keV/nucleon and ranges of a few hundred Å in chondritic material. Therefore, they can only be implanted in the outer skin of the material directly exposed to them and being very low energy-particles, do not induce nuclear reactions.

The elemental composition of solar wind as deduced from lunar sample studies is found to be broadly similar to the solar coronal composition (Geiss et al., 1972; Cook et al., 1980; Meyer, 1983). The Ne-isotopic composition was also measured in the solar wind composition (SWC) experiment. It was found to be $^{20}Ne/^{22}Ne = 13.7 \pm 0.3$ and $^{22}Ne/^{21}Ne = 33 \pm 4$ by Geiss et al. (1972). In general, lunar soils yield somewhat lower values normally ranging from $^{20}Ne/^{22}Ne = 12.3$ to 13.0 (Hohenberg et al., 1970; Kirsten et al., 1970; Pepin et al., 1970; Frick et al., 1975). The value of $^{20}Ne/^{22}Ne$ ratio was found to be 12.85 ± 0.1 by Eberhardt et al. (1970) in lunar ilmenite samples. In the present work the $^{20}Ne/^{22}Ne$ and $^{21}Ne/^{22}Ne$ have been taken to be 12.65 and 0.033 respectively (See Table III.1) for

lunar samples. It may be noted that higher values for $^{20}Ne/^{22}Ne$ have been found in the case of SW in meteorites (Pepin, 1967; Black, 1972 a).

(2) Solar Energetic Particles (SEP) : This represents the heavy component of the solar cosmic rays. While protons induce nuclear reactions, the SEP get implanted in the surface regions of lunar and meteoritic grains like SW but to a greater depth (significant flux is noticeable only upto a few tens of microns due to the steep fall in flux with energy). Limited results are available in literature on the elemental composition of SEP suggesting the SEP to be close to SW in elemental composition (Dietrich and Simpson, 1979; Mcguire et al., 1979; Cook et al., 1980). In Chapter IV of this thesis the problem of noble gas elemental and Ne-isotopic composition in solar flare particles (or SEP) is treated and the details are given there.

(3) Planetary Neon (Ne-A) : This component was earlier inferred from the study of carbonoceous chondrite by Pepin (1967). Black (1972 b) suggested that it could be a mixture of super solar wind (Ne-D) and Ne-E. Another proposition was that it could be result of mass fractionation of solar wind neon (Zähringer, 1962) but there several problems were recognized (Signer and Suess, 1963). The $^{20}Ne/^{22}Ne$ value for this component was deduced by Pepin (1967) by

finding the intersection of the trapped-cosmogenic composition mixing line defined by several carbonaceous chondrites (Mazor et al., 1970) with the SW-Atmospheric (terrestrial) mixing line. Now it is believed that this is an independent component and not a mixture of Ne-B and Ne-E (Reynolds et al., 1978). The values $^{20}Ne/^{22}Ne = 8.2 \pm 0.4$ and $^{21}Ne/^{22}Ne = 0.025$ are adopted in this study for planetary neon composition (Pepin, 1967). The experiments by Berkeley group (Reynolds et al., 1978) on the acid resistant, oxidizable residues from carbonaceous chondrites also yielded similar isotopic composition. They also demonstrated that the phases which showed planetary elemental composition for noble gases also showed planetary composition for neon isotopes.

(4) Neon-E : This component is present in minute amounts ordinarily, but has been of considerable interest with reference to the theories for its synthesis. Based on stepwise heating analysis of C1 and C2 carbonaceous chondrites, the presence of Ne-E was first suggested by Black and Pepin (1969). It is characterized by very low $^{20}Ne/^{22}Ne$ and $^{21}Ne/^{22}Ne$ ratios almost tending to be pure ^{22}Ne. Probably it is a nuclear component and exotic to the solar system (Podosek, 1978). Bern group (Eberhardt 1974; Eberhardt et al., 1978; 1981) carried out extensive analyses of Orgueil density-separates and deduced the Ne-E composition to be $^{20}Ne/^{22}Ne \leq 0.15$ and $^{21}Ne/^{22}Ne \leq 0.022$ indicating it to be

nearly pure ^{22}Ne. Eberhardt et al. (1979) attributed this to presolar grains while Lewis et al. (1979) interpreted it to be steller condensate. Heymann and Dzickaniec (1976) considered the production of pure ^{22}Ne through ^{22}Na ($T_{\frac{1}{2}}$ = 2.6 yrs.) by proton irradiation of solar nebula but several problems were realized with this scenario also (Clayton et al., 1977). Similarly other models also do not converge (Arnould, Norgaard, 1978; Sabu and Manuel, 1980) and final word is not said yet.

The two other (implanted/trapped) components not discussed here are Ne-D and atmospheric component. The Ne-D was attributed to premain sequence SW by Black (1972 a) and is characterized by high $^{20}Ne/^{22}Ne$ value of ~ 14 and low $^{3}He/^{4}He$. The atmospheric component refers to terrestrial atmosphere and its composition is taken from Nier (1950).

2. In-situ Produced Components : These components result from nuclear transformations (either spontaneous or induced e.g. spallation). Here we consider the products resulting from proton-induced spallation. The heavy particle flux is much lower in abundance and reaction thresholds are high. Hence the protons dominate the particle flux inducing nuclear reactions on suitable targets in extraterrestial samples. There are two main sources of energetic particle radiations : the galactic cosmic rays (GCR) and the

solar cosmic rays (SCR). The spallation neon isotopic ratios produced by these radiations are discussed below :

(1) Galactic Cosmic Ray (GCR) Induced Neon: Exploding supernovae are considered to be probable GCR sources. This is believed that their acceleration to high energies (GeV) can take place in the intersteller medium by Fermi mechanism (Fermi, 1949; 1954). The average GCR-proton flux ($\geq$1 GeV) has been estimated to be 1.7 protons cm^{-2} sec^{-1} (Webber, 1967) and has been shown to be constant over last 1 Gyr (Arnold et al., 1961) and during last few Myr (Tanaka and Inoue, 1979). In the inner solar system, the moon and other extra-terrestrial objects constantly record the effects of the GeV-protons. The GCR-particles (E 100 MeV) follow the following energy spectrum (Reedy and Arnold, 1972)

$$\frac{dJ}{dE}(E,d) = K(\alpha + E)^{-2.5} \qquad \text{III.1}$$

where K is a normalization constant and α determines the spectral shape. The three neon isotopes produced by interaction of protons on chondritic material have approximately equal abundance and in Table III.2 the isotopic compositions of GCR produced neon in Mg-rich (pyroxene) and Mg-poor (feldspar) minerals are given. The interior samples from lunar rocks and ordinary chondrites in general show pure GCR-neon and the observed neon isotopic ratios show small

TABLE III.2

EFFECTIVE PRODUCTION RATES AND END POINTS FOR COSMOGENIC NEON IN LUNAR SOILS*

	^{21}Ne Production rate** (10^{-8} cc STP $g^{-1}Myr^{-1}$)	Ne-isotopic ratio	
		$^{20}Ne/^{22}Ne$	$^{21}Ne/^{22}Ne$
SCR			
Pyroxene	0.127	1.67	0.63
Feldspar	0.05	0.628	0.43
GCR			
Pyroxene	0.18	0.856	0.873
Feldspar	0.086	0.76	0.768

* These values are calculated making use of results of Hohenberg et al. (1978) for production rates and those of Duraud et al. (1975) for residence time at different depths in the regolith. For meteorites, used production rates are one tenth of those given here.

**The GCR-production rates are valid for 20 g cm^{-2} depth. The chemical compositions used are as follows :

Feldspar : 0.02% Mg, 18% Al, 22% Si
Pyroxene : 18.5% Mg, 0.02 % Al, 21% Si

However, the values strongly depend on the chemical compositions and therefore valid only for the above composition. For different compositions, accordingly corrected values have been used.

variations with the location of the sample in the parent body of the given size and composition. Boschler et al. (1969) studied several mineral phases of ordinary chondrites. For Elenovka, the deduced GCR-Ne composition for pyroxene was $^{20}Ne/^{22}Ne = 0.856$; $^{21}Ne/^{22}Ne = 0.873$ and for feldspar $^{20}Ne/^{22}Ne = 0.797$; $^{21}Ne/^{22}Ne = 0.799$. Later, analysis of feldspar separate from the interior of lunar troctolite 76535 gave $^{20}Ne/^{22}Ne = 0.76 \pm 0.03$ and $^{21}Ne/^{22}Ne = 0.768 \pm 0.04$ essentially in agreement with the meteorite based values (Lugmair et al., 1976). In this thesis, the value for pyroxene is taken from Boschler et al. (1969) and that for feldspar is taken from Lugmair et al. (1976).

2. Solar Cosmic Ray (SCR) Proton induced component: The steeper energy spectrum of the SCR-protons results in the distinct isotopic signature for SCR-induced neon. The SCR proton effects are generally restricted to a depth of about 1 cm from the surface of the sample. To represent the energy spectrum of the SCR, two forms are commonly used :

(a) Power law in energy : (III.2)

$$\frac{dN}{dE} = KE^{-\gamma}$$

(b) Exponential rigidity shape: (III.3)

$$\frac{dN}{dE} = K' \exp\left(-\frac{R}{R_o}\right)$$

Here K and K' are constants; γ (gamma) is another constant (spectral index) defining steepness of the spectrum and ranges from 2 to 4 for different flares. The characterstic

rigidity R_o determines the steepness of the spectrum and is expressed in mega volts (MV) whose value ranges from 40 to 200 MV (Reedy and Arnold, 1972). Neither of these spectral representations covers the whole range of energy. The rigidity form has been found to be more appropriate for the range 10-100 MeV/nucleon which is the energy range of interest for nuclear interaction (Frier and Webber, 1963). This form was adopted for the calculation of cosmogenic production rates due to SCR by subsequent workers (Reedy and Arnold, 1972; Hohenberg et al., 1978). However, Bessel function in rigidity has also been shown to be a good fit to the observed proton and alpha-spectra (Mcguire et al., 1981).

B. NEON PRODUCTION RATES

1. GCR Produced Neon : In this study, for GCR-proton produced Ne in meteorites, production rate deduced by Nishiijumi et al. (1980) have been used as given in Table III.3. The production rate given by them is

$$P_{21} = 4.845 \times P_{21}(1.11) \times Fx(21.77 + (^{22}Ne/^{21}Ne)_m - 19.32)^{-1} \quad \text{(III.4)}$$

The normalization is with respect to L-chondrites with $^{22}Ne/^{21}Ne = 1.11$. The values of the constant are 1.0 for L and LL chondrites and 0.93 for H chondrites. The suffix 'm' indicates the measured value.

The GCR-production rates of Nishiijumi et al. (1980)

are considerably lower than those of Cressy and Bogard (1976) but are closer to the values reported by Hohenberg et al., (1978) after accounting for the differences in the exposure geometry of the meteorites and lunar samples. The composition-corrected GCR production rates thus calculated are given in Table III.2 and are in good agreement with the values (0.1 x 10^{-8} cc STP g^{-1} Myr^{-1} for feldspar and 0.11 to 0.21 x 10^{-8} cc STP g^{-1} Myr^{-1} for pyroxene grains) reported by Frick et al. (1975). For meteorites, values reported by Nishiijumi et al. (1980) have been used while for lunar rocks and soils those based on Hohenberg et al. (1978) are used in the present study.

2. SCR Induced Ne Production Rate : Hohenberg et. al.(1978) have given depth dependent Ne-production rate in different target elements based on Reedy-Arnold type spectrum (J=70 protons cm^{-2} $sec.^{-1}$ and R_o = 100 MV). While for lunar rocks applications of these values is relatively straight forward (except for erosion correction), continuous evolution due to micrometeorite-bombardment makes the situation complex in the case of soils. The soil grains do not have a fixed depth of irradiation all through their exposure history in lunar regolith. Instead they are continuously stirred. However, on a statistical basis, it could be considered that a grain starting its journey on top of the soil layer gradually goes down relative to top surface. Monte-Carlo

TABLE III. 3

^{21}NE PRODUCTION RATES IN METEORITES

Meteorite	P_{21} (10^{-8}cc STP g^{-1}Myr^{-1})	Reference
H-Chondrite	●.288*	Nishiijumi et al.(1980)
L, LL Chondrite	0.31*	Nishiijumi et al.(1980)
C3-O Chondrite	0.3	Mazor et al. (1970)

* Normalised to $^{21}Ne/^{22}Ne = 0.9$

calculations were made by Arnold (1975) and Duraud et al. (1975) to trace this trajectory with respect to time. Their results showed that the downward movement of the grain is not monotonic in nature and trajectory of the grain is zig-zag. For the residence time estimation, a straight line fit has been taken from the figure given in Duraud et al. (1975). In calculating the SCR induced Ne end points, the soil grains have been considered to be following this trajectory and residence times at different depths have been read from this figure.

Correspondingly, depth and composition dependent Ne-SCR production rates have been found by interpolation of the calculated Ne-production profile of Hohenberg et al. (1978). Nuemerical integration has been performed upto 1 cm to find the resultant average production rates and end point composition considering that, on average, the grain movements follow regolith evolution model of Arnold (1975) and Duraud et al. (1975). The production rates and Ne-isotopic ratios are given in Table III.2. As the flux-values used in these calculation were those for moon, the SCR-production rates for meteorites are expected to be lower by a factor of ten. Therefore for the gas-rich meteorites, the SCR production rates are accordingly corrected. The assumption is that meteorites were irradiated at about 3 AU distance from the Sun.

C. RESOLUTION OF DIFFERENT COMPONENTS

Reynolds and Turner (1964) introduced a method for presenting Ne-data in which by plotting $^{20}Ne/^{22}Ne$ and $^{21}Ne/^{22}Ne$ in three isotope Ne diagram one can study the mixing behaviour of the components. Composition of mixture of any two components (values normalized to the same isotope) falls along the line joining the compositions of the two individual components. In this type of presentation (Fig. III.1), a three component-mixtures have data points falling within the triangle defined by the three end points.

Fig. III.1 shows the various components of neon. Solar wind neon as determined in lunar ilmenite grains (Eberhardt et al., 1970) has highest ($^{20}Ne/^{22}Ne$) value while that based on pyroxene and feldspar grains show somewhat lower values The atmospheric composition (Nier, 1950) and Planetary composition (Pepin, 1967; Reynolds et. al., 1978) are also plotted. The GCR Ne composition has a spread, with feldspars having lowest $^{21}Ne/^{22}Ne$ ratio (0.768) and olivine the highest $^{21}Ne/^{22}Ne$ ratio (0.94 ± 0.1) as inferred by Lugmair et al. (1976). In the case of feldspars and pyroxenes the SCR-Ne fields are very different from GCR fields and also show different depth-dependence. All neon-data in this study will be presented in three isotope neon diagrams.

Components are resolved analytically. Quantitative procedures based on the knowledge of Ne compositions were developed for identification and resolution of different contributions from different reservoirs by Rao et al.(1978). The basis of resolution is isotopic ratio signatures. Not only are these ratios different in different reservoirs, they may also vary with depth of irradiation as in the case of SCR-produced component. Given the irradiation depth and chemical composition of the sample, it is possible to estimate the SCR-proton produced Ne-isotopic ratios. The techniques for decomposition of the neon isotopic mixtures to resolve SCR-Ne makes use of the above parameters viz. depth variation of SCR produced Ne-ratio and the differences in isotopic ratios of Ne from different components. For a given sample, the total measured ^{22}Ne can be equated to the sum of individual contribution, as shown below :

$$^{22}Ne_m = {}^{22}Ne_s + {}^{22}Ne_g + {}^{22}Ne_t$$

where subscripts m, s, g and t denote measured, SCR, GCR and trapped respectively. Simplifying and denoting SCR, GCR and trapped ^{22}Ne fractions by s, g and t respectively i.e.

$$s = \frac{^{22}Ne_s}{^{22}Ne_m}, \quad g = \frac{^{22}Ne_g}{^{22}Ne_m}, \quad t = \frac{^{22}Ne_t}{^{22}Ne_m}$$

we get $$s + g + t = 1 \qquad \text{(III.5)}$$

In a similar way ^{20}Ne and ^{21}Ne can be equated to contributions from different sources. As the observed ratio is result of combination of the ratios from these 3 sources, the following two equations can be written :

$$\left(\frac{^{20}Ne}{^{22}Ne}\right)_m = \left(\frac{^{20}Ne}{^{22}Ne}\right)_s x\ s + \left(\frac{^{20}Ne}{^{22}Ne}\right)_g x\ g + \left(\frac{^{20}Ne}{^{22}Ne}\right)_t x\ t$$

$$\left(\frac{^{21}Ne}{^{22}Ne}\right)_m = \left(\frac{^{21}Ne}{^{22}Ne}\right)_s x\ s + \left(\frac{^{21}Ne}{^{22}Ne}\right)_g x\ g + \left(\frac{^{21}Ne}{^{22}Ne}\right)_t x\ t$$

These equations can also be written as :

$$M_o = S_o\ x\ s + G_o x\ g + T_o\ x\ t \qquad \text{(III.6)}$$

$$M_1 = S_1\ x\ s + G_1 x\ g + T_1\ x\ t \qquad \text{(III.7)}$$

Here M is used to denote the measured isotopic ratios. The symols S, G and T are used for denoting Ne isotopic ratios due to SCR, GCR and trapped components respectively with subscripts 0 and 1 distinguishing $^{20}Ne/^{22}Ne$ and $^{21}Ne/^{22}Ne$ ratios respectively. Solving equations III.5, III.6 and III.7 gives

$$g = \frac{(M_o - S_o) - t\ (T_o - S_o)}{G_o - S_o} \qquad \text{(III.8)}$$

Value of g thus obtained can be substituted in III.7. Using equation III.5.

$$t = \frac{M_1 - S_1 + S_1 x\left(\frac{M_o - S_o}{G_o - S_o}\right) - G_1\ x\left(\frac{M_o - S_o}{G_o - S_o}\right)}{-S_1 + S_1 x\left(\frac{T_o - S_o}{G_o - S_o}\right) - G_1\ x\left(\frac{T_o - S_o}{G_o - S_o}\right) + T_1} \qquad \text{(III.9)}$$

Using equation III.5, $s = 1 - (g + t)$ (III.10

To find ^{22}Ne amount contributed by any reservoir, the coefficient , s , g and t can be used. Multiplication of the coefficient with the total measured ^{22}Ne gives the amount of ^{22}Ne contributed by that component. Thus

$$^{22}Ne_s = s \times {}^{22}Ne_m. \quad \text{(III.11)}$$

Multiplication of the $^{20}Ne/^{22}Ne$ or $^{21}Ne/^{22}Ne$ ratio with the ^{22}Ne in a particular reservoir gives the contribution of that component to the isotopes ^{20}Ne and ^{21}Ne. The ^{21}Ne obtained in this manner has been used for estimating the SCR-and GCR-exposure ages of the samples. Here the $^{20}Ne/^{22}Ne$ and $^{21}Ne/^{22}Ne$ values for SCR (S) and GCR (G) and trapped (T) are known from the literature (Hohenberg et al., 1978; Eberhardt et al. 1970 and also Chapter IV of this thesis).

The input parameters for these equations are the Ne-isotopic ratios in various components. In Table III.1 and III.2 are given the values for different reservoirs used in this study. The SCR-end points are depth and composition dependent and Fig. III.1 gives an idea of variation in different targets.

In the case of carbonaceous chondrite Isna where planetary and cosmogenic neon are present, two-component procedures are sufficient with planetary Ne and GCR-Ne as

two end points. Using the observed $^{20}Ne/^{22}Ne$ and $^{21}Ne/^{22}Ne$ values and the two end-point compositions spallogenic and trapped contributions have been resolved.

D. ESTIMATION OF IMPLANTED NEON

Light ions ($Z < 18$) do not form etchable tracks in glass and other mineral detectors such as feldspars and pyroxenes, thus making the estimation of the solar flare neon-flux from track studies impossible. The Fe-group nuclei form tracks and hence surveyor spectrum provides information about Fe-group particle - flux (Crozaz and Walker, 1971; Fleicher et al., 1971; Price et al., 1971). To infer the Ne-flux from Fe-flux one requires knowledge of Ne/Fe ratio in solar flares. Gloeckler (1979) has considered data from different sources and inferred that in 1 to 20 MeV/ nucleon energy range Ne and Fe are nearly equally abundant (Ne/Fe $\simeq$ 1.06) whereas in the Fe-rich flares the ratio is 2 but in co-rotating particle events, the same ratio is about 1 (Gloeckler, 1979). Cameron (1982) has given a value of 2.9 for the solar system Ne/Fe ratio. On the other hand, Cook et al. (1982) reported elemental obundances for 7 flares from Sep. '77 to May '78 and in selected four flares, they find Ne/Fe $\simeq$ 0.9 which is very different from the value adopted by Cameron (1982). If all the 7 flares reported by Cook et al. are considered, the Ne/Fe ratio is 1.1. For estimation of implanted SF-Ne, 1.0 has been used in this study.

To estimate the amount of implanted gases the information on Fe-group flux and spectrum is, necessary. The earlier direct measurements were made with detectors aboard rockets thus limiting the observation duration to a few minutes. The opportunity of studying relatively long term average iron-group nuclei flux and spectrum of solar flare particles came when a glass filter of Apollo-12 TV camera was returned to the earth in 1969 after exposure on lunar surface for a period of about 2.6 years. Detailed studies on this glass filter by Crozaz and Walker (1971), Fleicher et al. (1971) and Price et al. (1971) resulted in deducing long-term energy spectrum for solar flare Fe-group nuclei based on particle tracks and the spectrum adopted in this study (Fleicher et al., 1975) is as follows :

$$\left(\frac{dN}{dE}_{\geq 5 \text{Mev/nucleon}}\right) = 4.1 \times 10^{12} E^{-3.3} \text{nuclei cm}^{-2}\text{Myr}^{-1}\text{Sr}^{-1} (\text{Mev/nucleon})^{-1} \quad \text{(III.12)}$$

At energies < 5 MeV/nucleon, the values are read from the 'reassesed' spectrum as given in Zinner (1980) :

$$\left(\frac{dN}{dE}_{<5 \text{Mev/nucleon}}\right) = 3 \times 10^{12} E^{-2.8} \text{nuclei cm}^{-2}\text{Myr}^{-1}\text{Sr}^{-1} (\text{Mev/nucleon})^{-1} \quad \text{(III.13)}$$

Based on these two spectra, implanted neon (SEP-Ne) estimates are made by integrating upto 20 MeV energy as contribution to implanted component by particles > 20 MeV/nucleon is very small. The lower limit of Energy for integration is governed by the etching. This limit is taken in accord with the thickness of etched layer based on range energy curves given

by Lal (1972). However, it may be added that more than one spectra have been deduced to represent the SEP and they considerably differ (e.g. see Blanford et al., 1974; Hutcheon et al., 1974 and the reviews by Hartung, 1980 and Zinner, 1980). Thus the estimates of implanted SEP-neon suffer from large uncertainties.

CHAPTER IV

NOBLE GAS COMPOSITION OF THE RECENT AND ANCIENT SOLAR ENERGETIC PARTICLES

The present study is an effort to understand the isotopic composition of Ne emitted in Solar Flare events using lunar samples and meteorites as detectors. The composition of the solar energetic particles (hereafter SEP)* is of interest for several reasons. Not only does it help us to understand the composition of the Sun, it also contributes to our understanding of the mechanisms operating in the Sun during particle acceleration.

The significance of the solar energetic particles was duly recognized when the similarities between the photospheric and SEP-composition were demonstrated based on the particle tracks in the emulsion stacks exposed to the SEP (Biswas and Fichtel, 1965; Lambert, 1967; Durgaprasad et al., 1968; Bertch et al., 1972). In other words it meant that study of the SEP offers an opportunity to sample the solar material (Cameron, 1973). As a result, now SEP-composition

---

*Hereafter, the event of solar flare will be referred to as solar flare (or SF) and the energetic particles emitted in these flares will be referred to as the solar energetic particles (or SEP) or SF-particles.

has been accepted as representing the solar system composition wherever meteoritic data are imprecise or not available (Cameron, 1973; 1982). Solar energetic particle-measurements are given preference over the solar wind measurements for deducing the composition of the Sun because being high energy particles the SEP are subject to less fractionation.

It is in this perspective that the study of the problem of SF-Ne composition has become important. The SCR consist mostly of protons and alpha-particles and a smaller fraction ($\sim$1%) of heavier particles. Later, in Chapter V, the effects of protons will be discussed. But here the study is confined to the resolution and characterization of the implanted solar energetic particles.

A. MEASUREMENT OF SEP-COMPOSITION : EARLY ATTEMPTS

Elemental abundances are prone to chemical and mass-fractionation. However these problems are much less serious in isotopic ratios and therefore the study of isotopic ratios can yield valuable information. As neon shows a wide range of well defined isotopic compositions in different reservoirs, it provides opportunity to trace the source composition and to characterize the source material. Photospheric measurements may provide such information. But for a relatively cool star like our Sun (photospheric temperature $\sim$ 5800^{o}K), measurement of neon in photosphere is difficult

due to its high ionization potential (21.6 eV) and the chromospheric measurements are unreliable due to high errors associated.

1. Direct Measurements : The direct measurements of SEP-Ne remained inaccessible till the data from Charged Particle Telescopes (CPT) flown aboard the satellites and spacecrafts in the last decade became available. By that time, techniques had been perfected to the extent of making isotopic resolution possible by improved methods for the energy-loss measurements and path-length-determination. These improvements (Garcia-Munoz et al., 1977; Mewaldt et al., 1979) provided data with better resolution compared to the earlier values for SEP-neon composition reported by Webber et al. (1973) which covered planetary as well as the solar wind value for $^{20}Ne/^{22}Ne$ ratio. These CPT-instruments were carried aboard the satellites IMP-8 and ISEE-3. Increased activity of the Sun around 1978 aided the isotopic and elemental study of the solar energetic particles. Of the many measurements made, those of direct relevance to the present study are results on SEP-Ne isotopic composition reported by Chicago and Caltech.groups (Dietrich and Simpson, 1979; Mewaldt et al., 1979) who measured the SEP-Ne-isotopic ratio in 28-49 and 11-26 MeV nucleon^{-1} energy ranges respectively. Based on these experiments, they reported a value of 7.7 (+ 2.3, - 1.5) and 7.6 (+ 2.0, - 1.8) respectively for

$^{20}Ne/^{22}Ne$ ratio in solar flare neon. What was more significant was their suggestion that the Ne in the Sun has planetary composition. This conclusion was based on the similarity between the observed value of $\simeq 7.7$ with planetary neon value of ~ 8.2 (Pepin, 1967; Reynolds et al., 1978; see Chapter III also). This inference triggered an interesting debate regarding the neon composition of Sun and the present work has direct bearing on this problem.

The CPT-measurements of the solar energetic particles span over a few years and values for individual flares vary widely. Therefore it is important to know whether the CPT-data really yield a value which can be considered to represent average value over the long history of the Sun. As variations in the Ne isotopic ratio from flare to flare are large, direct measurement have certain unavoidable limitations despite excellent resolutions achieved.

2. Long Term (Average) SEP-Composition: To study solar flare composition averaged over geological past, we require detectors which have been exposed to solar flare radiation over long time periods. Lunar soils were recognized as potential detectors for collecting SW - and SEP and have been successfully exploited in the last decade (Eberhardt et al., 1970; Hohenberg et al., 1970; Pepin et al. 1970; Heyman et al., 1975; Crozaz, 1977 and many others).

That implanted solar flare particles can be present in the lunar soil grains is not a novel idea. Lal and Rajan (1969) and Pellas et al. (1969) were the first to show SEP-effects in the meteoritic crystals (even before lunar samples arrived) by measuring the charged particle-track-densities and their gradient with depth. They showed that these grains had been irradiated by solar flare particles. Later work by Wilkening (1971) and Macdougall et al. (1974) showed that these records are accumulated during the regolith history of the meteoric material. As early as 1972, Black had suggested that gas-rich meteorites could be having implanted SF-gases in grains from dark portion of these meteorites. Based on the observed data points of neon-analysis of bulk samples of lunar fines and gas-rich meteorites, he inferred a value of $^{20}Ne/^{22}Ne = 10.6 \pm 0.3$ for SEP and termed this neon component Ne-C. Price and Rajan (1973) made use of the published data on Khortemiki (Eberhardt et al., 1965) to show that the trapped ^{20}Ne and ^{36}Ar in this sample were nearly equal to the estimated amounts of these two gases due to solar flare implantation. A few years later, Leich et al. (1975) carried out an elegant experiment involving sequential etching of lunar ilmenite grains (0.6 to 1.3 microns) and mass-spectrometric analysis of the etched residues. The aim of their experiment was to identify the SEP-component in the observed gases. Around that time, several workers had reported preferential enhancement of heavier elements at low energies based mainly on the

charged particle track studies in rocket-borne detectors (e.g. Price et al., 1971; Mogro-Campero and Simpson, 1972). Therefore, Leich et al. looked for any enhancements in ratios of heavy to light elements such as $^{36}Ar/^{4}He$, $^{36}Ar/^{20}Ne$, $^{86}Kr/^{36}Ar$ and $^{132}Xe/^{36}Ar$ in ilmenite grains as etching removed the implanted SW sequentially. Failure to observe any such systematic trends coupled with the fact that they didn't find $^{20}Ne/^{22}Ne = 10.6$ as inferred by Black (1972), made them point out that their search was inconclusive. In fact, in some cases, they found values closer to the solar wind values. Solar flare-correlated phenomena such as particle tracks have also been studied in great detail (Lal, 1972; Fleicher et al. 1975 and many others referenced therein) but isotopic determination is not possible by particle track techniques.

Establishing the presence and composition of SEP-Ne demands identification, resolution and estimation of this component. Resolution of implanted SEP in lunar soils is generally plagued by the overwhelmingly dominating solar wind. Taking clue from the pioneering experiments of Eberhardt and his co-workers (Eberhardt et al., 1965) on Khortemiki, etching of grain-surfaces was considered to be an appropriate approach to remove the major amount of surface-sited solar wind from the lunar grains. As the range of solar wind ions is $\lesssim 0.1$ micron, etching of 1 micron thick surface layer should be considered sufficient to remove

the major amount of solar wind.

In Chapter III, the SEP-energy spectrum and the estimations of implanted SEP-Ne in the etched lunar soils were discussed. Estimates of implanted SF-Ne in etched lunar soil grains studied here are given in Table IV.1 for different soil samples. The lower limit of integration (over energy) is taken in correspondance with the thickness of etched layer and thus the loss of implanted SF-gases during etching is taken into account. The etching estimates are made separately for different soil samples studied here and range from 2 to 5 microns for feldspars ("well etched") and 7 to 11 microns for the pyroxene grains ("heavily etched"). However, not much reliance should be placed on the estimates of implanted SEP-neon as the uncertainty associated with the rate or flux-measurement is very high (Hartung, 1980).

Estimation of implanted neon in the case of gas-rich meteorites is somewhat difficult. As the gas-rich meteorites are believed to have been irradiated in the regolith of their parent-bodies during early period of solar system-formation (Kothari and Rajan, 1978), they should have accumulated SF-noble gases. Anders (1975, 1978) estimated that meteorites of this type should contain nearly three orders of magnitude lower gas amounts compared to the lunar soils. This estimate is based on the $1/R^2$ dependence of the solar wind flux (R is

TABLE IV.1

OBSERVED AND EXPECTED SEP-Ne IN ETCHED LUNAR MINERALS

Sample	Mineral	Size (μm)	Etched thickness (μm)	Expected* ^{20}Ne (cc STP g^{-1})	observed SEP-^{20}Ne cc STP g^{-1}
14148	Pyroxene	40 - 90	~11	1.0×10^{-6}	1.7×10^{-5}
14148	Pyroxene	90 - 200	~ 9	1.5×10^{-6}	1.3×10^{-5}
14148	Feldspar	200 - 500	~ 2	1.0×10^{-5}	1.4×10^{-4}
69921	Feldspar	200 - 500	~ 3	6.0×10^{-5}	1.6×10^{-5}

*These amounts can be treated as correct only within a factor of 10 due to uncertainties associated with the spectrum, flux and estimates of etched layer. The estimates of the thickness of the etched layer are made from mass loss and the power law size-distribution from data given by King et al. (1972) for the soil 14148. Similar size distribution is 'assumed for the other mature soil 69921.

the heliocentric distance) and higher cratering rates in the region of asteroidal belt at that time. The solar flare particles also nearly follow the inverse square law for radial dependence of flux (e.g. see Lee, 1976) so the effect is also expected to be correspondingly lower in gas-rich meteorites. Based on the data from stepwise heating experiments on gas-rich meteorites, an attempt is made here to infer the ancient SEP-neon-composition.

B. RESULTS ON LONG TERM (AVERAGE) NOBLE GAS COMPOSITION IN SEP

In this section , results obtained from lunar and meteoritic samples are presented in two parts viz. isotopic and elemental composition.

1. Neon Isotopic Composition : The neon isotopic composition in SEP has been deduced using information from the following sources : (i) Etched lunar soil feldspar grains, (ii) Etched lunar soil pyroxene grains and (iii) Gas-rich mateorites. While the first two yield information about the SEP-Ne in the recent past, the gas-rich meteorites yield information about the SEP-Ne during the early stage of the solar system history.

The relevance of the three isotope neon diagram for presentation of neon-data was described in Chapter III. The

end points used are same as those discussed in Chapter III and given in Table III.1. Even though the SW-Ne composition based on SWC (Solar Wind Composition) experiment was found to be $^{20}Ne/^{22}Ne = 13.7 \pm 0.3$ and $^{21}Ne/^{22}Ne = 0.0335$ (Geiss et al., 1972), the composition of SW-Ne observed in lunar soil samples is $^{20}Ne/^{22}Ne = 12.65$, $^{21}Ne/^{22}Ne = 0.033$ and has been used as SW-end point (Eberhardt et al., 1970; Frick et al., 1975) in this study.

(1). Lunar Feldspar-Based Result : The stepwise-heating data on different etched feldspar size fractions from lunar soils 69921 (200 - 500 microns), 14148 (200 - 500 microns) and 61221 (200 - 500 microns) are presented in Table IV.2 and the results are plotted in Fig. IV.1. The data of Bhai et. al. (1978) on mildly etched feldspar from 14148 (90 - 200 microns) are also plotted for comparison. The feldspar samples 69921 (200 - 500 microns), 14148 (200 - 500 microns) and 61221 (200 - 500 microns) are all well etched samples. It is estimated that in these cases 1 to 5 micron thick layers of the grain surfaces are removed (see Table IV.1). Therefore, they should be almost free from solar wind. The residual solar wind if any, should show-up in the first (600^{o}C) temperature fractions during stepwise heating mass-spectrometric analysis. If one assumes that long term average SEP-Ne has planetary composition then

TABLE IV.2 a

NEON-ISOTOPIC RATIOS* IN ETCHED LUNAR FELDSPAR GRAINS OF (200-500 MICRONS)

Temp (^{o}C)		69921		14148		61221	
		20/22	21/22	20/22	21/22	20/22	21/22
600		11.43	0.088	11.95	0.038	5.943	0.430
	±	0.1	0.002	0.18	0.001	0.090	0.006
1000		10.153	0.136	11.10	0.063	7.610	0.313
	±	0.05	0.001	0.11	0.001	0.080	0.003
1200		n.m.	n.m.	9.22	0.155	n.m.	n.m.
	±			0.14	0.002		
1600		3.866	0.566	7.63	0.271	6.819	0.34
	±	0.007	0.010	0.15	0.005	0.13	0.007
SUM		10.455	0.129	11.38	0.055	6.845	0.361
	±	0.219	0.003	0.37	0.001	0.183	0.01

*The Ne-amounts and the Ar-data will be reported in Chapter V.
The isotopic ratios are written just as ratios of mass-numbers instead of full symbols. The entry 'n.m.' denotes that sample was not heated at this temperature

TABLE IV.2 b

NEON ISOTOPIC RATIOS IN ETCHED FEILDSPAR

GRAINS FROM SIZE FRACTIONS OF LUNAR SOIL 61221

Temperature (°C)	61221 (40-90 microns) Neon			61221 (90-200 microns) Neon		
	20/22	21/22	22*	20/22	21/22	22*
600	4.304 ± 0.07	0.542 0.08	40.5 0.5	2.979 0.04	0.6102 0.009	40.12 0.5
900	7.236 ± 0.1	0.340 0.004	36.3 0.5	7.179 0.08	0.3457 0.004	42.86 0.5
1600	3.364 ± 0.07	0.666 0.012	25.6 0.4	5.166 0.1	0.4820 0.009	18.85 0.3
SUM	5.108 ± 0.076	0.501 0.032	102.4 0.81	5.152 0.070	0.4751 0.0067	101.83 0.74

*Gas amounts in 10^{-8}cc STP g^{-1}.

The isotopic ratios are written just as ratios of the mass-numbers instead of the full symbols.

FIGURE CAPTION

Fig. IV.1 The implanted SEP-Ne in the etched feldspar grains from lunar soils. The GCR-feldspar end point is taken from Lugmair et al. (1976). The isotopic composition of the SW-Ne is dependent on the retentivity of the mineral also. The higher temperature-data for 69921 and 14148 soils give a value of 11.73 $\pm$ 0.25 on back-extrapolation. These points do not define a single line because of different relative SCR- and GCR- contributions. The data for 24087 (200 - 500 microns) are taken from Bhai et al. (1978).

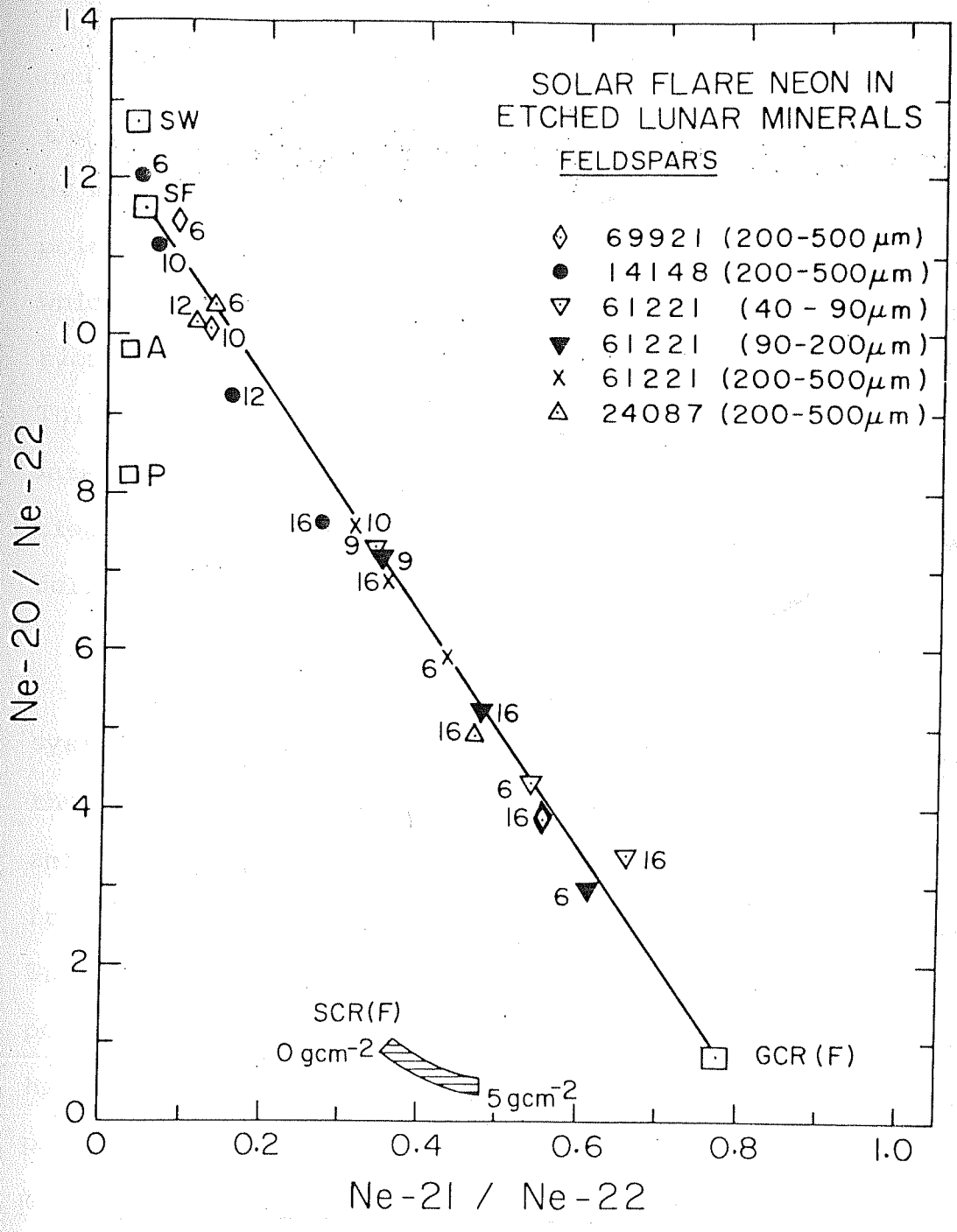
SOLAR FLARE NEON IN
ETCHED LUNAR MINERALS
FELDSPARS
69921 (200-500 μm)
14148 (200-500μm)
61221 (40 - 90μm)
61221 (90-200μm)
61221 (200-500μm)
24087 (200-500μm)
SW
SF
A
P
SCR(F)
0 gcm-2
5 gcm-2
GCR (F)
Ne-20 / Ne-22
Ne-21 / Ne-22
0
2
4
6
8
10
12
14
0.2
0.4
0.6
0.8
1.0

FIG. IV.1

some of the data points for etched feldspars should be close to the planetary Ne-end point and the other data points should fall along the line joining the planetary and the spallation end point. As can be seen, once 600°C temperature is crossed, the higher temperature data points tend to fall along a line; or more precisely, fall within a band which spans from an end point slightly below the solar wind to the spallation end which is different from the end point defined by GCR-spallation alone. This is termed 'resultant spallation' end point. This resultant end point is obtained by extrapolation of the data points towards spallation end and represents a proportional mixture of GCR-spallation and SCR-spallation neon in feldspar soil grains which will be discussed in Chapter V.

A survey of the observed data points indicates a systematic trend. With increase in the gas-release temperature the isotopic ratio changes from implanted to the spallation end point of the feldspars from soils 69921 and two size fractions (90 -200 microns and 200 - 500 microns) of 14148. The 600°C points have higher $^{20}Ne/^{22}Ne$ value than other temperature fractions. This is understandable in view of the higher $^{20}Ne/^{22}Ne$ value for the loosely bound implanted component. The 600°C temperature point of 14148 (90 - 200 microns) has a value of $\simeq$ 12.5 for this ratio while well etched (200 - 500 microns) size fraction of the same soil has a value $\simeq$ 12.0. For no other soils under investigation, this ratio has value $>$12.0. This suggests that the

etching techniques employed here effectively removed the implanted SW-gases from these soil grains.

The behaviour of (200 - 500 microns) fraction of feldspars from the immature soil 61221 is interesting. This soil is less mature. The 600°C point has $^{20}Ne/^{22}Ne = 5.94$ (Table IV.2a) but the next temperature fraction shows a higher $^{20}Ne/^{22}Ne$ value of 7.69. This may be explained if the release properties of the SF-and SW-gases are considered. The penetration depth for solar energetic particles is much higher than for the SW-particles. As etching results in the removal of SW, the first temperature fraction is mostly a mixture of some implanted SEP-and spallation neon. However, this temperature may not be enough to release most of SEP (which are relatively deeper sited) but would have been sufficient to release most of SW-gases. This seems to be consistent with the conclusions of Baur et al. (1972) who showed that release-temperature for the implanted ions is proportional to the energy of injection. This qualitatively explains why one observes a high $^{20}Ne/^{22}Ne$ value in 1000°C fraction. The 1600°C points for 61221 as also in the case of all other soils are always close to the spallation end point as one would expect. A similar trend is obtained for the other two size fractions viz. (40 - 90 microns) and (90 - 200 microns) of this soil (Table IV.2a, 2b)

The other soil 69921 (200 - 500 microns) is also well-etched (~2 microns) though not as much as 61221. The 600° temperature fraction of 69921 has $^{20}Ne/^{22}Ne \approx 11.5$. One can notice a progressive trend towards the spallation end point with increasing temperature of sample-heating.

What makes the low temperature points of 14148 (90 - 200 microns) feldspars interesting is the decrease in the $^{20}Ne/^{22}Ne$ value upto about 12 without any corresponding change in the $^{21}Ne/^{22}Ne$ value which one expects in case the $^{20}Ne/^{22}Ne$ value is pulled down due to spallation contribution. This strengthens the inference that the gas released in the low temperature fractions is dominated by SEP-component. The same trend can not be expected in the case of 61221 because degree of irradiation in the 61221 soil is much less ($N_H/N \simeq 0.1$) compared to that in 14148 ($N_H/N \simeq 0.8$).

The data points of feldspars from 14148 (200 - 500 microns) and 69921 (200 - 500 microns) have been used for a straight line fitting using the procedure by York (1966). A separate line is fitted to the data from (40 - 90), (90 - 200) and (200 - 500) micron size fractions of feldspar grains from the soil 61221. This procedure takes error in both the ratios into account. The best fit line obtained is

$$\left(\frac{20}{22}\right)_{SEP} = -(15.34 \pm 1.18) \times \left(\frac{21}{22}\right)_{SEP} + (12.26 \pm 0.22)$$

for 14148 and 69221 samples. For the feldspars from 61221 soil, the best fit line is given by

$$\left(\frac{20}{22}\right)_{SEP} = -(14.24 \pm 0.83) \times \left(\frac{21}{22}\right)_{SEP} + (12.05 \pm 0.35)$$

These lines cut the SW-Planetary component tie line close to $^{21}Ne/^{22}Ne = 0.033$ and it has been taken as the value for SEP-Ne ratio. The $^{20}Ne/^{22}Ne$ in SEP so deduced is 11.73 ± 0.25 and 11.58 ± 0.36 for the two cases respectively. The error includes error of fitting as well as that of measurement. Hereafter the line based on 14148 and 69921 will be referred to as Feldspar-line unless noted otherwise. The reason for error being large is uncertainty in the $^{21}Ne/^{22}Ne$ value for the SEP-Neon which is taken to be ± 0.007.

(2) Lunar Pyroxene Based Results : Here the results for various size fractions of pyroxene samples are presented. The data are given in Table IV.3 and the ratios are plotted in Fig. IV.2. The soil samples studied viz. pyroxene from 14148 (40 - 90 microns), 14148 (90 - 200 microns) and 24087 (40 - 200 microns) were heavily-etched (7 to 11 microns of grain surface removed) as described in Chapter II. The data on unetched lunar soil 10084 (bulk) as reported by Pepin et al. (1970) are also plotted for the purpose of comparison. In addition, earlier data reported by Padia et al. (1977) on unetched 24087 (bulk) have been re-analysed using procedures described in the Chapter III and

TABLE IV.3

NEON-ISOTOPIC RATIOS IN ETCHED LUNAR PYROXENE GRAINS*

Temp (°C)	14148(40-90 Mic.) 20/22	14148(40-90 Mic.) 21/22	14148(90-200 Mic) 20/22	14148(90-200 Mic) 21/22	24087(45-200 Mic) 20/22	24087(45-200 Mic) 21/22	24087 bulk sample** 20/22	24087 bulk sample** 21/22
600	10.87	0.124	10.01	0.156	10.76	0.123	12.31	0.0336
	± 0.10	0.004	0.15	0.003	0.15	0.004	0.14	0.0011
900	8.61	0.236	6.94	0.381	8.86	0.252	11.91	0.037
	± 0.06	0.002	0.06	0.005	0.04	0.004	0.10	0.0010
1600	3.73	0.609	4.93	0.524	2.29	0.756	11.12	0.0820
	± 0.10	0.012	0.15	0.020	0.07	0.022	0.11	0.0015
SUM	8.26	0.285	7.95	0.306	9.44	0.216	11.73	0.0488
	± 0.12	0.005	0.18	0.008	0.14	0.004	0.37	0.0017

* The details of Ne data and the other noble gas data will be reported in Chapter V.

**Data of this bulk sample (first reported in Padia et al., 1978) have been re-analysed as discussed in the text.

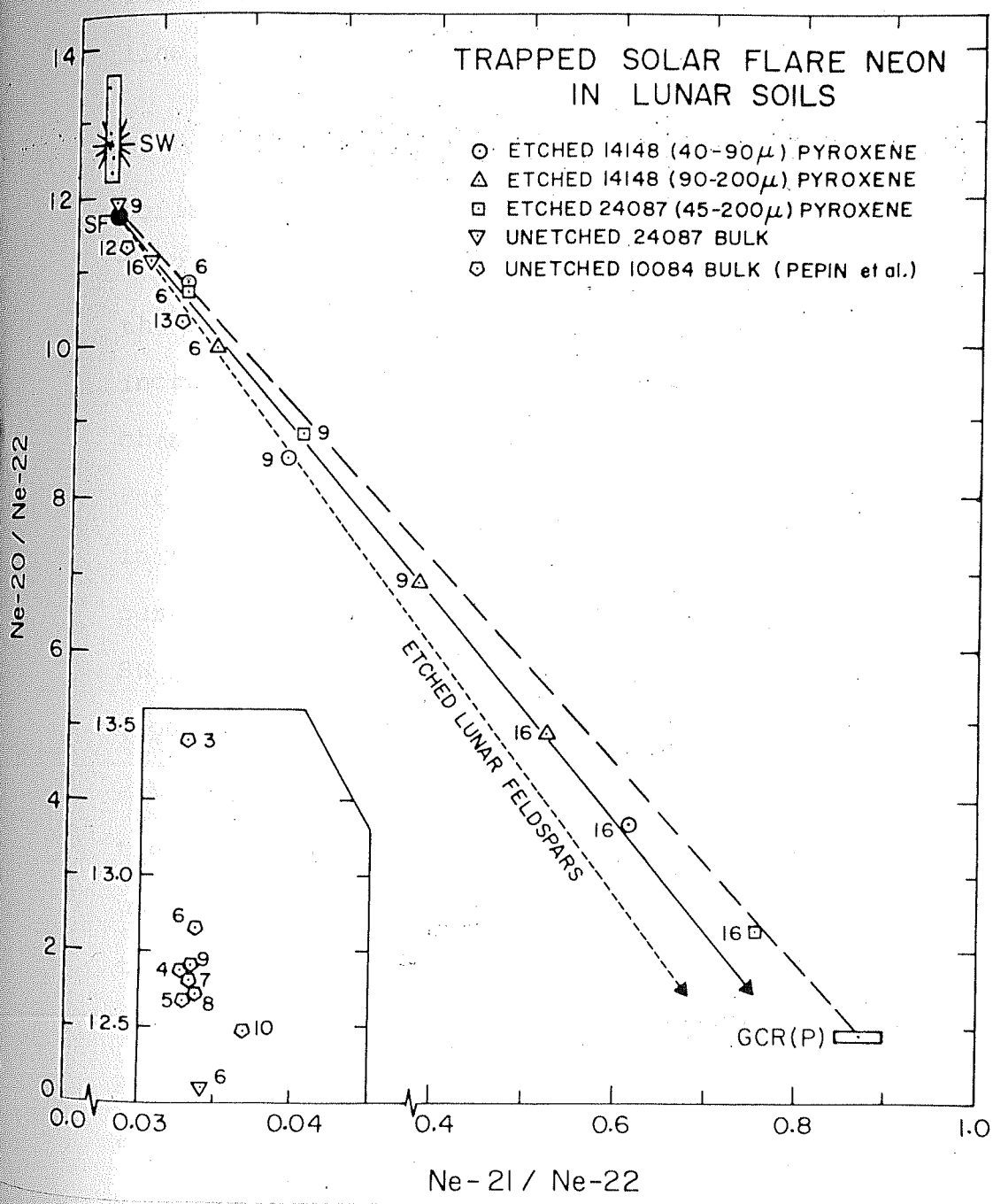

Fig. IV.2 The etched pyroxene-data showing the presence of SEP-neon.

have been plotted in the same Fig. IV.2. However, the data for bulk sample are not incluled for fitting the straight line.

The low temperature lata points for the unetched soils 10084 and 24087 are plotted as inset in the Figure IV.2. The striking feature of the low temperature points of these soils is the steep fall in the $^{20}Ne/^{22}Ne$ value with increase in the release-temperature without any accompanying change in $^{21}Ne/^{22}Ne$ values as was also observed for feldspars. But in unetched samples this feature is more pronounced than in the case of etched samples. This behaviour of low temperature points seems to be typical of a binary mixture of SW and SF components. The values reported by Hohenberg et al. (1970) for unetched bulk sample from lunar soil 10084, 59 also show (not plotted here to preserve clarity) a similar trend. This decreasing trend in $^{20}Ne/^{22}Ne$ ratio continues upto $^{20}Ne/^{22}Ne \simeq 12$ and thereafter data points begin to move towards spallation end point. To characterise the second component we make use of the data points of the etched pyroxene from 14148 (40-90 microns), 14148 (90 - 200 microns) and 24087 (45 - 200 microns) which define a very good straight line. Since etching has removed the SW, the grains contain implanted SF-gases and spallation (SCR+GCR) gases. The behaviour of the data points is as expected from such a mixture. The straight line fitted to the data points is

given by

$$\left(\frac{20}{22}\right)_{SEP} = -(14.06 \pm 0.78) \times \left(\frac{21}{22}\right)_{SEP} + (12.26 \pm 0.23)$$

The SF-Ne composition ($^{20}Ne/^{22}Ne$) thus inferred is 11.8 ± 0.25 for $^{21}Ne/^{22}Ne = 0.033 \pm 0.007$.

It is worth noting that despite different slopes, both feldspars (14148 and 69921) and pyroxenes yield similar values of about 11.8 for the $^{20}Ne/^{22}Ne$ ratio in SF-Ne of the recent past. The Fig. IV.2 also shows the 'feldspar' line plotted for comparison. The higher slope of the feldspar line compared to that for the pyroxene-line can be understood in terms of their chemical compositions. Feldspars are free from magnesium and hence have lower $^{21}Ne/^{22}Ne$ in its SCR-induced component. As a consequence, the 'resultant' spallation end point for feldspars has lower $^{21}Ne/^{22}Ne$ value than pyroxene-end point. So the tie lines for the two are different as seen in the figure. The reason why the data points in the case of feldspars show a spread, will be discussed in Chapter V.

(3) Gas Rich Meteorities : The study of gas-rich meteorites Pantar, Leighton was carried out with the idea of comparing contemporary and ancient SF-Ne composition. The stepwise heating data for Pantar and Leighton obtained in this work have been combined with the available data on two other

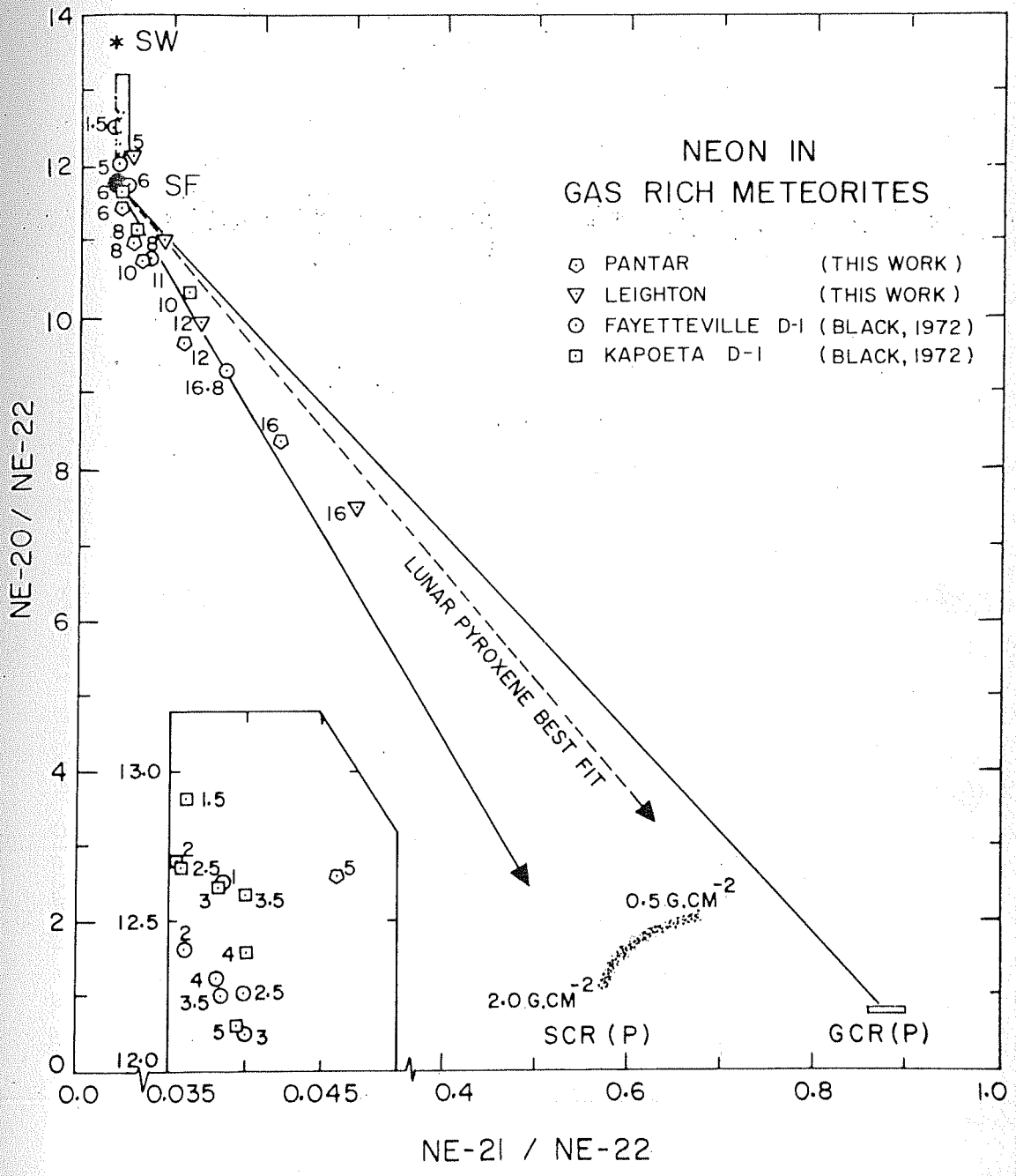

Fig. IV.3

Stepwise heating Neon data in gas-rich meteorites. The points give a value of about 11.7 ± 0.35 on back extrapolation for $^{20}Ne/^{22}Ne$ in the SEP. Numerals beside data points are temperatures in hundreds of ^{o}C.

TABLE IV. 4

NEON ISOTOPIC RATIOS IN GAS RICH METEORITES

Temperature		Pantar (dark)		Leighton (dark)	
		20/22	21/22	20/22	21/22
500		12.65	0.0459	12.13	0.0548
	±	0.15	0.0007	0.14	0.0060
600		11.38	0.0529	–	–
	±	0.15	0.0006	–	–
800		10.96	0.0567	10.98	0.0881
	±	0.11	0.0006	0.14	0.0010
1000		10.73	0.0670	–	–
	±	0.10	0.0007	–	–
1200		9.83	0.1110	9.74	0.1304
	±	0.10	0.001	0.10	0.0015
1600		8.38	0.2173	7.50	0.3049
	±	0.12	0.0030	0.11	0.0040
SUM		10.78	0.0752	10.82	0.0950
	±	0.15	0.0010	0.18	0.0030

gas-rich meteorites Fayetteville D-1 and Kapoeta D-2 (Black, 1972) and plotted in Fig. IV.3. Table IV.4 gives the measured isotopic ratios in Pantar and Leighton. The inset shows low temperature data points of these meteorites. A qualitative similarity with the lunar soils is exhibited by data points of both these meteorites in the low temperature region. However, the temperature intervals are larger for Pantar and Leighton and hence a comparison is difficult in the low temperature region. As can be seen in Fig. IV.3, the trend of the meteorite points is different from the lunar soil points. These points tend to spallation end points which have lower $^{21}Ne/^{22}Ne$ values than expected. But despite this, these data points also, when extrapolated back, indicate a $^{20}Ne/^{22}Ne$ value of about 11.7 for SEP. The straight line fitted to those data points of Pantar, Leighton and Fayetteville (D1 and D2) which have $^{20}Ne/^{22}Ne < 12$ is

$$\left(\frac{20}{22}\right)_{SEP} = -(17.13 \pm 1.49) \times \left(\frac{21}{22}\right)_{SEP} + (12.25 \pm 0.18)$$

In principle each meteorite should define a line if the spallogenic gas amount in them are mixtures of SCR and GCR contributions in different proportions. But the points show a somewhat constant relative amounts of Ne from these two components.

C. NOBLE GAS ELEMENTAL RATIOS IN SEP

An independent characterization of the residual gas components present in the etched mineral grains can be done by

comparing their elemental ratios. Below is examined whether the residual gas has 'planetary' elemental composition or not. Planetary component is characterized not only by low $^{20}Ne/^{22}Ne$ but also by higher abundance of heavier noble gases compared to solar gases also (Signer and Suess, 1963; Reynolds et al., 1978) as given in the Table IV.5. The usual way of presenting the noble gas elemental data is to plot the normalized abundance (with respect to ^{36}Ar) against the mass number. The Figure IV.4 shows the planetary and solar noble gas components plotted in this format. Since different isotopes of a noble gas would be produced by different processes, to characterize the residual (or trapped) gas we have chosen only those isotopes whose abundances are less affected by in-situ production. Therefore ^{4}He has been chosen for He and ^{20}Ne has been chosen to represent Ne. For krypton and xenon, the isotopes ^{84}Kr and ^{132}Xe have been chosen.

The elemental ratios characteristic of solar wind and planetary composition are plotted in Fig. IV.4. In this figure the elemental ratios measured for the etched feldspars for the size-separates of 69921 (200 - 500 microns), 14148 (200 - 500 microns) and 24087 (45 - 200 microns) are plotted. The $^{20}Ne/^{36}Ar$ ratio for the ilmenites (Leich et al., 1975) and the for pyroxenes of Kirsten et al. (1972) are also plotted. The value from the direct (CPT)

TABLE IV.4

ELEMENTAL AND ISOTOPIC RATIOS IN DIFFERENT NOBLE GAS RESERVOIRS

Reservoir	Source	Neon 20/22	Neon 21/22	$^{20}Ne/^{36}Ar$	$^{36}Ar/^{132}Xe$	Ref.
Solar Wind	Lunar Soils	12.6	0.033	>33	∿ 16000	a, b
Solar Wind	SWC-experiment	13.7 ± 0.3	0.0335			c
SEP(28-49 MeV nucleon^{-1})	Direct Charged Particle Telescope	$7.7^{+2.3}_{-1.5}$	-	32^{+27}_{-15}	-	d, e
SEP(11-26 MeV nucleon^{-1})	Measurements of solar flares	$7.6^{+2.0}_{-1.8}$	<0.11		-	f
SEP(∿1MeV/nuc)	Inferred from gas rich meteorites, lunar soils and breccias	10.6 ± 0.3	-	-	-	g
Planetary	Measured in acid resistant, oxidizable residues of carbonaceous chondrites	8.6	-	0.18	∿ 90	h
Planetary	Inferred from carbonaceous chondrites	8.2 ± 0.4	.025	-	-	i

a. Eberhardt et al. (1970)
b. Pepin et al. (1970)
c. Geiss et al. (1972)
d. Mewaldt et al. (1979) and Mewaldt et al. (1983)
e. Cook et al. (1980)
f. Deitrich and Simpson (1979)
g. Black (1972)
h. Reynolds et al. (1978)
i. Pepin (1967)

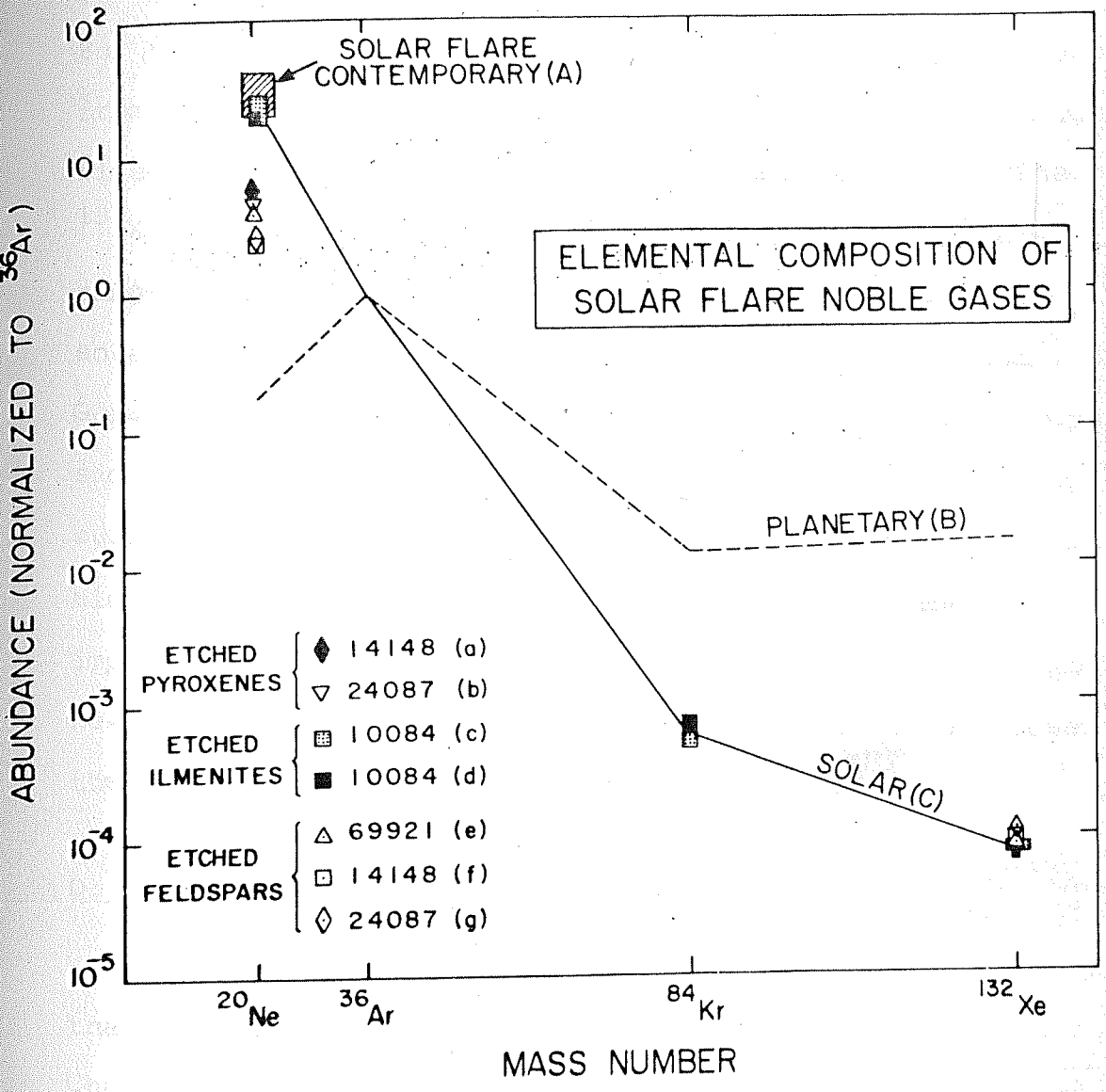

Fig. IV.4

The elemental ratios in the etched lunar grains. Their similarity with the solar composition is evident. Data from Leich et al., 1975 (c,d) and Bhai et al., 1978 (g) are plotted. A, B and C are from cook et al., 1980; Reynolds et al., 1978 and Eberhardt et al., 1972.

measurement of SEP by Cook et al (1980) is also plotted. For the feldspars studied in this work, this ratio ranges from 3 to 6. The contributions of spallation do not significantly affect these ratios as mentioned earlier. The $^{132}Xe/^{36}Ar$ ratio measured in the etched feldspar grains ranges from 8×10^{-5} to 1×10^{-4} which agrees with the solar wind value within error limits (Eberhardt et al., 1970; Geiss, 1972). All the above observations support the conclusion that the noble gases we are observing after etching the surface of the lunar grains, are closer to the solar wind elemental composition than to the planetary. This is an important observation and consistent with the finding about Ne-isotopic composition which has been shown to be closer to the solar wind than to the planetary composition.

D. DISCUSSION

The results of SF-Ne composition being closer to SW than planetary neon ratios is not in agreement with the Charged Particle Telescope (CPT) measurements of Dietrich and Simpson (1979) and Mewaldt et al. (1979). The value of $^{20}Ne/^{22}Ne = 11.8 \pm 0.25$ obtained here is closer to the value of about 12.6 for the SW-Ne deduced from lunar soil studies (Eberhardt et al., 1970). The value deduced by Dietrich and Simpson (1979) and Mewaldt et al. (1979) from the CPT-based experiment were about 7.7 (+ 2.3,-1.5). What was more important was the authors' suggestion that the Ne in the Sun

is planetary in composition based on the fact that the observed value of about 7.7 is close to the planetary neon value of 8.2 $\pm$ 0.4 which was found in carbonaceous chondrites (Pepin, 1967; Black, 1972 and Reynolds et al., 1978). This suggestion has far-reaching consequences. Solar flares are believed to represent the composition of the sun and this essentially means solar system-abundance (Cameron 1973). To take planetary composition to represent the solar composition appears inconsistent. Not only isotopic but also the noble gas elemental composition in etched lunar samples has been found to be similar to the solar wind.

One important feature of the SEP-composition is the variability in isotopic as well as elemental ratios. Models have been proposed for the SEP-acceleration to explain how different charged states and consequently different rigidities R(R=pc/Z*, where Z* is the effective charge on the ion) of particles can govern their entry into the Fermi acceleration zone on the Sun. Model by Korchak and Syrovatski (1950), originally proposed for galactic cosmic rays, can explain the preferential acceleration of heavier elements to differing degrees (Price et al., 1971; Cartwright and Mogro-Campero, 1973; Crawford et al., 1975). Variations of several orders of magnitude have been found in $^{3}He/^{4}He$ ratio in solar flares. Fisk's mechanism (1978) based on heating of ambient $^{3}He^{++}$ in the lower carona of Sun, can

explain such He-isotopic variations but Ne isotopic composition variations to-date, remain puzzle. For discussion purpose we are considering the results of Dietrich and Simpson (1979) which are essentially similar to the results of Mewaldt et al. (1979). The results of Dietrich and Simpson (1979) are based on 7 flares. Two of them were in 1974, and the remaining five in 1977-78. The total number of ^{20}Ne - events considered for analysis was 112 and that of ^{22}Ne was 16. The spallation effects did not interfere as inferred by them on the basis of absence of ^{21}Ne. The resolution in these experiments is excellent and the calibration data show no spill over of neighbouring isotopes. But the ^{22}Ne counts varied from 0 to 6 in the 7 flares indicating the degree of variability and also that the observed differences in the isotopic composition are genuine flare to flare variations. The important question, therefore, is whether averaging of measurements from a few flare-observations can give a value which can be called representative of solar composition or not. Another important question is whether Sun can have planetary composition. The source of planetary component has been briefly discussed in the Chapter III eventhough no consensus exists on this aspect of noble gases. The phases which retain the planetary gases (Reynolds et al. 1978; Moniot, 1980) are probably fine grained carbon (Anders , 1981) and they are found to release gases at high temperature. But being implanted component,

solar flare-gases are expected to be released at lower temperature. So it is unlikely that the planetary-component is a result of SEP-implantation. One could try to interpret the observed Ne-data points as a mixture of contributions from Planetary, solar wind and GCR but in that case one would expect the high temperature points to line up along the planetary-GCR tie-line which is not found (Fig. IV.1.2 and 3). The value of $^{20}Ne/^{22}Ne$ for solar system abundance adopted by Cameron (1973) was based on C1-meteorite data (and hence, planetary) because of unavailability of SEP-observations. But C-1 matrix composition can be taken to represent the composition of primitive solar nebula only for nonvolatile or less volatile elements and not for rare gases and H,C,N,O as they are not easily condensible (Meyer, 1978). All these considerations along with the variability of SEP-data suggest that the CPT-based values, howsoever precise, can not be taken as representative of long term value of SEP-composition.

As for the elemental composition, large variations have been found by various workers (e.g. Dietrich and Simpson, 1979; Mason and Gloeckler, 1979). In these 7 flares, Fe/o ratio was found to be varying from 0.031 to 0.22. However, the Fe/O and Ne-20/Ne-22 were completely independent of each other.

It is important to add that the Ne/Ar ratio also indicate solar wind like values for the SEP (Figure IV.5). The Ne/Ar values are similar in the solar wind (27.4 ± 9) reported by Geiss et al. (1970), solar system-abundance given by Cameron (1982) and the SW found by Marti in Gas-rich meteorite Pesyanoe (1969). Leich et al. found a value of about 20 for the same ratio in lunar ilmenites from soil 10084 after mild (0.61 to 1.3 micron) etching. In the case of pyroxenes of soil 12070, Kirsten et al. (1971) obtained a nearly similar $^{20}Ne/^{36}Ar$ ratio of about 10-15 in the pyroxene and ilmenite grains after varying etching. The measurement of 5 (individual) lunar soil olivine crystals by Kiko et al. (1978) gave values close to 25 (though one value was as low as 9) while feldspar from lunar soil had been shown to have $^{20}Ne/^{36}Ne$ value as low as 1.2 (Kirsten et al., 1971). A somewhat similar value of about 15 in all the samples whether unetched, or etched to different degrees, is probably indicative of similarity in compositions of these two components. Wieler et al. (1982) have pointed out that the $^{20}Ne/^{36}Ar$ ratio in retained SEP may vary from 3 to 10 in lunar feldspars. The value of 32 (+ 27, -15) obtained by Cook et al. (1980) from CPT-measurements aboard the Voyager-1 and Voyager-2 spacecrafts is not inconsistent with the solar wind value of 27.4 ± 9 deduced from SWC-experiment of Geiss et al. (1972) and the ilmenite-based value of > 33 reported by Eberharhardt et al. (1970). The feldspar-based

FIGURE CAPTION

Fig. IV.5. The figure shows the normalized $^{20}Ne/^{36}Ar$ for the SEP and SW as deducted by different methods. Normalization is with respect to the average value as measured by Kirsten et al. (1971) in unetched pyroxene. The hexagons and inverted triangles are from Kirsten et al. (1971). The other values are from the following.

Planetary	:	Reynolds et al. (1978)
SEP (Ilmenite) Squares	:	Leich et al. (1975)
Filled triangles	:	Kirsten et al. (1971)
SEP (CPT)	:	Cook et al. (1980)
SW (Feldspar)	:	Etique et al. (1980)
SW (SWC)	:	Geiss et al. (1972)

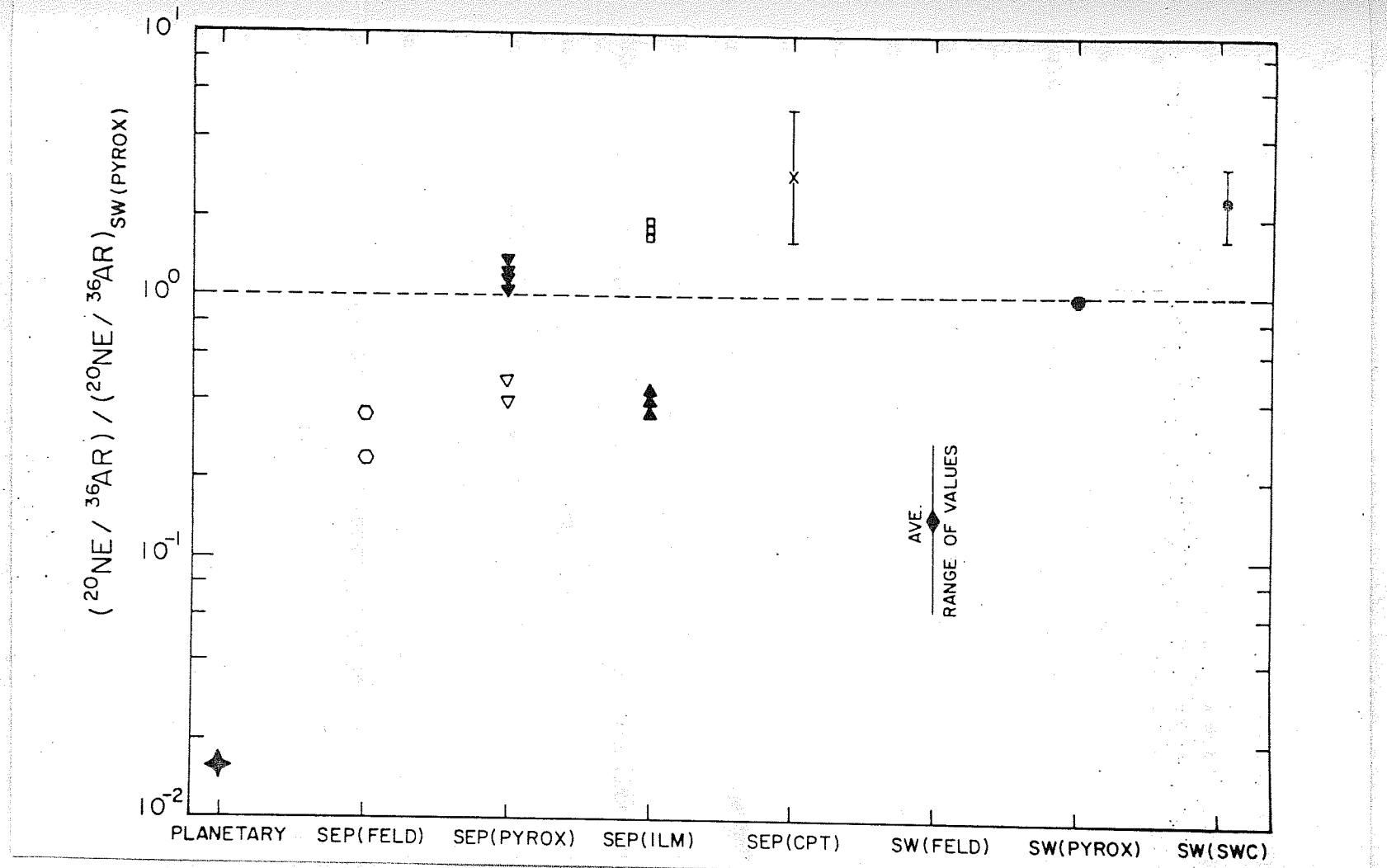
10^1
10^0
10^{-1}
10^{-2}
$(^{20}NE/^{36}AR)/(^{20}NE/^{36}AR)_{SW(PYROX)}$
AVE.
RANGE OF VALUES
PLANETARY
SEP(FELD)
SEP(PYROX)
SEP(ILM)
SEP(CPT)
SW(FELD)
SW(PYROX)
SW(SWC)

FIG. IV.5

value is comparatively low (partly due to diffusion) but still more than an order of magnitude higher than the planetary $^{20}Ne/^{36}Ar$ ratio of 0.18 (Reynolds et al., 1978). All these values for $^{20}Ne/^{36}Ar$ are summarized in Fig. IV.5 with normalization to the value obtained by averaging lunar pyroxene data of Kirsten et al. (1971). In this study no Kr-measurements were made so Kr/Ar values are not available for the feldspars and pyroxenes but the values obtained by Leich et al. (1975) for this ratio in etched ilmenites, are plotted in the Fig. IV.4. The $^{132}Xe/^{36}Ar$ ratio measured in the etched feldspar grains (8×10^{-5} to 1×10^{-4}) agrees with the solar wind value within error limits (Eberhardt et al., 1970; Geiss et al., 1970). The solar wind noble gases are lighter in elemental as well as isotopic composition (Geiss et al., 1972; Marti, 1969). It is therefore not unexpected that the SEP which resemble the SW in elemental composition should also be isotopically lighter compared to the planetary composition. However, as discussed before, the variations in flares are genuine. It is therefore important to examine whether the differences in the results by charged particle telescope method and by those used in this study are inherent to the techniques. Table IV.5 offers a comparison between the two techniques viz. etched lunar soil-based measurements and the CPT-measurements. Both methods refer to measurements at $\sim$ 1 AU. The difference in the two techniques is that the CPT-measurements are limited over a narrow energy range

(11 - 50 Mev nucleon^{-1} energy range in these two cases) while soil samples accumulate the particles over a wide range of energies. The greatest advantage of using soils is the long duration of sampling. The soils were exposed to the solar radiations typically over a few million years thus accumulating neon which is several million times higher than what CPT can sample over short time periods. As it is only a few flares which dominate the total flux (Webber, 1967) in a solar cycle, the CPT measurement may be atypical of the long term composition. The flux in $<$ 11 MeV nucleon^{-1} is expected to be much higher than that in $>$11 MeV nucleon^{-1} range indicating that what CPT sampled did not represent the major fraction of the solar energetic particles. Thus the major differences between the two methods is that the lunar soil-and meteorite-based results represent long-term-averaged value covering almost entire range of energy of solar energetic particles in contrast with the direct observations which are based on a few flares and sample these particles over a limited energy range. Black (1983) has indeed argued for the energy-dependence of the neon-isotopic ratio as was noted by him in the case of $^{3}He/^{4}He$ data of Anglin et al. (1971) and Webber et al. (1975). Besides this, the variations observed from flare to flare are large and averaging of measurements from a few flare-observations may not give representative value of the composition.

Lunar soil-based results reported by Etique et al. (1981) and Wieler et al. (1982) and those reported here are in agreement within limits of error and represent long term average for $^{20}Ne/^{22}Ne$. The value of 11.8 ± 0.25 as given by lunar soil feldspars and lunar soil pyroxene and about 11.7 ± 0.35 given by gas-rich meteorites are for different time windows and hence it is concluded that the time averaged SEP-Ne-isotopic composition and SEP-noble gas elemental composition is not planetary and is closer to the solar wind composition. This also implies that assuming the SEP-composition to be representative of the bulk solar composition, the composition of the Sun is not planetary and resembles the solar wind composition.

CHAPTER V

COSMOGENIC EFFECTS OF THE SOLAR COSMIC RAY PROTONS IN LUNAR SOILS

Solar cosmic ray bombardment of lunar and meteoritic materials brings about in them a variety of physical and chemical changes. In this Chapter the results of the study of the neon isotopic changes induced by solar protons in lunar soils are presented.

In general, the observed noble gas-abundances in the extra-terrestrial samples are due to a super-position of effects accumulated over a number of short intervals as the exposure of the lunar grains to SCR does not take place in a fixed position and also their exposure is not continuous in time.

By resolving the isotopic excesses, the surface exposure ages of the lunar soils can be estimated using the available knowledge of SCR flux, SCR-spectrum and the specific isotope-production rates. While the radioactive isotopes by SCR-protons have been extensively used to study the surface exposure histories of lunar samples (Shedlovsky et al., 1970; Herr et al., 1971; Herpers et al., 1973; Kohl et al., 1978), the noble gases have remained, in that context, unexploited.

The attempts to use them for the above purpose were thwarted partly by the lack of knowledge of suitable proton-spallation-cross-section values and partly by the fact that the SCR-produced noble gases constitute a relatively small fraction of the observed noble gas inventory which is swamped by the enormous amount of implanted solar wind particles. In addition, the SCR-exposure ages are typically a few tens of Myr while the GCR-induced production continues over hundreds of million years. In other words the SCR-produced noble gases have to be deciphered against the high background of implanted SW and SEP and also in the presence of volume-correlated GCR-component.

Noble gases provide integrated information over long time-intervals whereas the radioactive isotopes refer to the recent acquisition or production depending on its decay constant (or the half-life). However, the advantage of noble gas-based methods also lies in this fact because the application of radioactive isotopes to the exposure age determination can not be extended to much longer time scales due to the limitation of their mean lives ($\simeq$ 10 Myr using ^{26}Al or ^{53}Mn). Rao et al. (1971) had indicated the presence of SCR-induced ^{132}Xe in lunar fines by showing the correlation between the SCR-tracks and the excess ^{132}Xe. Gopalan and Rao (1975) and Frick et al. (1975) examined the Xe-and Ne-isotopic compositions respectively in lunar soils and showed that

the SCR-induced Xe and Ne were indeed responsible for their deviation from the SW-GCR tie line. However, the uncertainty in the production rates at that time was quite large prohibiting a quantitative estimation of the SCR-effects. Besides, the observed amounts especially of Ne were dominated by the solar wind implanted component. In the studies by Gopalan et al. (1977) and Bhai et al. (1978) the size-and mineral-separates were subjected to the mass-spectrometric analysis after mild etching. These experiments needed improvement on several counts. The etching was not sufficient to remove the SW-component; the SEP-contribution was not known and the production rates as well as production ratios were not well known. The SCR-induced Ne production rates and ratios used in these studies were based on integration only upto 45 MeV energy. Considering that the flux of protons in greater than 45 MeV range appreciably contribute to the cosmogenic neon (due to SCR), use of production-values obtained by integration upto 45 MeV production rates was not correct. In the last few years, a number of low energy proton spallation cross-section results and production rates for SCR-proton induced noble gases have become available (Walton, 1974; Walton et al., 1976 a; Walton et al., 1976 b; Hohenberg et al., 1978). In the present study, the resolution procedures make use of the isotopic ratios calculated on basis of above work. The purpose of this chapter is to develop a technique for isolating the

SCR-produced Ne and determining model surface exposure ages using neon as a tool.

A. DEPTH-AND COMPOSITION-DEPENDENCE

The cosmogenic effects are mainly due to the protons whose abundance is nearly an order of magnitude higher than the alpha particles. Also the threshold energies for nuclear reactions are higher for alpha particles and they have lower range than protons in lunar and meteoritic materials. Therefore, it can be considered that the protons alone are responsible for the cosmogenic production of neon by SCR. The SCR-protons are energetic enough to induce nuclear reactions but they are attenuated fast due to their low energies. Therefore the SCR-proton produced neon has strong depth-dependence. The depth-dependence of the Ne-isotopic ratios is a consequence of change in the energy spectrum of the incident particles (Reedy and Arnold, 1972) due to preferential energy losses by low energy particles as they traverse through matter. The composition-dependence arises from the fact that in high energy-proton-interections, there is no preference shown for the production of a particular isotope in a particular target element while in the low energy proton interactions, excitation functions are very different for different elements (Frick et al., 1975; Walton, 1974; Walton et al., 1976 a; Walton et al., 1976 b). Fig. V.1, V.2 and V.3 are adopted from Walton (1974). For

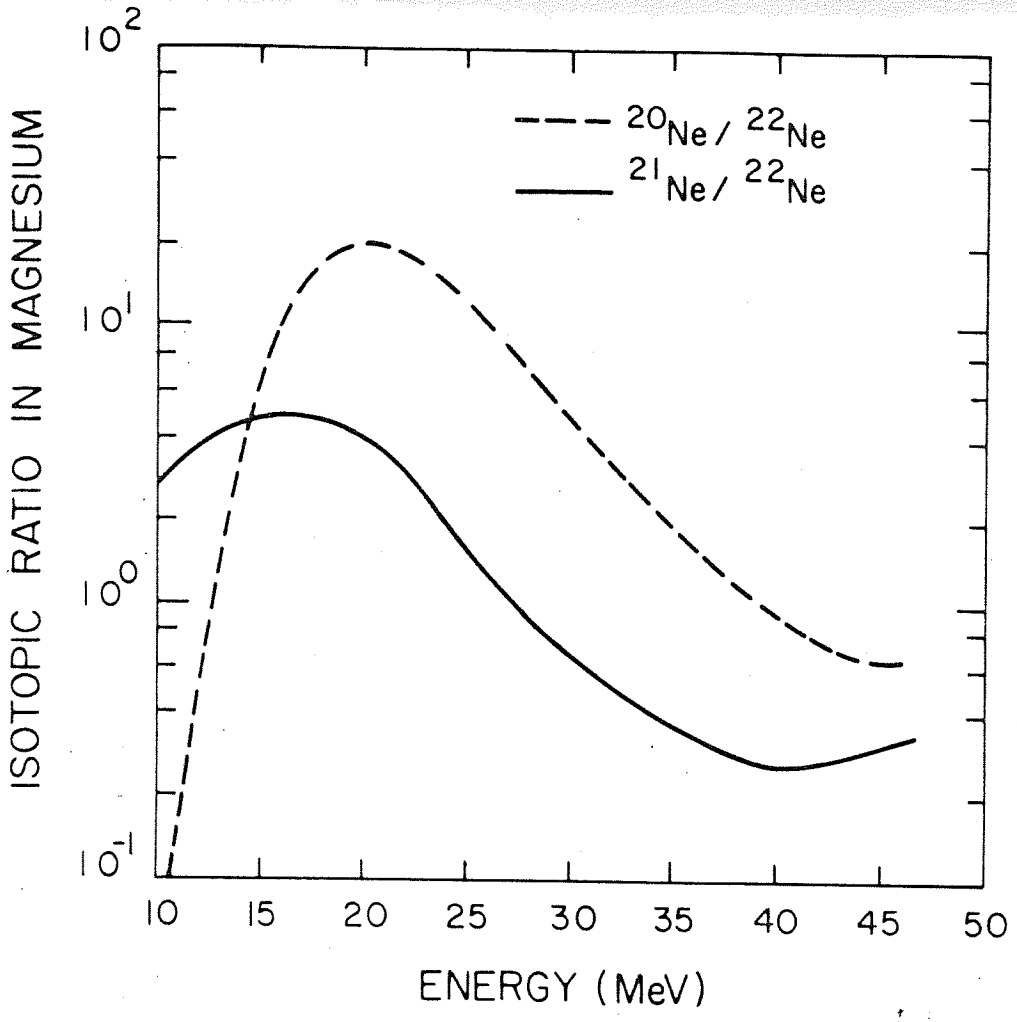

FIG.V.1 SCR PROTON PRODUCED NEON RATIOS IN MAGNESIUM (ADOPTED FROM WALTON, 1974)

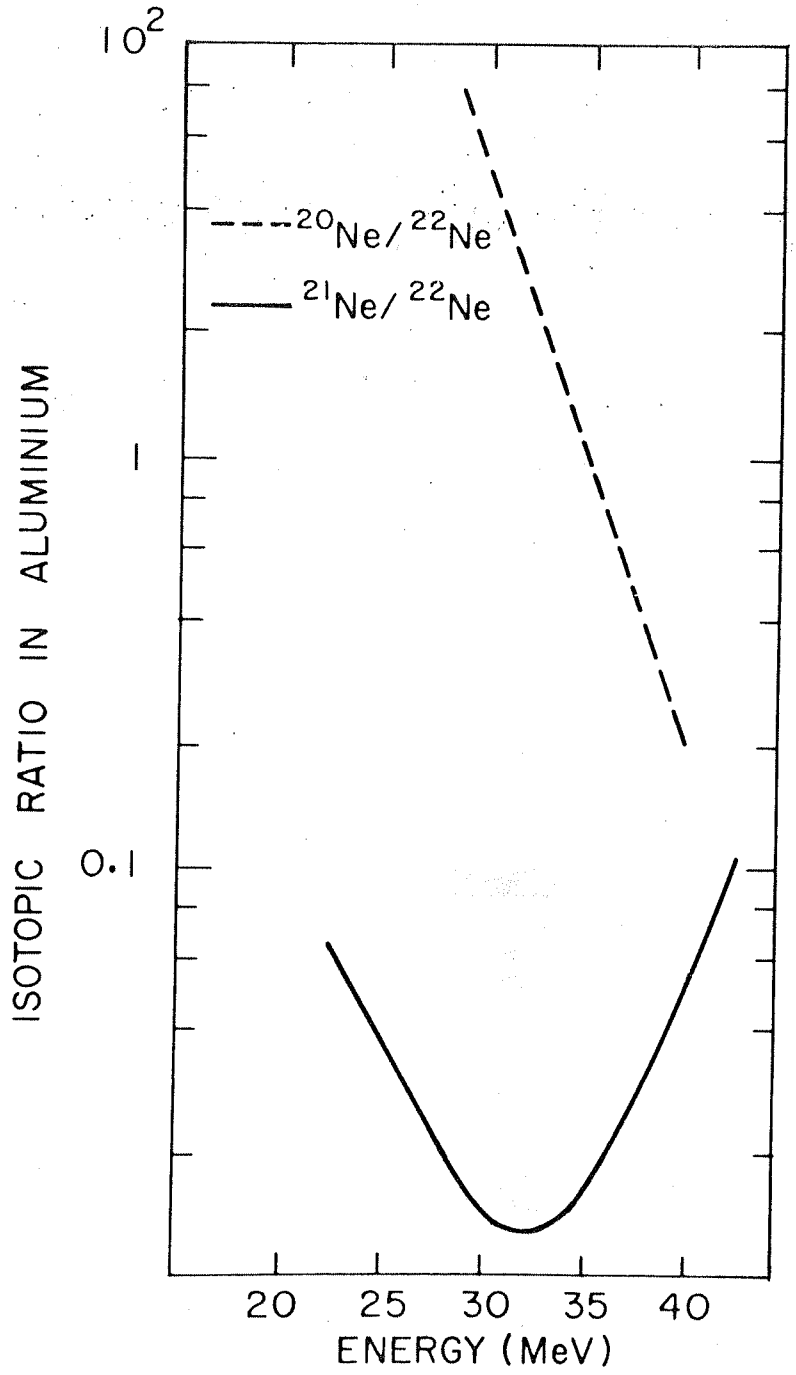

FIG V.2 SCR-PROTON PRODUCED NE-RATIOS IN AL

(ADOPTED FROM WALTON, 1974)

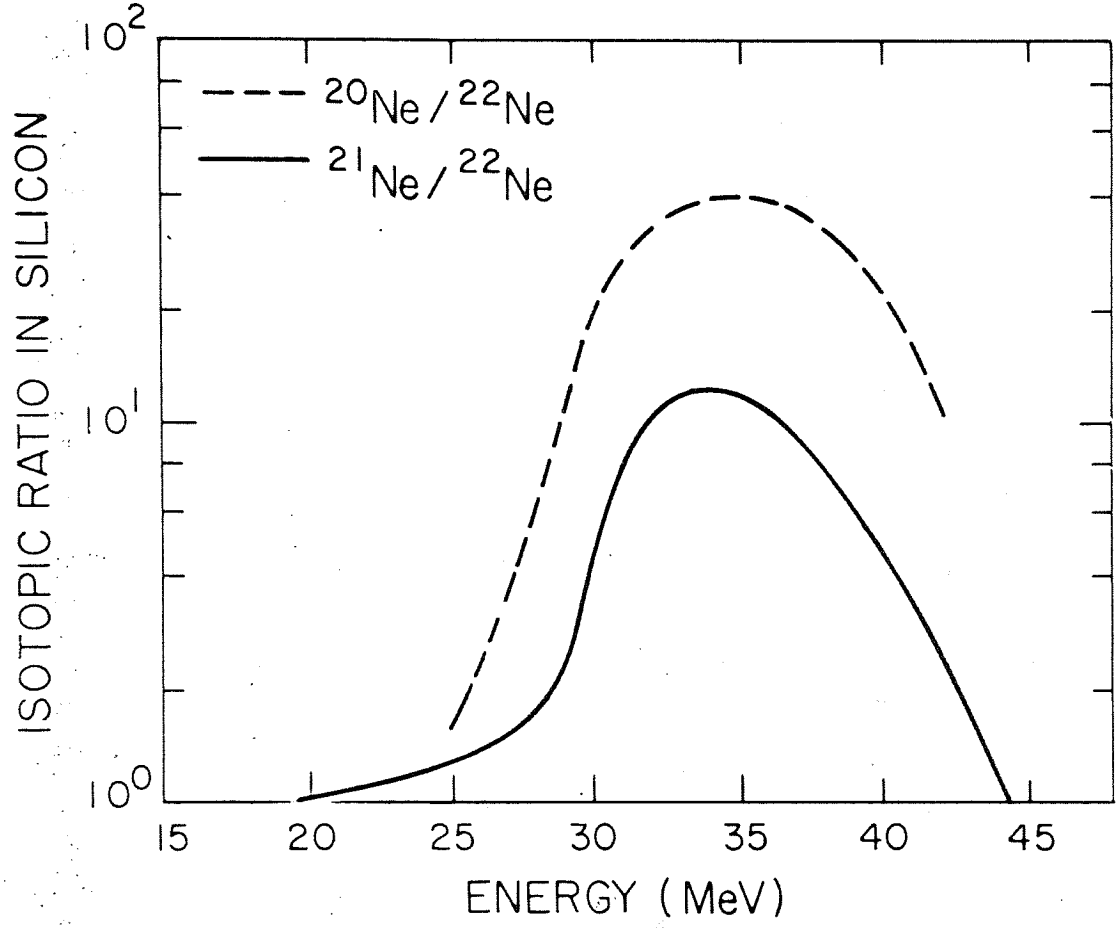

FIG.V.3. SCR PROTON PRODUCED NE ISOTOPIC RATIOS IN SI (ADOPTED FROM WALTON, 1974)

the sake of clarity, experimental points are not plotted and only best fit curves are shown. The differences in excitation functions are apparent for the three target elements Mg, Al, and Si commonly present in silicate minerals. This behavior leads to some interesting consequences. While the $^{21}Ne/^{22}Ne$ value is very high in Mg, it tends to be very low in aluminium. In the case of GCR-induced neon, in contrast, all isotopes are produced in approximately equal amounts. Considering that the ^{21}Ne-production rate in Mg is nearly six times of that in Al and at about 5 g cm^{-2}, it is twice of that in aluminium, one expects that in Mg-rich samples SCR-produced $^{21}Ne/^{22}Ne$ ratio will be closer to the GCR-induced neon ratio. In fact, in the near surface region of lunar samples, SCR $^{21}Ne/^{22}Ne$ ratio can be somewhat higher than the GCR $^{21}Ne/^{22}Ne$ value. In Al the ^{21}Ne production is very low and ^{20}Ne-production is relatively high (Fig. V.2). The depth and composition-dependence of the SCR, make selection of samples very important. Besides, the neon-retentivity in different minerals is also dependent on their crystal-structure and this sometimes leads to the variation in isotopic ratios due to diffusion of neon. These considerations suggest that the bulk samples are not suitable for such studies. Therefore grain size fractions from mineral separates from lunar soils were selected for this study. The etching of these samples greatly aided in reducing SW-interference. The

residence time for soil grains in the top one cm being typically of the order of 20 to 30 Myr (e.g. Arrhenius et. al., 1971), the SCR-effects in noble gases are expected to be observable in etched samples.

B. MATURITY OF THE SOIL SAMPLES

Some of the aliquot samples were analysed for charged particle tracks in order to determine the maturity of the samples and for some samples data from published literature were made use of, as referred to, wherever necessary.

Mineral grains which reside close to the lunar surface show very high track densities ($\geq 10^8$ cm^{-2}) and due to steep SCR energy spectrum, show a steep fall in track-density in going from edge to the centre (Lal and Rajan, 1969; Pellas et al., 1969). The abundance of such grains in a soil sample is a measure of its maturity. The higher the fraction of irradiated grains in a sample, the higher should be the residence time of the soil on the lunar surface. The fraction of irradiated grains, denoted here by N_H/N, is used as a measure of their maturity. Grains with track densities exceeding 10^8 cm^{-2} or displaying track density gradients were considered irradiated grains (N_H).

Fig. V.4 shows the value of N_H/N in the various soils. All the soils considered in this study except 61221 are

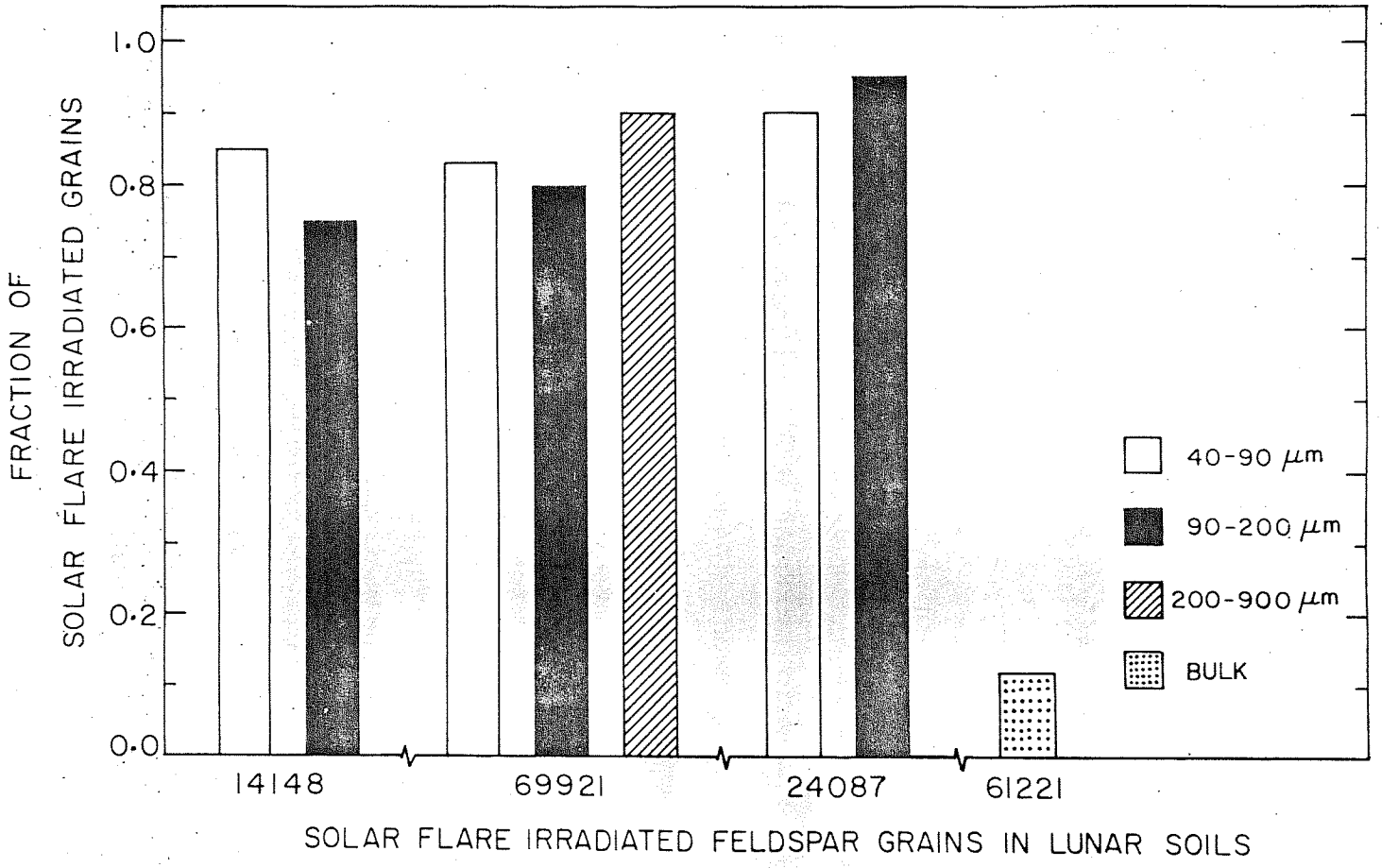
FRACTION OF
SOLAR FLARE IRRADIATED GRAINS
1.0
0.8
0.6
0.4
0.2
0.0
14148
69921
24087
61221
40-90 μm
90-200 μm
200-900 μm
BULK
SOLAR FLARE IRRADIATED FELDSPAR GRAINS IN LUNAR SOILS

FIG. V.4

mature and therefore are expected to contain appreciable amount of SCR-induced component. The feldspar fraction of 14148 (40-90 microns) and 14148 (90-200 microns) have 85% and 75% irradiated grains respectively (Bhai et al., 1978). The soil 24087 (45-200 microns) is also a mature soil (Bhai et al., 1978) with the same size fractions having over 90% irradiated grains. From the soil 69921, the feldspar fraction has been studied and its three size fractions show 80 to 90% irradiated grains. Thus all these soils are mature soils. As a test case, we have studied feldspars from a soil 61221 which is immature by the same criteria and it is expected that the SCR effects should be very small in this sample. The feldspar grains from soil 61221 were analysed for tracks which showed a small fraction (0.12) of irradiated grains.

It is important to mention here that the tracks showing steep density-gradients are formed by the heavy ($Z \geqslant 18$) solar energetic particles (mostly Fe-group nuclei) during residence of grains in the top ($\sim$ 0.1 mm) of the regolith. The SCR-proton induced component, on the other hand, is a result of SCR-proton-interactions (having energy upto $\sim$ 100 MeV) and their effective depth is close to about a centimeter. Thus even if all grains have not accumulated solar flare tracks it is possible that they may have been irradiated by solar protons. But a high N_H/N value suggests

residence of grains in the near surface region of a longer duration (thus resulting in increase in track density in a larger fraction of grains) which in turn indicates a longer duration for exposure to solar cosmic rays also.

The track-data along with several other parameters (Chapter II) give us a qualitative idea whether to expect cosmogenic effects of SCR in these samples. As pointed above, except for the soil 61221, these soils are quite mature and one expects to observe the SCR-proton produced neon in these samples.

C. RESULTS

The results obtained here are presented in two parts in this section. First it is shown that SCR-neon is present in neon observed in etched mineral separates from lunar soils. Next, using the SCR-Ne contents, their surface-exposure ages have been calculated using procedures described in the Chapter III. It should be emphasised that on absolute scale the calculated ages may not be correct. But they can be treated as good indicaters of maturity. Considering the various input parameters that have to be used, these ages at best serve as model ages. As the deviations of the experimental points from the trapped-GCR tie-line are seldom very large, in the single step-analysis, the effects get smeared out due to the dominating trapped component. It is only on

etching and stepwise-heating analysis that the SCR component can be clearly resolved. At low temperatures, where the trapped component dominates and the data points fall close to the trapped end points, SCR-contribution in the released gases is expected to be small but at the higher temperatures, relatively more of spallation (SCR + GCR) neon is released and appreciable deviation from the trapped-GCR tie line in the data points begins to occur.

1. Presence of SCR-produced Neon : The noble gas data for the etched (200-500 microns) size fractions of feldspars from soil 69921, 14148 and 61221 are presented in the Tables V.1, V.2 and V.3. The neon data for these soil samples were earlier presented in Fig. IV.1 along with several other samples. Here neon data for these three samples only are plotted in the Fig. V.5. The pyroxene data for two different size fractions of soil 14148 are presented in Table V.4 and V.5 and plotted in the Fig. V.6.

Deviations of the experimental data points from the trapped-GCR tie-line is indicative of the presence of an additional component viz. the presence of the SCR-components. In Fig. V.5 and V.6 such deviations are evident. The points representing high temperature points fall along the line which joins the trapped (SEP) composition to a composition intermediate between the GCR-composition and the

TABLE V. 1

ISOTOPIC COMPOSITION OF NEON AND ARGON IN ETCHED FEIDSPARS FROM LUNAR SOIL 69921 (200-500 MICRONS)

Temperature (^oC)		Neon			Argon		
		20/22	21/22	22*	38/36	40/36	36*
600		11.429	0.088	90.46	0.216	0.90	81.98
	±	0.100	0.005	2.00	0.003	0.02	4.50
1000		10.153	0.136	153.49	0.253	4.68	430.99
	±	0.050	0.001	3.06	0.004	0.02	22.00
1600		3.866	0.566	6.35	0.349	9.75	145.85
	±	0.007	0.01	0.20	0.050	0.02	8.00
SUM		10.455	0.130	250.30	0.270	5.33	658.83
	±	0.219	0.003	3.61	0.018	0.28	23.84

* The gas amounts are in 10^{-8} cc STP g^{-1}.

TABLE V. 2

THE ISOTOPIC COMPOSITION OF NEON AND ARGON IN ETCHED FEIDSPARS FROM LUNAR SOIL 14148 (200-500 MICRONS)

Temperature (^oC)		Neon			Argon		
		20/22	21/22	22*	38/36	40/36	36*
600		11.95	0.038	464.0	0.188	22.24	868.0
	±	0.18	0.001	15.0	0.0025	0.73	45.0
1000		11.1	0.062	772.0	0.197	2.47	3273.0
	±	0.11	0.001	23.0	0.0035	0.01	65.0
1200		9.22	0.155	18.46	0.196	2.07	1099.0
	±	0.14	0.002	0.35	0.003	0.004	50.0
1600		7.63	0.271	3.06	0.208	4.99	205.0
	±	0.15	0.005	0.12	0.003	0.01	8.0
SUM		11.38	0.055	1257.52	0.196	5.63	5445.0
	±	0.36	0.001	27.46	0.005	0.22	94.0

* The Gas amounts are in 10^{-8} cc STP g^{-1}.

TABLE V.3

THE ISOTOPIC COMPOSITION OF NEON AND ARGON IN FELDSPARE FROM LUNAR SOIL 61221 (200-500 MICRONS)

Temperature (^oC)		Neon			Argon		
		20/22	21/22	22*	38/36	40/36	36*
600		5.94	0.430	50.38	0.220	181.70	171.6
	±	0.09	0.006	1.5	0.03	3.6	8.C
900		7.61	0.313	60.08	0.289	8.88	176.21
	±	0.08	0.004	1.8	0.005	0.25	8.0
1600		6.8	0.340	27.79	0.332	7.100	338.87
	±	0.100	0.005	0.84	0.006	0.250	15.64
Total		6.84	0.361	138.25	0.293	57.19	686.68
	±	0.183	0.010	2.49	0.014	2.69	19.37

*The gas amounts are in 10^{-8} cc STP g^{-1}.

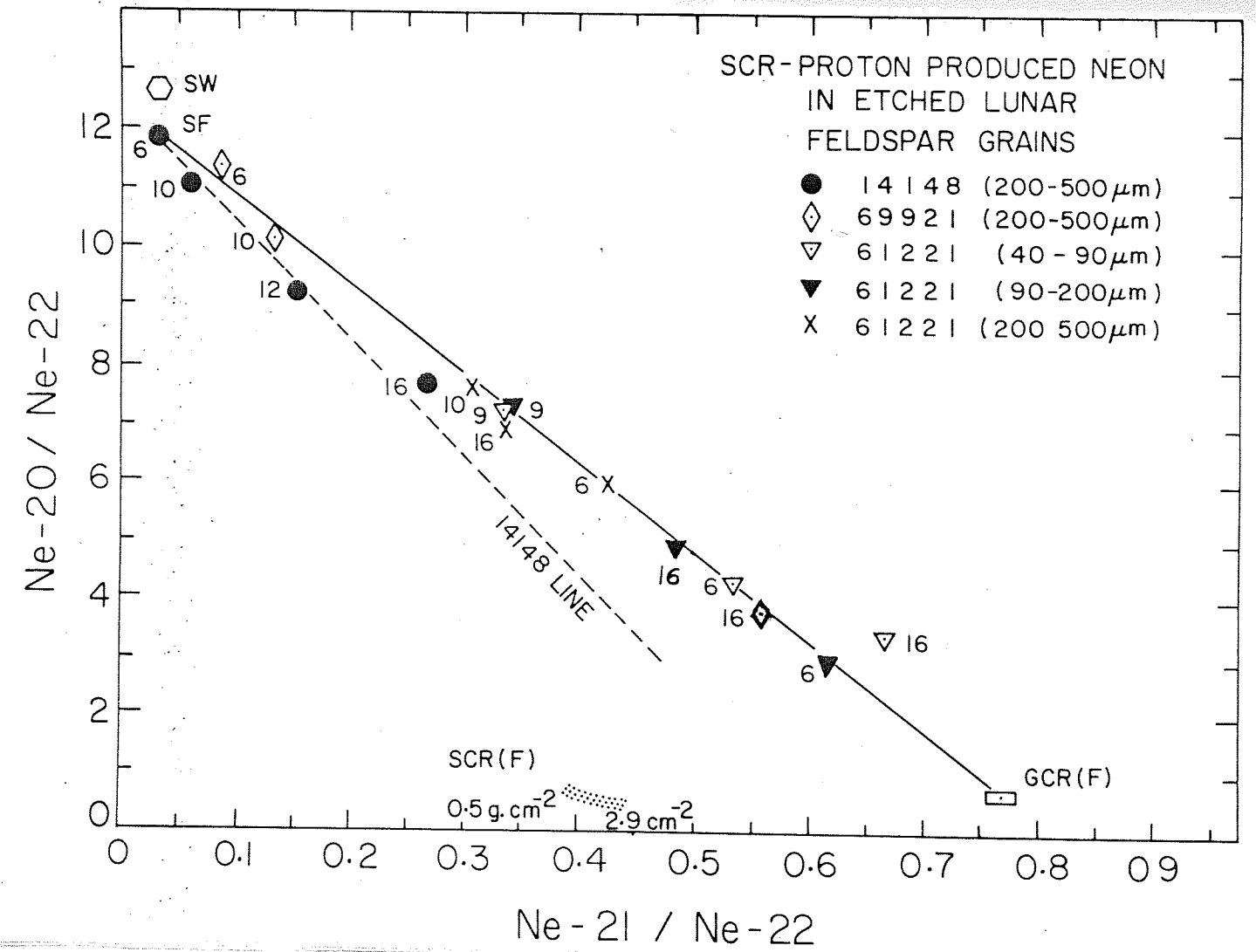

Fig. V.5 The Ne-data from stepwise heating mass-spectrometric analysis of etched lunar feldspars. The mature soils show deviation from the trapped - GCR tie live

TABLE V.4

NEON AND ARGON IN ETCHED PYROXENE GRAINS FROM LUNAR SOIL 14148

(40 - 90 MICRONS)

Temperature		Neon			Argon		
(^{o}C)		20/22	21/22	$^{22}Ne^{*}$	38/36	40/36	36^{*}
600		10.87	0.124	79.1	0.246	20.89	58.38
	±	0.10	0.004	1.2	0.003	0.40	3.00
900		8.61	0.236	84.9	0.363	18.50	47.32
	±	0.06	0.002	1.2	0.005	0.35	3.00
1600		3.73	0.609	51.9	0.796	42.45	30.63
	±	0.10	0.012	0.8	0.015	2.00	1.50
SUM		8.26	0.285	215.9	0.408	24.80	135.54
	±	0.18	0.005	1.9	0.019	1.23	4.50

* Gas amounts in 10^{-8} cc STP g^{-1}.

TABLE V.5

NEON AND ARGON IN ETCHED PYROXENE GRAINS FROM LUNAR SOIL 14148
(90 - 200 MICRONS)

Temperature (^{o}C)		Neon			Argon		
		20/22	21/22	$^{22}Ne^{*}$	38/36	40/36	36^{*}
600		10.01	0.156	84.9	0.255	83.38	92.64
	±	0.15	0.003	2.0	0.004	1.6	4.5
900		6.94	0.381	34.0	0.325	65.67	33.69
	±	0.07	0.005	0.7	0.005	1.3	1.6
1600		4.93	0.524	46.5	0.337	11.3	120.04
	±	0.15	0.020	0.4	0.014	0.3	6.00
SUM		7.95	0.306	165.4	0.304	45.84	246.37
	±	0.18	0.008	2.2	0.14	2.24	7.67

* Gas amounts in 10^{-8} cc STP g^{-1}.

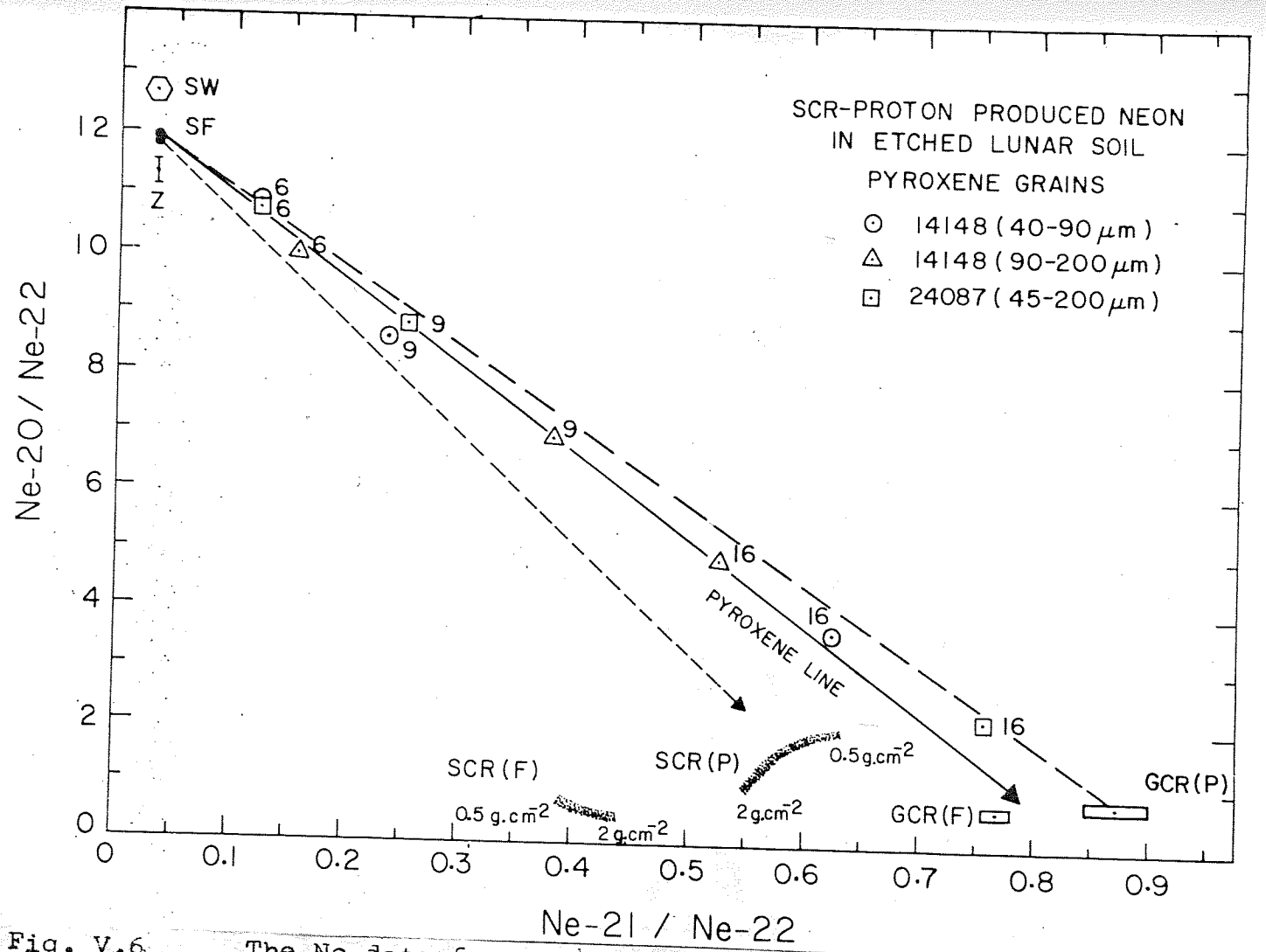

Fig. V.6 The Ne-data from stepwise heating mass-spectrometric analysis of etched lunar pyroxeres. In the case of these soils, the deviation can be seen.

SCR-field, depending on the relative contributions of SCR- and GCR-spallation neon contents. The composition of the trapped component has been taken in accordance with the SEP-Ne values deduced in the Chapter IV viz. $^{20}Ne/^{22}Ne = 11.8$ and $^{21}Ne/^{22}Ne = 0.033$. The SCR-fields for the feldspars and the pyroxenes have been estimated using the production rates given by Hohenberg et al. (1978). The depth-markers indicate the neon composition ensuing due to proton-irradiation occuring at that given depth. If all the samples had fixed spallation-end points then all the stepwise-data-points would fall along a single tie line i.e. SEP-spallation line. But each soil has had its unique exposure history and therefore some differences in the resultant spallation end point can be expected depending upon the relative durations of exposure to the SCR-and GCR-protons.

2. Exposure Ages : Having deduced the composition of the SEP-Ne which dominates the neon in mature samples after removal of SW by etching techniques, estimation of the SCR-proton produced Ne becomes possible. The SCR-and GCR-proton-produced neon-amounts have been calculated using the SEP-Ne composition deduced in chapter IV and the analytical procedures discussed in chapter III. The relevant production rates and end points used in this analysis have also been discussed in the chapter III. The surface exposure ages of soils deduced by SCR-Ne method represent the inte-

grated residence time in the top one centimetre of the lunar regolith and these ages are only model ages. As the amount of SCR-proton produced neon is very small below one centimetre most of the observed SCR-neon is a result of accumulated production during the residence of these grains in the top one centimetre of the lunar regolith. The GCR-exposure age, in contrast, refers to the integrated residence time in $\sim$1 metre of the regolith and therefore is expected to be, in general, higher than the SCR-age.

The SCR-and GCR-exposure ages calculated for the soils 69921 (200-500 microns), 14148 (200-500 microns) and 61221 (200-500 microns) using the feldspar fractions are given in Table V.6. For these three samples the SCR ages are $\geq$21 Myr, 145 $\pm$50 Myr and 4.2 $\pm$ 1.5 Myr respectively. The GCR exposure age for these soils are 213 $\pm$23 Myr 260 $\pm$ 30 Myr and 525 $\pm$ 50 Myr respectively using a GCR production rate of 0.09 cc STP g^{-1} Myr^{-1}. In the case of 69921, a limit is provided because the first temperature fraction (600°C) was suspected to be containing some SW and hence was not included for the three component analysis to find the SCR-exposure age.

Pyroxene samples were well etched (chapter II) and consequently all the experimental points lie within the triangle defined by SEP, SCR and GCR compositions indicating rather complete removal of SW-neon. As pyroxene grains are

TABLE V.6

SCR-AND GCR-EXPOSURE AGES FOR LUNAR SOILS

Sample (Mineral, size-fraction)†	$^{21}Ne^{*}$		Exposure Age (Myr)	
	SCR	GCR	SCR	GCR
14148 (F, 200 - 500)	7.4	25.6	145±50	260±30
14148 (P, 40 - 90)	16.3	40.6	165±60	260±30
14148 (P, 90 - 200)	12.5	34.8	127±45	222±25
69921**(F, 200 - 500)	1.1	19.2	≥20.8	213±23
61221 (F, 200 - 500)	0.21	47.3	4.2±1.5	525±58

*Gas amounts in 10^{-8}cc STP g^{-1}.

**The limits are placed because the first temperature fraction has not been included for S,G,T analysis (see section C)

† The symbols F and P denote feldspar and pyroxere respectively. The size is expressed in microns.

believed to be more retentive in the case of neon, results for these samples are considered to be more definitive compared to feldspars.

The data for etched pyroxene size-separates are given in Table V.4 and V.5 and the exposure ages are given in Table V.6. Using an SCR-production rate of 0.098×10^{-8} cc STP g^{-1} and amounts given in Table V.6, the SCR-ages for 40-90 and 90-200 microns fractions of 14148 pyroxene are 165 ± 60 Myr and 127 ± 45 Myr, very close to the value of 145 ± 50 Myr deduced from feldspars from the same soil 14148. Considering GCR-^{21}Ne amounts in these two samples i.e. $(40.6 \pm 8) \times 10^{-8}$ cc STP g^{-1} and $(34.8 \pm 6) \times 10^{-8}$ cc STP g^{-1} the exposure ages for these two pyroxene fractions are 260 ± 30 Myr and 222 ± 25 Myr using a production rate of 0.156×10^{-8} cc STP g^{-1} Myr^{-1}.

The errors in the GCR-exposure ages are mainly due to the uncertainties in partitioning of Ne-mixtures and the errors in the mass-spectrometric measurements. The errors in the SCR-ages have similar problems and additionally they suffer from the uncertainties in production rate which have been determined by combining depth-profile of production rate with the knowledge of residence time at different depths (see Chapter III).

The discussion is based on observed deviations of the experimental points from the trapped (SW/SEP)-GCR tie line and on the resulting isotopic excesses given in Table V.6. These deviations can not be explained in terms of any components other than SCR. The contributions from Ne-E, atmospheric or planetary component to the lunar samples are too small (if any) to explain the observed trend. The amount of neon produced by SCR is normally a small fraction of the total neon in the lunar sample but the contribution shows up clearly on etching and stepwise-heating analysis. The presence of SCR-produced neon is consistent with the other observed features of solar cosmic rays such as particle-tracks and cosmogenic radionuclides. Also we attempt to trace whether these isotopic excesses could be qualitatively correlated with the degree of solar flare-irradiation as evidenced by other independent criterion such as SF-tracks.

Along with the results of mature soils, those for the immature soil 61221 have also been presented. The immature nature of this soil makes it suitable to bring out the contrast in the behaviour of two kinds of samples : those exposed to the SCR for an appreciable duration (mature soils) and the others either not exposed to the SCR at all or exposed for a very short duration (immature soils). The

difference in the behaviour of the immature soil 61221 and the mature soils such as 69921 or 14148 is evident at the outset as seen in the FIG. V.3. In the case of 61221, it is important to note that all the temperature points for all three etched size fractions follow the same trend without showing any significant deviation from the SEP-GCR line. However, while one should expect to see, in general, such deviations in mature soils, occasionally it is possible to have samples considered 'mature' but not showing SCR-Ne component in some cases. The reason may be that different maturity indices do not refer exactly to the same situation on the lunar surface. For instance a soil sample with surface exposure in the recent few Myr can have saturated radioactivity for short lived radionuclides but if the integrated surface exposure duration is only a couple of Myr, the amount of SCR-component (cosmogenic) may not be very high.

This is one possible reason why the soil 61501 studied by Etique et al. (1981) did not show significant deviations from trapped-GCR line as other soils like 69921, 14148 and 24087 (studied here) even though 61501 contains a good fraction of track rich grains (Bhandari et al., 1972; Wieler et al., 1982) but it is submature to immature as deduced from FMR-scale (Morris, 1978) and low carbon values (Wszolek et al., 1973). It is therefore, suggested that even

though 61501 sample spent enough time (a few Myr) in top 1 mm which was sufficient for accumulation of SF-tracks, prior to this epoch, it could have possibly been buried deeper ($\gtrsim$1 cm) thus accounting for the small amount of SCR-produced Ne.

The table V.6 contains the SCR and GCR exposure ages for the soils studied here.

The SCR-exposure age for the immature soil 61221 is deduced to be about 4.2 $\pm$ 1.5 Myr. The following comments about the GCR age of this soil are in order. This soil has been earlier studied for He, Ne, and N by different groups. Walton et al. (1973) determined its GCR exposure age to be 250 Myr based on the observed ^{21}Ne amount of 43 x 10^{-8} cc STP g^{-1} in bulk sample. The GCR-^{21}Ne determined in this study is also similar to this : 47 x 10^{-8} cc STP g^{-1} in feldspar (200-500 microns) fraction but the deduced age of 525 $\pm$ 50 Myr is nearly a factor of two higher. The discrepancy is due to the production rates used. The production rate used by Walton et al. (1973) was 0.17 x 10^{-8} cc STP g^{-1} Myr^{-1} which is rather high even after considering that they studied bulk sample which may contain higher-magnesium than in pure feldspars. The soil 61221 is a plagioclase rich soil and using the bulk composition given by Rose et al. (1973), the GCR-^{21}Ne production rate is estimated to be 0.10 x 10^{-8} cc STP g^{-1} Myr^{-1}. Use of this

production rate and the amount reported by Walton et al. (1973) yields a GCR exposure age for this soil as 430 Myr considering irradiation at a depth of 20 g cm^{-2}. The ^{15}N-based exposure age given by Becker and Clayton (1977) is 370 Myr for this soil and the ^{126}Xe-based age quoted by them is 530 Myr which is in agreement with the value deduced here. The conclusion of Marwin and Mosie (1980) about 61221 being an old but immature soil is confirmed here from track and neon studies.

A detailed study is undertaken in the case of soil 14148 using two size-fractions (40-90 microns and 90-200 microns) from its pyroxene separate and one size-fraction (200-500 microns) from its feldspar separate. Considering the maturity of the soil, it is expected that the data points for these samples show appreciable deviations from the trapped and GCR-mixing line. Table V.6 contains the SCR and GCR-exposure ages for this soil after deducing the SCR-^{21}Ne excess and using appropriate SCR production rates. There are two points noteworthy about the SCR-ages of these samples. The SCR exposure ages for (40-90 microns) and (90-200 microns) in the case of pyroxene separates are about 165 and 130 Myr respectively and in the case of feldspar (200-500 microns) it is 145 Myr. Within the assigned errors of about $\pm$ 50 Myr they agree with each other indicating the reliability of the decomposition procedures. But these ages

are rather high compared to the surface exposure ages of lunar soils deduced by other methods such as particle tracks. The observed exposure ages can be high provided the grains were allowed to reside at the surface for a longer duration i.e. during a particular epoch of the surface bombardment the micrometeoritic flux was less intense compared to other time periods. Alternatively it could be that the proton flux was somewhat higher than the present value of 70 p cm^{-2} sec^{-1} on which the SCR production rate used here are based.

The surface exposure ages of the soil 14148 was determined by quartile track density method using GCR-particle-tracks and was found to be 20 Myr (Bhandari et al., 1972). Considering the difficulties associated with the quartile track density method at high track densities ($\sim 10^8$ cm^{-2}), the measured age of 20 Myr could be an underestimate and the exposure age of the soil can be revised upwards to a maximum of 50 Myr (J.N.Goswami, personal communication). Also the SCR-^{21}Ne based age has uncertainty associated with it which arise from several factors discussed in section C. But in this case the lower limit for SCR exposure age of pyroxene fractions (90-200 micron) is about 100 Myr. Thus there seems to be a descrepancy of about a factor of two between the exposure ages determined by these two techniques. As the SCR-^{21}Ne techniques developed here

makes use of the time-dependence of depth of irradiation (Duraud et al., 1975), it is believed to be closer to the real situation. It may be relevant here to point out that the ages based on quartile track density method yield consistently lower values than those based on average track-density method by a factor of 2 to 5 (Fleicher et al., 1975) If the extent of uncertainty is that large, than the discrepancy between track and noble gas based ages could be considered to be less significant. But if quartile track density based age has an upper limit of 50 Myr and SCR-^{21}Ne based age has lower limit of $\sim$80 Myr then the only way to make the ages from the two methods compatible with each other is to consider the possibility that the average proton flux during the irradiation epoch of soil 14148 was nearly twice the present accepted value of 70 protons cm^{-2} sec^{-1} for SCR flux. It may be mentioned that some radionuclide-based results have been reported indicating a higher SCR-proton flux (Shukla et al., 1983).

The advantage of the SCR-neon based method lies in its applicability to samples whose surface exposure ages range beyond the resolvablity and saturation-limits of track and radionuclide methods (about 10 Myr). While the track and radionuclide methods become progressively inaccurate at higher exposure ages, the SCR-neon based ages improve in accuracy with increasing surface exposure ages because

detection of the SCR-neon signals in the mass spectrometer become easier. This method takes into account the variation in the depth-history of the grains and uses the time-integrated production rate for age-estimation. Admittedly, the histories of individual soils and different grains in the same soil differ considerably from one another and the SCR-Ne method has several difficulties to surmount. Its dependance on the choice of end points is important and the end points such as for SCR-neon, depends on the cross-section values for the SCR-proton reactions on the target elements. Not all cross sections are measured upto 200 MeV which is the energy range over which SCR-protons are effective. This is in addition to the uncertainties in the regolith-dynamics model. But despite the uncertainties, discussed in section C, this procedure has potential for estimation of surface exposure ages (residence time in the top 1 cm of the regolith) and with improved models for regolith-dynamics and knowledge of end-point compositions, it holds promise as reliable method to study the solar proton fluxes over time scales exceeding 10 Myr. Using lunar soils of different antiquities (from lunar soil cores) one can use this techniques for studying the solar flare proton fluxes at different stages of its evolution during the late history of Sun.

CHAPTER VI

EARLY ACTIVE SUN : CLUES FROM GAS-RICH METEORITES

Our Sun like all other stars has evolved with time, but there is no direct way of knowing about the intermediate stages of its evolution. While the astronomical evidence for several young stars suggest a highly active (T Tauri-like phase during their early phases of evolution, any such evidence for our Sun can be obtained from the fossil records trapped in lunar and meteoritic grains. Lunar samples, being free from ablation-effects do provide records of solar activity upto several hundred million years back from now but they do not date back to the epoch representing the early evolution of the Sun. The possibility that such records can be found in gas-rich meteorites is what makes the study of gas-rich meteorites interesting. In this chapter an attempt is made to decipher the records of early active Sun in the gas-rich meteorites.

A. ISOTOPIC ANOMALIES AND THE EARLY IRRADIATION

During the last decade several isotopic anomalies such as in ^{26}Mg and ^{107}Ag were discovered (Clayton et al., 1973; Kaiser and Wasserburg, 1983). Hypothesis of local irradiation was offered as one of the explanations. This hypothesis explains, though not without difficulties, the production

of pure ^{22}Ne through ^{22}Na and of ^{26}Mg through ^{26}Al by proton-irradiation with a flux equivalent to 10^{23} protons cm^{-2} Myr^{-1} at 1 MeV. (Heyman and Dziczkeniec, 1976). A study of heavily radiation-damaged fine sized grains from C1 meteorite Orgueil (Audouze et al., 1976) suggested a lower limit of about 3×10^{18} protons cm^{-2} at 0.1 MeV This was based on observations of high density of tiny crystallites presumably due to VH-nuclei of 0.1 MeV energy. For producing enough ^{26}Al to melt the planetary cores the minimum required fluence at an optimum energy of 40 MeV was calculated to be 4×10^{18} protons cm^{-2} by Schramm (1971). Recently Kaiser and Wasserburg (1983) also considered proton-irradiation as a possibility to explain their observations of Pd-correlated excess ^{107}Ag in some ataxites and an octahedrite Grant. While their observations are also consistent with GeV proton-irradiation, they have preferred irradiation by 30 MeV protons of solar origin which dispenses with the high shielding ($\sim$1 metre) needed to produce secondary neutrons. It need be pointed out that the fluence-estimates based on radionuclides are strictly lower limits because decay accompanies the production and much higher fluence is required to produce the same effect if the irradiation duration is long. Many such features were suggested in the past to be due to effects of solar particles. An attempt is made in this chapter to identify the cosmogenic effects of solar cosmic ray protons to which dark portions of the gas-rich meteorites were presumably exposed in the ancient past.

B. GAS-RICH METEORITES

The records of low energy solar radiations are confined to the outer layers of the meteorites and are normally lost by them when they fall through the atmosphere and their outer layer gets ablated. But some meteorites known as gas-rich meteorites have these records preserved which were presumably acquired in their parent-body regoliths in the ancient past. These meteorites are brecciated meteorites containing material once upon a time irradiated by solar particles. These meteorites are characterized by the presence of the light clasts in the dark host matrix. The darkening of the matrix is generally attributed to its finer grain size. some consider it to be result of admixing of some extraneous phase such as carbonaceous material as orginally suggested by Müller and Zähringer (1966), Major and Anders (1967). However, the nearly identical chemical composition of the light and dark portions in these meteorites suggest a common source for both the phases (König et al., 1964, Begeman and Heinzinger, 1969) but exotic clasts were also discovered in the dark portions (Wilkening, 1976).

1. Regolithic Origin : These meteorites contain enormous noble gas amounts. First discovery of Pesyanoe as a Gas-rich meteorite (Gerling and Levskii, 1956) was followed by many more such discoveries (Zähringer and Gentner, 1960; König et al., 1961; Hintenberger et al., 1962; König et al.

1962; Signer and Suess, 1963; Manuel and Kuroda 1964; Manuel 1967). Eventhough these meteorites display light and dark structures, dark texture of the samples does not ensure enrichment of high noble gas contents in them. However, the vice-versa is true. Siting of these gases remained obscure until the experiments of Eberhardt et al. (1963) who showed the excess gases to be confined to outer $\sim$0.1 micron of the grains by etching away the grain-skins and measuring the residual gases. Suggestion of Suess et al. (1964) for solar wind origin of these gases received confirmation when lunar samples arrived in 1969. But before lunar samples arrived, Lal and Rajan (1969) and Pellas et al. (1969), based on their observation of high track density and track gradient in crystals from these meteorites had proposed that these grains had been exposed to solar flare particles in the past. Detailed studies and comparison with lunar soil revealed assymetric irradiation pattern and it was this similarity with the lunar soils which led Wilkening (1971), Rajan (1974) and McDougall et al. (1974) to conclude regolithic origin for these meteorites.

2. Gas-rich Mateorites and Lunar Soil : Detailed account of the interesting debate over origin of the various features of the gas-rich mateorites was given by Suess et al. (1964), Wilkening (1971), McDougall et al. (1974). Here, only those characteristics of the gas-rich meteorites are

outlined which bring out their comparative features with lunar soils and breccias. Several lunar breccias show the light and dark structure similar to that in the gas-rich meteorites. The dark portions of lunar and meteoritic breccias and the lunar soils contain regolith-components i.e. mineral grains showing SF-irradiation features such as high track densities but the percentage of such grains is smaller in meteorites compared to lunar soils (Crozaz and Dust, 1977; Goswami et al., 1976). Trapped noble gas content of these meteorites have also been found to be lower correspondingly (Anders, 1975). As the cratering flux for meteorite-parent bodies several Gyr ago is expected to have been higher than for the moon in the recent past and the lower gravity causes major portion of the impact ejecta to escape from the meteorite parent body, the mean residence time of the material on the regoliths is lower. All these factors combined together indicate a less mature regolith on gas-rich meteorite-parent-bodies which is also evidenced by the absence of amorphous layers on silicate grains from meteorites in contrast with those in lunar soils (Bibring et al., 1974). Further, agglutinates are absent in gas-rich meteorites (Kerridge and Kieffer, 1977; Rajan et al., 1974). Due to larger distance from the Sun, the flux of solar wind is also lower by an order of magnitude at the asteroidal belt following inverse square law-dependence (Parker, 1963). Similarly the SCR flux is also expected to be lower at the

location of meteorite-parent-bodies i.e. asteroidal belt. Based on emperical reasoning, Anders (1975, 1978) estimated three orders of magnitude lower noble gas concentration in the gas-rich meteorites compared to lunar soils which is in agreement with the observations.

3. Epoch of Irradiation : Despite the difficulties listed above, gas-rich meteorites score over the lunar-samples in one respect : the antiquity. These meteorites have presumably witnessed early activity of our Sun which lunar samples have not or if they have, they have lost the records of ancient irradiation i.e. of about 4.6 Gyr ago. Meteorites formed nearly 4.6 Gyr ago and it is likely that they acquired their regolith-features at that time. However, it is difficult to establish that the irradiation of the meteorites took place about 4.6 Gyr ago. Poupeau et al. (1974) inferred from the possible high cratering rate history (manifested in low track-density, low gas-concentration etc.) of these meteorites that the irradiation was ancient and at a time when cratering flux was higher. Price et al. (1975), on the other hand, opined that the idea of ancient irradiation is more an assumption rather than a proven fact. Brecciation is an ongoing process in the solar system as evidenced by 1.2 Gyr old xenolith in St. Mesmin (Schultz and Signer, 1977) but many xenoliths do date back to about 4.6 Gyr. Based on ^{244}Pu fission-tracks in whitlockite grains

from gas-rich meteorites Fayetteville, Weston and St.Mesmin, Kothari and Rajan (1982) dated the last track erasing event to have occured about 4.5 Gyr ago. Considering the low track retention charasteristics of whitlockite grains and near absence of any track-resetting features in them (Pellas and Storzer, 1981) suggest the possibility that the regolith exposure was old. Evidence showing long association of adjascent crystals (McDougall et al., 1974) as was found with ^{244}Pu-tracks in the case of carbonaceous chondrites may hold clue to this long standing problem.

C. STUDY OF ANCIENT SCR-ENERGY SPECTRUM

The qualitative similarities of gas-rich meteorites with lunar soils and lunar breceias suggest that the SCR-signatures well studied in lunar samples can be searched for in meteorites. Attempts were made in the past to deduce the ancient SCR spectrum using particle tracks (Rajan, 1974). However, as minor dust coating can always flatten the track profile in a given sample, flatter (harder) spectral shapes, whenever found, were dismissed as artifacts. The approach adopted was to take the steepest observed spectrum as the correct spectrum of solar flare Fe-nuclei. Rajan (1974) compared the spectra deduced from several gas-rich meteorites with those from lunar rock crystals from documented samples. It was found that Kapoeta, Breitcheid, lunar soil grains, a grain from a breccia, surveyor camera glass and a vug from

the lunar rock 15499 showed nearly similar spectral shapes. Some suggestion of steeper energy spectrum was found in the case of Fayetteville. However, it was concluded by Rajan (1974) that SCR-spectrum in the last 4 Gyr or so has remained unchanged.

Two points may be noted about these observations. One is that the track measurements were confined to outer 100 microns or less of meteoritic grains and the other is that normally flattening is observed at the low energy end of the spectrum. This flattening at 3 AU may be genuine because, as Lee (1976) pointed out, the low energy (< 15 MeV/nucleon) SEP-flux falls as R^{-3} rather than R^{-2} where R is the heliocentric distance. The track-studies refer to the solar flare nuclei of energy upto about 10 MeV nucleon^{-1} (100 micron range corresponds to about 10 MeV nucleon^{-1} in silicate material) while the experiments reported in this chapter are aimed at deciphering the records of the solar flare proton component ($\gtrsim 10$ MeV) which can induce nuclear reactions.

D. RESULTS

Results of the stepwise heating data on two gas-rich chondrites Pantar (H-5) and Leighton (H-5) are presented in Table VI.1 and VI.2.

The neon data for these two meteorites are plotted

TABLE VI.1

NEON IN GAS-RICH METEORITE PANTAR

Temp:		20/22	21/22	22*
Pantar-Dark				
500		12.65	0.0459	1.388
	±	0.15	0.0007	0.040
600		11.38	0.0529	3.106
	±	0.15	0.0006	0.060
800		10.96	0.0567	5.680
	±	0.11	0.0006	0.110
1000		10.73	0.0670	4.405
	±	0.10	0.0007	0.088
1200		9.8	0.1110	2.856
	±	0.10	0.0010	0.050
1600		8.38	0.2173	1.091
	±	0.12	0.0030	0.035
SUM		10.78	0.0752	18.5269
	±	0.15	0.001	0.17
Pantar-Light				
600		1.099	0.831	0.224
	±	0.001	0.008	0.006
1000		0.752	0.907	0.450
	±	0.15	0.012	0.009
1600		1.6607	0.831	0.408
	±	0.020	0.012	0.010
SUM		1.167	0.8636	1.082
	±	0.253	0.180	0.015

TABLE VI.2

NEON IN LEIGHTON (DARK)

Temperature		20/22	21/22	22*
500		12.13	0.0548	9.74
	±	0.14	0.006	0.12
800		10.98	0.0881	7.88
	±	0.14	0.0010	0.15
1200		9.74	0.1304	7.32
	±	0.10	0.0015	0.14
1600		7.50	0.3049	0.88
	±	0.11	0.0040	0.17
SUM		10.82	0.0950	25.81
	±	0.18	0.0030	0.29

* Gas amounts in 10^{-8}cc STP g^{-1}.

FIGURE CAPTION

Fig. VI.1 The stepwise heating data points in the gas-rich meteorites show a trend similar to that shown by lunar soils. However, the deviation from the SEP (or SW) - GCR tie line is more for the meteorites. The SCR- field shown is for the pyroxenes under present lunar conditions. The inset shows the low temperature points for these meteorites in detail. The data for Fayetteville D-1 are taken from Black (1972 a). Other available data sets for Fayetteville (Black, 1972 a; Manuel, 1967) are not plotted here but they also show similar deviation.

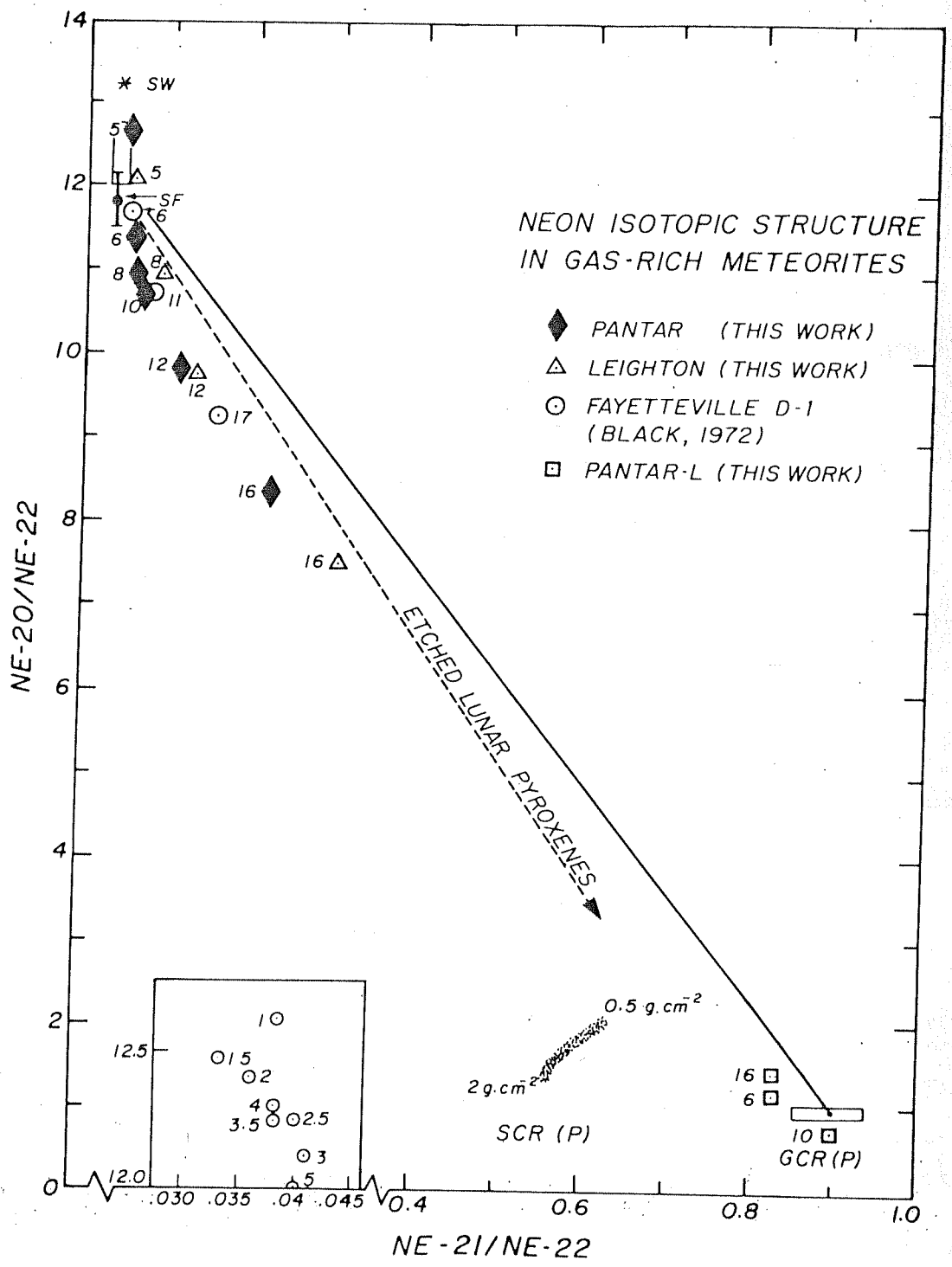
NEON ISOTOPIC STRUCTURE
IN GAS-RICH METEORITES
PANTAR (THIS WORK)
LEIGHTON (THIS WORK)
FAYETTEVILLE D-1
(BLACK, 1972)
PANTAR-L (THIS WORK)
ETCHED LUNAR PYROXENES
0.5 g.cm⁻²
2 g.cm⁻²
SCR (P)
GCR (P)
SW
SF
NE-20/NE-22
NE-21/NE-22

FIG. VI.1

in Fig. VI.1 along with data on Fayetteville D-1 (Black, 1972). The Ne-data for pantar light is presented in Table VI.1.

1. The Neon Data : The similarity between the trend of data points of gas-rich meteorites and that of lunar soils is evident. The data points show a deviation from the tie-line between SW and GCR and more precisely that joining SEP to GCR. Because of etching, the lunar soil data-points fell somewhat below the SW-end point. But in the case of meteorites they fall close to the solar wind-end point. Thereafter the $^{20}Ne/^{22}Ne$ ratios decrease as shown in the Fig. VI.1, but the change in the $^{21}Ne/^{22}Ne$ ratio is very small until temperature of about 800-1000^{o}C is reached. It is at these temperatures and above that the spallation components start showing up. However, the GCR-exposure duration of the lunar soils being much longer, their high temperature points could move much closer to the GCR-end points in the three isotope neon diagram. Pantar was analysed in six temperature steps. The 500^{o}C temperature datum point falls close to the SW-end point as expected. The following points show lower $^{20}Ne/^{22}Ne$ ratio and higher $^{21}Ne/^{22}Ne$ indicating progressive release of the spallation component. However, upto 1000^{o}C, the data points are still close to the SW-SEP tie-line and only at high temperature they show a clear evidence for the

spallation component. The Ne-composition in the Pantar-light sample is in complete contrast with all the three temperature data points falling near the GCR-end point (Fig. VI.1).

Leighton was analysed in four temperature-steps. The first temperature fraction shows a lower $^{20}Ne/^{22}Ne$ value than Pantar though the trend shown by Leighton (dark) points is similar to that shown by Pantar (dark). The Total $^{20}Ne/^{22}Ne$ value for these two meteorites are 10.78 and 10.82 respectively.

In view of the variability of the trapped gas-contents in different samples of gas rich meteorites, comparison of gas amounts with literature values is difficult. However, the ^{22}Ne amount of 1.08×10^{-8} cc STP g^{-1} measured in Pantar (Light) is in agreement with that of 1.04×10^{-8} cc STP g^{-1} in Pantar (Light) analysed by Hintenberger et al. (1962) and Hintenberger et al. (1964). The Pantar (Light) data is also plotted in Fig. VI.1 for comparison and all the points fall close to the GCR-end point, showing that it is almost pure GCR-spallation neon.

2. Neon Isotopic Excesses : The deviation of the data points from the SW/SCR tie line or SF-GCR line is a noteworthy feature in this study which indicates isotopic

excesses. It is to be expected that a third component is responsible for this shift. The possibility of the carbonaceous material being responsible for the shift can be ruled out based on several arguments. Müller and Zähringer (1966) were the first to suggest the possibility of a carbonaceous carrier phase to explain the high abundance of the noble gases in the dark portions of gas-rich meteorites. However, subsequent experiments showed that the source of the excess noble gases was not any carbonaceous carrier but solar wind (Eberhardt et al., 1965). Wilkening (1976) suggested that about mm sized carbonaceous chondrite material could be present in the dark portion of gas-rich meteorites. This idea was put forward to explain the excess volatile elements in these phases. However, this suggestion was examined by Bart and Lipshutz (1981) who concluded that the excess volatile-abundance did not correspond to C1 or C2 composition. According to McSween et al. (1980, 1981) and Dreibus and Wänke (1980), these excesses volatile elements are a result of mobility in the parent-body-interior rather than any extraneous component. If the dark portions are nearly free from carbonaceous chondrite-meterial, the presence of planetary gas component in the dark part will be negligible. Moniot (1980) has indeed shown that the planetary gases are present in the ordinary meteorites only in insignificant amounts.

3. Decomposition into Various Components Constituting the Mixtures : With the result of chapter V before us, as earlier discussed, we know of one such component which can lead to the production of observed deviations in the experimental points. The presence of SW-gases and abundance of track-rich grains (Lal and Rajan, 1969; Pellas et al., 1969) suggest that the dark portions of gas-rich meteorites were subjected to SCR-irradiation in the ancient past. Below, this proposal of SCR-irradiation is examined considering two cases. In one we consider that the neon observed in the dark portions of the gas-rich meteorites is a mixture of SW, SEP (or SF), GCR-spallation and ancient SCR-spallation. In the other we consider incorporation of a component which is highly enriched in ^{22}Ne compared to ^{20}Ne or ^{21}Ne. The procedures discussed in Chapter III have been used to resolve the observed amounts into different components.

The end points for SW, and GCR are chosen as described in Chapter III and for SEP as discussed in Chapter IV.

(1) SCR-proton Irradiation : The isotopic signatures of the SCR-protons are distinct from those due to the GCR. The difference arises due to their different energy spectra. It follows that the difference in the proton spectra of SCR- can result in production of a different neon isotopic composition. To explain the deviation

of the meteorite data points, what is needed is a component with low $^{21}Ne/^{22}Ne$-ratio. The SCR-protons with contemporary spectrum produce a $^{21}Ne/^{22}Ne$ ratio of about 0.6 in pyroxene (Chapter III, V). But with this ratio the meteorite data points cannot be explained and a different spectrum is needed. Considering the narrow range of $^{21}Ne/^{22}Ne$ ratios one is allowed, the limits on the energy range of the protons seem to be stringent. As is clear from Fig. 1 of Chapter V, in Mg the lowest possible $^{21}Ne/^{22}Ne$ ratio occurs at nearly 30-40 MeV energy. At both lower and higher energies, this ratio becomes larger. These excitation functions for Ne-production by low energy protons have been reported by Walton et. al. (1976 a, b) as discussed earlier in Chapter V. It is therefore concluded that the energy spectrum of the solar protons responsible for the production of Ne with low $^{21}Ne/^{22}Ne$ is a pulse-shaped spectrum peaking around 35 MeV with the low energy protons sufficiently suppressed, rather than the usual power law. Alternatively the spectrum can be steep with a lower cut off at about 30 MeV. Since flux is considered to fall steeply with energy, the high energy part of the spectrum does not contribute significantly to the total neon production as the proton flux in the high energy region is low. It is interesting to note that a harder energy spectrum may not be appropriate due to higher $^{21}Ne/^{22}Ne$ which would result at low energies. With these considerations in mind, the ^{21}Ne amount due to different components have been

calculated and presented in the table VI.4. The table includes SCR and GCR produced ^{21}Ne under 2 entries A and B. The values under entry 'A' refer to ^{21}Ne amounts resolved using the combination of $^{20}Ne/^{22}Ne = 1.0$ and $^{21}Ne/^{22}Ne = 0.2$. The values under B are those resolved using 1.0 and 0.25 combination. The GCR and SEP-values used are those given in Chapter III and Chapter IV respectively. In addition to Pantar and Leighton, Fayetleville D-1 data (Black, 1972) has also been considered for analysing because it is a well known gas-rich meteorite. As better GCR-production rates have become available recently (Nishiijumi et al., 1981), the GCR exposure ages given are the re-calculated ones. The GCR exposure ages found in this study using dark portions of Pantar, Leighton and Fayetteville are about 2, 4 and 20 Myr as against the value of 3, 6 and 30 Myr based on measurements on the light part (Schultz and Kruse, 1978; Hintenberger et al., 1962; Signer and Suess, 1963; Manuel and Kuroda, 1964). One notices that the GCR-exposure ages deduced in these model calculations are lower than the values based on the analysis of the light portions of the same meteorites. This may partly be due to compounding of errors in choosing different end points or may be genuine. For instance Weston is known to have had complex exposure history with different exposure ages for different parts (Schultz et. al., 1972).

TABLE VI. 3

SCR AND GCR PRODUCED NEON IN GAS-RICH METEORITES AND THEIR EXPOSURE AGES

Meteorite	^{21}Ne*		GCR-Exposure ages (Myr)	
	SCR	GCR	Model	Literature**
Case A:				
Pantar	0.23	0.62	2	2.9, 3.2
Leighton	0.16	1.32	4.4	5.7
Fayetteville+	1.62	6.41	21.4	30.0
Case B:				
Pantar	0.31	0.54	1.8	2.9, 3.2
Leighton	0.22	1.25	4.1	5.7
Fayetteville+	2.2	5.84	19.5	30.

Case A and B refer to the choice of SCR-end points of (1,0.2) and (1,0.25) respectively.

*Gas amounts in 10^{-8}cc STP g^{-1}.

**Exposure ages are recalculated using production rate given by Nishiijumi et al., 1980 (see text). The ages are based on ^{21}Ne amounts reported in this work (Pantar); Hintenberger et al.,1961 (Pantar); Signer and Suess, 1963 (Pantar); Schultz and Kruse, 1977 (Leighton) and Manuel and Kuroda, 1964 (Fayetteville).

+Based on data for Fayetteville D-1 (Black, 1972).

(2) Incorporation of the Pure ^{22}Ne Phase : The observed trend of neon-isotopic structure in these meteorites need lowering of the $^{21}Ne/^{22}Ne$ ratio. It was shown above that this is possible by considering SCR-irradiation. However another possibility for explaining the Ne-trend has been considered viz. addition of a pure ^{22}Ne phase to the dark portion of these meteorites. In fact, this also leads to deviation of the points from SW (or SF)-GCR tie line. While considering admixture of pure ^{22}Ne phase or incorporation/production of pure ^{22}Ne, SW and GCR are two end points and pure ^{22}Ne is the third end point. In this case all the data points are considered (unlike the previous case where only data points below SEP-composition were considered for the three component analysis.) The GCR ages deduced in this manner (given in column B of Table VI.4) are in agreement with the values deduced from the ^{21}Ne concentration in the light parts or deduced from the inferred cosmogenic ^{21}Ne in relatively gas-poor parts (Manuel and Kuroda, 1964; Schultz and Kruse, 1978). Since the ^{22}Ne amounts needed to explain the deviations in data points are small ($\leq 1 \times 10^{-8}$ cc STP g^{-1}), detection of nearly pure ^{22}Ne is difficult. At present it is difficult to explain how the pure ^{22}Ne could have been incorporated in the dark portion of the meteorite. It is possible that the light portions of the gas-rich meteorites received additional GCR-exposure on the parent body and the agreement of the ages deduced with pure ^{22}Ne as a component is fortuitous.

TABLE VI. 4

GCR EXPOSURE AGES OF GAS-RICH METEORITES (CONSIDERING MIXING OF PURE ^{22}Ne-COMPONENT)

Meteorite	^{22}Ne*		^{21}Ne*		GCR-Exposure-age (Myr	
	^{22}Ne Phase	GCR	^{22}Ne Phase	GCR	Model	Literature**
Pantar (H-5)	1.81	1.00	-	0.87	2.9	2.9, 3.2
Leighton (H-5)	1.89	1.98	-	1.7	5.7	5.7
Fayetteville (H4-H6)	18.9	10.3	-	9.0	30	33

* Gas amounts in 10^{-8}cc STP g^{-1}.

** The sources for the GCR- ages are same as in Table VI.3.

4. Flux Requirement : The acceptance of SCR-irradiation-scenario for explaining the isotopic excesses seen in the gas-rich meteorites needs two conditions to be fulfilled. One is conditions on the ancient Sun and of the interplanetary medium which result in high abundance of about 35 MeV proton flux or a very steep energy spectrum with a low energy cut off around 35 MeV. The second is availability of very high proton fluxes.

From Table VI.4, we can see that the ^{21}Ne required to be produced by 30-40 MeV proton beam is about 0.2 to 1 x 10^{-8} cc STP g^{-1} sample. Using a cross section of 25 mb at this energy (Walton, 1974) and irradiation of $\sim$200 micron-grains, the proton fluence at 3 AU is calculated to be 0.8 to 4 x 10^{17} protons cm^{-2}. If we consider that 200 micron grains spend nearly 10^4-10^5 Yrs (Duraud et al., 1975; Shoemaker et. al., 1970) at the surface, then flux turns out to be nearly 10^4 protons $cm^{-2}sec^{-1}$. But this flux estimates hold good at a distance of about 3 AU. Considering the inverse square law radial dependence of flux, the flux at 1 AU should be 10^5 protons cm^{-2} sec^{-1}. Besides this, average residence time on meteorite parent body is expected to be lower so that this flux is the lower limit. However, the solar proton flux in the recent past has been estimated to be 70 protons $cm^{-2}sec^{-1}$ (Reedy and Arnold, 1972; Kohl et al., 1978; Rao and Venkatesan, 1980) with a power law spectrum. This indicates about three

orders of magnitude higher average proton flux during the epoch of irradiation of the gas-rich meteorites i.e. about 4.6 Gyr ago.

E. DISCUSSION

The discussion is based on two main conclusions reached in section D.

(i) The dark portions of gas-rich meteorites contain material irradiated by solar flare protons with an energy spectrum which peaks at about 30-40 MeV energy.

(ii) During the irradiation epoch of the gas rich meteorite, the solar flare proton flux was nearly three orders of magnitude higher than the contemporary flux.

1. Generation of the Pulse-shaped Spectrum : A qualitative attempt is made here to understand the possibilities of generation of 30 to 40 MeV energy protons in solar flares in the ancient past. Acceleration of particles due to collisions with the moving magnetic field configurations (magnetic mirrors) results in a power law energy spectrum (Fermi, 1949) but all the spectral features of solar flare particles can not be accounted for by this mechanism alone. The basic physical process responsible for the accelecation

of the solar flare particles to high energies is mostly due to anhilation of the magnetic field lines in the flare region as proposed by Petscheck (1964) and Sonnerup (1970) and others which results in a rapid conversion of magnetic energy into kinetic energy.

A set of processes combined together can yield the desired spectral shape i.e. flux peaking at ~ 35 MeV. As the magnetic field lines tend to force the charged particles to follow them, a minimum energy is required for the charged particles for crossing the given magnetic field lines. Price et al. (1971) and Cartwright and Mogro-Campero (1973) have suggested that injection of particles into the acceleration zone of solar flares on the Sun is rigidity (or equivalently energy) dependent. After the entry, the protons gain energy and remain confined to the acceleration region untill the surrounding magnetic pressure is unable to hold them (Dorman and Miroschnichenko, 1976). Magnetic fields in the sun-spots can be several thousand gauss and above the chromosphere also they can be of the order of a few hundred gauss (e.g. Elliot, 1973; Švestka, 1976). But in the early stages of the evolution of the Sun, these fields could be still higher (Fowler, Greenstein and Hoyle, 1962). In the young stars, magnetic fields indeed have been found to be much higher (Skunamich, 1972). Thus for the young Sun, the escape of particles from the acceleration zone would also

be more difficult for a given energy. Bryant et al. (1965) and Simnett (1971) drew attention to several observations of contemporary solar flares suggesting trapping of the electrons and protons on Sun. Simnett (1971) has cited examples of flares which were accompanied by emission of electromagnetic radiations such as X-rays and ultraviolet rays but no particle enhancements were observed at earth. In these cases the propagation could not be responsible for the absence of particles because of favourable location of the flare on solar surface i.e. on the western limb. Earlier McDonald and Desai (1971) had also suggested the possibility of storage of protons ($\sim$ 10 MeV) to explain their observation that particle flux increases in the late stages of the flares. Meerson and Rogacheviskii (1983) discussed instability in cyclotron wave in the corona and inferred that it is possible to trap protons of about 10 MeV for several days. However, storage alone can only delay the release of low energy protons and yield a steeper spectrum in the late phase of the flare. Our observation on gas-rich meteorites need complete or nearly complete suppression of $<$30 MeV protons and not just delayed release. If the protons are stored in the coronal fields, they will undergo coulumbic energy losses. As a result, as pointed out by Krimigis (1973), the low energy flux would be degraded and it may even lead to a peak shaped energy spectrum at the low

energy-end. This was in fact the criterion applied by Krimigis (1973) to test the storage hypothesis for solar particles. Such degradation, however, had been observed only at very low energy of 0.3 MeV (Krimigis and Verzariu, 1971) and therefore one may infer that such storage is not operative on contemporary Sun. Newkirk (1973) gave estimates of columbic energy losses during such storage and inferred that such storage on the Sun is not possible unless one invokes conditions favourable to low columbic losses because otherwise 10 MeV protons could not survive the storage time of a few days. However, in the case of early Sun one can use similar considerations to imply that under conditions of high magnetic fields on the Sun, higher storage time could result in loss of low energy particles yielding a proton energy spectrum having a peak at about 35 MeV. Eventhough this suggestion looks ad hoc, it does not seem to be impossible. One serious difficulty it faces is maintaining the ordered high magnetic fields in the coronal region to allow trapping of protons for long periods. Considering the high flaring rate on the ancient Sun, the efficiency of Coulumbic loss processes and the time interval between successive flares (because flares can disrupt the magnetic loops) have to be high.

The other stage where generation of such spectrum could be aided is the traversal through the interplanetary

medium. Reedy and Arnold (1972) have demonstrated the effect of proton-traversal through material on their spectrum. The more is the amount of matter traversed, the more is the resulting spectrum close to the desired pulse shape.

The effect of these two processes may lead to a decrease in the flux but as will be shown in the next subsection, the available flux may even then be sufficient. The relative flux of high energy particles ($\sim$ 35 MeV) may further increase due to fact that >15 MeV particle flux falls as R^{-2} as against R^{-3} dependence for <15 MeV flux (R is the heliocentric distance) as inferred by Lee (1976). This is applicable to the conditions of present interplanetary magnetic field. It may be added here that Kaiser and Wasserburg (1983) also suggest a high flux of 30 MeV protons in the early solar system to explain their observations on excess ^{107}Ag in iron meteorites.

2. High SCR-Flux : While it is important to have 30-40 MeV proton flux to explain the observed neon isotopic excess in gas-rich meteorites, this criterion is not sufficient to account for the observed excesses. To explain these isotopic excesses a fluence of 10^{18} protons cm^{-2} (or a flux of $\sim 10^4$-10^5 protons $cm^{-2}sec^{-1}$) is required at 3 AU considering a residence time of $\sim 10^5$ years on the regolith of the gas-rich meteorite parent bodies.

There are enough astronomical evidences available to suggest that stars during their early phase of evolution before entering their Main Sequence should be very active. Based on observation of stars in Hyades and Pleides steller clusters, Skunamich (1972) showed that the Ca II line strength (f) falls off as inverse of root of the age of the star (t) $f \propto 1/(t)^{1/2}$. Using Ca II line strength as indicator of the age of the star (and of chromospheric activity), Feigelson (1979) related the soft X-ray flux, as measured by instruments aboard HEAO satellite and the age of the stars. He argued that if Hudson's estimate (Hudson, 1978) of variation in proton flux as fourth power of X-ray luminosity can be applied in general, then comparing with younger stars in Hyades, the proton flux of the young sun ($\sim$ 4.6 Gyr ago) should have been about 10^5 times the present flux because stars in Hyades show 30 times higher X-ray luminosity. This estimate is consistent with the requirements deduced from the gas-rich meteorites. What is more important is that this proton flux does not produce other anomalies such as ^{26}Al, ^{50}V etc. (Audouze et al., 1976) which require much higher flux. Another important observation is by Worden et al. (1981) who deduced proton fluxes of the orders of 6×10^{34} sec^{-1} and 6×10^{35} sec^{-1} for B P Tau and T Tau which are equivalent to proton fluxes of 10^7-10^8 protons cm^{-2} sec^{-1} at 1 AU. All these observations are consistent with the idea that the fluxes of protons from

the early Sun could have been very high.

The ^{107}Ag anomaly (Kaiser and Wasserb rg, 1983) can be explained even by GeV proton flux due to GCR as pointed out by them but the flux requirement is so high that it is not consistent with the present understanding of galactic cosmic rays. So they suggest that low energy protons ($\sim$30 MeV) are responsible for the production of ^{107}Ag isotopic anomaly seen in iron meteorites.

Results of an experiment reported recently (Caffee et al., 1983) are important from the point of view of conclusions reached in this work. The Ne-measurement in (individual) irradiated grains from the gas-rich meteorite howardite Kapoeta revealed enormous ^{21}Ne concentration ($\simeq 17 \times 10^{-8}$ cc STP of $^{21}Ne\ g^{-1}$) in them. This high amount of ^{21}Ne can not be attributed to the SW implantation based on various other evidences and hence cosmogenic production is suggested to be the likely mechanism. It is noteworthy that the low temperature fraction (800°C) of the sample shows SW-composition ($^{20}Ne/^{22}Ne = 12.7$) and the high temperature point (1900°C) falls near the SCR-field (20/22 = 2.37, 21/22 = 0.79) estimated for the pyroxenes using contemporary SCR spectrum, deduced for lunar samples by Hohenberg et al. (1978). This result may apparently look contradictory to the results arrived at in the case of H-chondrites in this work where the present SCR-field does not seem to be consistent with

the observations. The difference may be attributed to the fact that irradiation in Kapoeta could have been relatively recent. Kapoeta has clasts with lower formation age of ~3.6 Gyr (Papanastassiou et al., 1974) even though the formation ages are about 4.5 Gyr. But the meteorites Pantar, Leighton and Fayetteville so far have not shown evidences for brecciation events later than 4.6 Gyr. Their formation ages are also about 4.6 Gyr.

All these evidences are suggestive of higher proton flux during the early history of the Sun. However, the generation of proton fluxes enriched in ~35 MeV protons is not straight forward but the SCR-irradiation scenario is preferred because it is possible to envisage conditions of high SCR-flux because of lot of support from the astronomical observations. Production of pure ^{22}Ne with less than 10 MeV proton flux and very low $\frac{21}{22}$ ratio was considered by Audouze et al. (1976). But conditions on the ancient sun, seem to be more favourable for higher energy protons. These models suggest a higher proton flux from the Sun in the epoch of irradiation of the gas-rich meteorites during the early solar system history. However, the scenario involving irradiation by ~35 MeV protons gives lower GCR-exposure ages for the meteorites which is a difficulty. As Niederer and Eberhardt (1977) did find presence of nearly

pure ^{22}Ne in Dimmit (though in very minute amount) which is a gas-rich meteorite, probably similar studies on other gas-rich meteorites will help in settling the issue.

CHAPTER VII

NOBLE GASES IN METEORITES AND LUNAR ROCKS

In the course of its orbit around the Sun, earth sweeps about 10^{10}g of material every year which includes bodies ranging in size from a micron to about a metre. However, only a minute fraction of it survives the atmospheric journey to reach earth to be recovered as meteorites. Before the arrival of lunar samples, meteorites were the only extraterrestrial material available.

Meteorites have always been objects of curiosity - scientifically and otherwise. First it was by way of their spectracular arrival and associated myths and then by the tremendous amount of information they were found to carry. Although it is chondrites which dominate the inventory of meteorites, the first meteorites to be identified as extraterrestrial material were irons. The evidence of slow cooling rates and uniform distribution of olivine in the pallasite Pallas and the exotic composition (pure iron with minor amount of nickel) of Otumpa meteorite prompted Chladni to conclude that they were of extraterrestrial origin. In subsequent years, meteorites became subjects of extensive and intensive investigation. While they are useful in providing information about the solar system processes (Chapter VI),

they continue to remain interesting in their own rite. As discussed in the Chapter I, the GCR-exposure age of a sample defines the duration for which it was accessible to the galactic cosmic rays (GCR). The GCR-exposure age, therefore, is indicative of certain event in the history of the sample. The GCR-exposure ages of lunar rocks have been used to infer the time of the cratering event responsible for excavating the rocks from the interior of the regolith. The dates of formation of the North Ray and South ray craters on moon were determined in this manner (Behrmann et al., 1973).

The cosmic ray exposure ages of the meteorites being considerably lower than the age of the solar system, indicates that it is relatively recently that the meteorites became accessible to the interacting protons. The range of the GCR-protons being of the order of a metre, GCR-exposure age must indicate an excavation event which exposed the meteorites to the galactic protons. A peak around 5 Myr in the exposure age distribution of H-chondrite meteorites, , similarly, denotes the parent body fragmentation event (Zahringer, 1962). These fragments, knocked out of the parent body orbits, may later get captured by the earth's gravitational field though after spending considerable ($\sim$ Myr) time in space. But the noble gas records in meteorites are not the result of the GCR-irradiation alone. They contain information about a variety of processes (Wasson, 1974): processes

which occured in the nebula, those during their collisional and irradiation history and also during their life as planetary body. Chondrites could have been derived from comets, asteroids or earth-approaching-bodies such as Apollo-Amor objects (Anders, 1964; Wetherill, 1971; Zimmerman and Wetherill, 1973). The optical evidence for carbonaceous chondrite like material on asteroids have also been found (Chapman et al., 1975). But the fragility, volatile abundance and low exposure ages of carbonaceous chondrites are features suggesting cometary nuclei as their parent bodies also. Recent compositional evidence from antarctic meteorites suggest interesting possibilities of some of the meteorites being lunar in origin also (Warren et al., 1983). The origin of meteorites is, however, still an unsettled issue and contradictory evidences exist. While comets cross the earth's orbit, it is doubtful that they have differentiated material as nucleus. Besides, gas-rich meteorites which had regolith-history are unlikely to have origin on comets (Wetherill, 1974). Anders (1978)believes most of stony meteorites to be from asteroidal belt . The carbonaceous chondrites are believed to have escaped igneous metamorphism. Different classes of mateorites have different noble gas components in them and these records point to their evolutionary history. The study of Isna was aimed at finding planetary component of noble gases in it and determining its cosmic ray exposure age. The analysis of Allan Hill meteorite (AH 77216,18)

a find from Antarctica, was taken up because the track study by Goswami (1980) indicated presence of pre-compaction track records in it. The results for gas-rich meteorites of H-group were reported in Chapter VI. Here the results of noble gas analysis of L-3 chondrite AH # 77216,18 are presented. The GCR-exposure ages of three lunar rocks are also estimated and presented.

B. ISNA: C3-O METEORITE

The stony meteorite Isna was found in 1970 in Egypt (Methot et al., 1975). The carbonaceous chondrites are generally considered to represent the most primitive and chemically unaltered material in the solar system even though they do contain features indicative of hydrothermal alteration (McSween, 1979). Isna is not a fall but observed high ^{60}Co activity of 130 ± 40 dpm, suggests that its terrestrial age is less than 15 yrs (Herpers et al., 1983).

(1) Noble Gases in Isna and GCR Exposure Age: The Table VII.1 and VII.2 give the light noble gas-data and Xe-data respectively obtained by stepwise heating mass-spectrometric analysis. The ^{3}He and ^{4}He concentration in Isna have been found to be 0.13 x 10^{-8} cc STP g^{-1} and 930.4 cc STP g^{-1} respectively. Kirsten et al. (1980) have reported similar values in their total melt experiment.

TABLE VII.1

ELEMENTAL AND ISOTOPIC COMPOSITION OF LIGHT NOBLE GASES IN ISNA-1

Temperature (°C)		He		Ne			Ar		
		3/4	4*	20/22	21/22	22*	38/36	40/36	36*
600		0.000149	322.8	5.347	0.354	0.023	0.175	320.97	2.02
	±	0.000002	15.0	0.200	0.008	0.002	0.004	16.10	0.02
900		0.000133	520.2	5.591	0.319	0.062	0.179	7.68	108.60
	±	0.000002	25.0	0.150	0.006	0.004	0.003	0.35	3.30
1200		0.000095	49.9	6.119	0.298	0.030	0.184	19.31	27.12
	±	0.000001	2.5	0.184	0.006	0.003	0.002	0.96	1.40
1600		0.000228	37.5	5.514	0.347	0.021	0.186	9.39	7.03
	±	0.000003	2.0	0.200	0.020	0.002	0.003	0.90	0.35
SUM		0.000140	930.4	5.654	0.325	0.136	0.180	14.30	144.72
	±	0.000006	29.3	0.351	0.020	0.006	0.007	0.60	3.60

*Gas amounts in 10^{-8} cc STP g^{-1}.

TABLE VII.2

ELEMENTAL AND ISOTOPIC COMPOSITION OF XENON IN ISNA-2

Temp. (°C)		124	126	128	129	130	131	134	136	132 (10^{-12} cc STP g^{-1})
		(Normalized to 132_{Xe})								
600		0.00420	0.00380	0.0751	1.0396	0.1535	0.7964	0.3889	0.3314	226.8
	±	0.00008	0.00008	0.0010	0.0012	0.0016	0.0080	0.0040	0.0033	4.6
900		0.00470	0.00440	0.0822	1.2856	0.1629	0.8159	0.3954	0.3437	172.1
	±	0.00009	0.00008	0.0010	0.0150	0.0017	0.0080	0.0040	0.0035	3.4
1200		0.00450	0.00400	0.0812	0.1719	0.1627	0.8177	0.3844	0.3194	3993.0
	±	0.00005	0.00005	0.0000	0.0014	0.0017	0.0082	0.0040	0.0032	60.0
1600		0.00470	0.00400	0.00837	1.1827	0.1627	0.8137	0.3782	0.3149	210.1
	±	0.00006	0.00004	0.00009	0.0012	0.0018	0.0085	0.0040	0.0032	5.2
SUM		0.00450	0.00400	0.0811	1.1701	0.1622	0.8164	0.3847	0.3207	4602.0
	±	0.00009	0.00008	0.0017	0.0218	0.0034	0.0168	0.0080	0.0066	60.0

The Ne data are given in Table VII.1 and plotted in Fig. VII.1. The total Ne isotopic ratios obtained in this study are $^{20}Ne/^{22}Ne = 5.65 \pm 0.35$ and $^{21}Ne/^{22}Ne = 0.325 \pm 0.02$. All the points representing various temperature fractions fall close to the tie-line joining planetary and galactic cosmic ray (GCR) components. Kirsten et al. (1980) reported $^{20}Ne/^{22}Ne = 6.969$ and $^{21}Ne/^{22}Ne = 0.348$. The ^{22}Ne amount measured here is $(0.136 \pm 0.007) \times 10^{-8}$ cc STP g^{-1} which is close to the concentration of 0.112×10^{-8} cc STP g^{-1} reported by Kristen et al. (1980). While measurement errors in He and Ne are small, diffusion losses of ^{3}He and ^{4}He during its terrestrial residence can not be ruled out. The amounts of cosmogenic ^{3}He and ^{21}Ne in Isna are 0.13×10^{-8} cc STP g^{-1} and 0.0442×10^{-8} cc STP g^{-1} respectively. The correction for trapped gases yield cosmogenic $^{22}Ne/^{21}Ne = 1.01$ which is much lower than the lower limit of 1.08 given by Cressy and Bogard (1976) for applying shielding corrections. Using the ^{21}Ne production rate of 0.3×10^{-8} cc STP g^{-1} Myr^{-1} (Mazor et al., 1970) and ^{3}He production rate of 2×10^{-8} cc STP g^{-1} Myr^{-1}, the GCR exposure ages for Isna are calculated to be 0.14 ± 0.06 Myr and 0.07 ± 0.04 Myr. The isotopic ratio of Ar suggests a nearly pure trapped component. For want of Ca-concentration no attempt has been made here to calculate ^{38}Ar-based GCR exposure age.

The Ne based exposure ages for other C3(O) chondrites

FIGURE CAPTION

Fig.VII.1 Neon isotopic compositions of some chondrites and lunar rocks are shown. The numerals near the data points denote temperatures in hundreds of degree centigrade. The presence of the planetary neon in Isna and that of SW-Ne in AH 77216, 18 is evident. The lunar rock samples are from rock-interior and neon is dominated by the GCR produced neon. Being breccias, they do contain small amounts of SW - neon. The difference between the data-points of Mg-bearing 79215 rock and the two Mg-free rock samples is also seen. The GCR field has the end points of feldspar and pyroxenes as the boundary. The filled symboles represent sum of the individual temperature fractions.

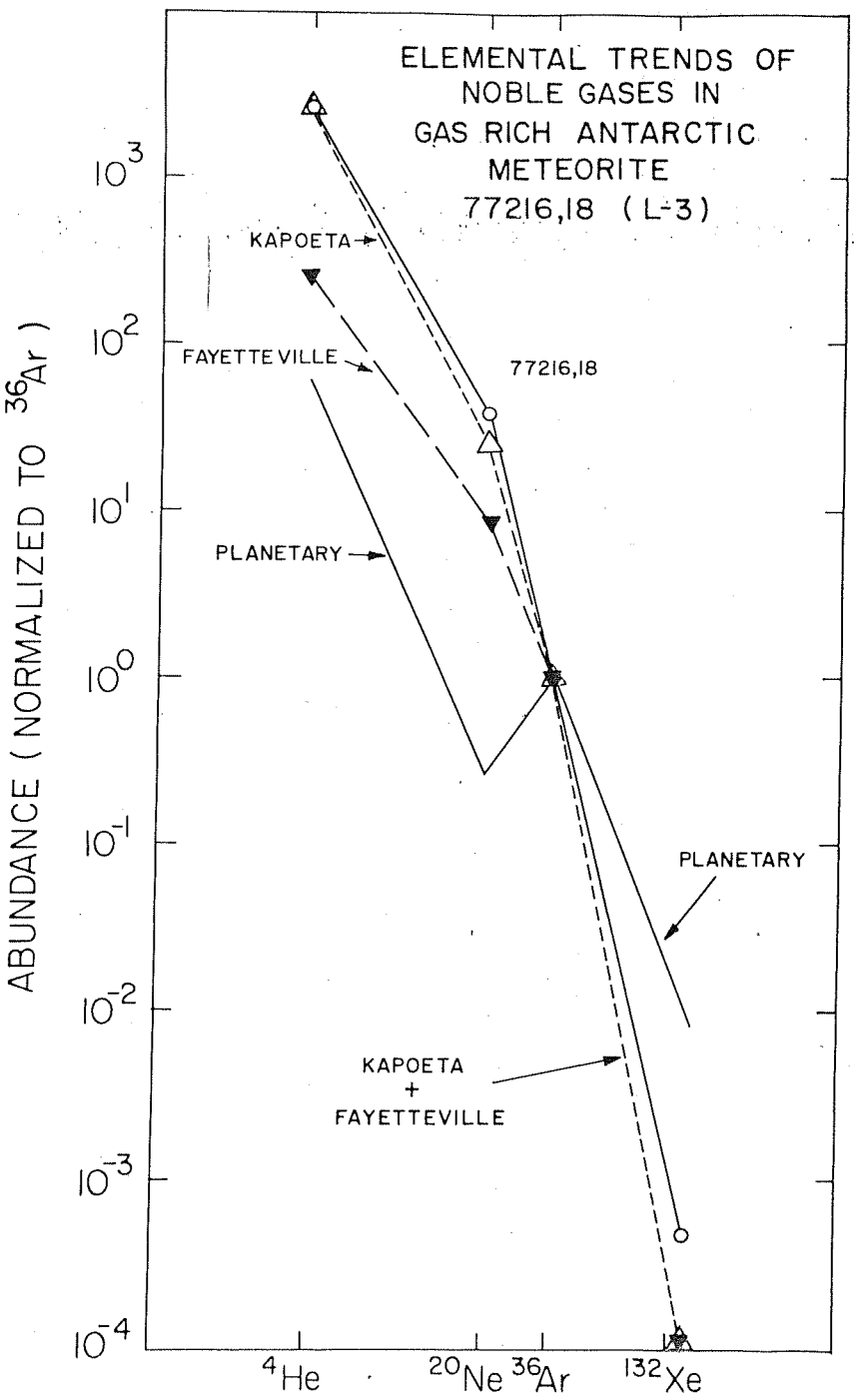

Fig. VII.2 Noble gas elemental abundances in the gas-rich L-3 meteorite AH 77216, 18. For comparison the Kapoeta and Fayetteville data from Black (1972 a) and planetary values from Reynolds et al. (1978) are also plotted.

are all greater than 4 Myr and Isna has the lowest GCR exposure age of about 0.14 Myr in this group. The low exposure age is further evidenced by the absence of particle tracks in olivine and pyroxene grains in Isna. About 50 mineral grains from Isna were examined for tracks without any success.

The xenon data obtained in the step wise heating runs of Isna, are given in Table VI.2. The Xe isotopic compositions of Isna is similar to that of average carbonaceous chondrite (AVCC). The $^{129}Xe/^{132}Xe$ ratio is 1.2 for Isna whereas the same ratio is about 2.0 for Kainsaz, Felix and Lancé but the ^{132}Xe contents are roughly same i.e. about 0.55 x 10^{-8}cc STP/g for all these four chondrites.

(2) Noble Gas Elemental Composition and Classification of Isna : Based on petrological and chemical studies, Methot et al. (1975) classified Isna as a C3(O) carbonaceous chondrite. Here classification of Isna is attempted based on the noble gas isotopic composition.

The $^{36}Ar/^{132}Xe$ ratios for C2 and C3(O) chondrites are 89 and 242 respectively (Mazor et al., 1970) and for Isna, it is 284 which agrees roughly with the C3(O) meteorites. The $^{20}Ne/^{36}Ar$ ratio for Isna is about 0.0053 (0.005, Kristen et al., 1980) and this value could be considered to be closer to the average value of 0.03 for C3(O) rather than

0.3 for the C2 meteorites. The noble gas elemental abundance pattern for Isna i.e. ^{20}Ne : ^{36}Ar : ^{132}Xe pattern, seems to be similar to that of Lancé, Kainsaz and Ornans except for Ne (Alaerts et al., 1979). It may be that some Ne has been lost from Isna during its terrestrial surface residence. But from a chemical point of view, Isna does not seem to be a weathered meteorite, as it has most of the iron in Fe^{O} and/or Fe(II) state (Methot et al., 1975). Probably the low ^{20}Ne observed in Isna, relative to other C3(O) meteorites, can be attributed to loss during metamorphism as it belongs to metamorphic stage III according to the petrologic criteria (McSween, 1977). However, the matrix to chondrule ratio of 0.4 (McSween, 1977) and the noble gas data indicate that Isna belongs to the group of Felix and Lancé (Stage II metamorphism) rather than Warrenton.

B. ANTARCTIC METEORITE AH# 77216, 18

Study of nuclear track records had revealed the presence of pre-compaction solar flare irradiation records in Antartic L-3 chondrite AH-77216 (Goswami, 1980). The track-rich phases of such meteorites are also known to have accumulated solar wind gases during their pre-compaction surface exposure. In order to study the irradiation history of this meteorite, mass spectrometric analysis for isotopic and elemental composition of noble gases has been carried out. Based on petrographic features and field relation, sample

77216 is likely to be a fragment in a multiple fall to which samples 77215, 77217 and 77252 are associated.

The aliquot sample of this meteorite showed 16% of irradiated grains where back ground track density was 4×10^6 tracks cm^{-2} (Goswami, 1980). The sample 77216,18 was analysed in three different temperature-steps. The analysis has yielded $^{20}Ne/^{22}Ne$ = 10.12, 9.53 and 7.71 at 900°C, 1200°C and 1600°C respectively with average value of 9.8 for this sample (Table VII.3). Neon isotopic ratios as well as $^{38}Ar/^{36}Ar$, given in Table VII.3 indicate presence of an appreciable contribution from GCR spallation. The GCR exposure age for this sample is calculated to be 20 ± 4 Myr using the production rates given in Chapter III. The Ne-data are plotted in Fig. VII.1 and the noble gas elemental ratio in Fig.VII.2.

The trend of Ne ratios on a three-isotope diagram (Fig. VII.1) is similar to that seen in other gas-rich meteorites though the Ne isotopic ratios are, however, somewhat lower due to dilution by spallation. The confirmation for the solar origin of the excess gas in 77216,18 comes from the noble gas elemental abundance pattern shown in Fig.VII.2.The abundance pattern (normalized to ^{36}Ar) for AH-77216,18 demonstrates striking similarity with Kapoeta (Black, 1972 a) which is a gas-rich howardite and is distinct from planetary pattern. The $^{132}Xe/^{36}Ar$ point for AH 77216,18 has, however, more error as the first temperature

TABLE VII.3

NOBLE GAS ISOTOPIC COMPOSITIONS IN AH 77216,18

Temp. (°C)	He		Ne			Ar		
	3/4	4*	20/22	21/22	22*	38/36	40/36	36*
900	0.000574	71025.3	10.12	0.1000	72.11	0.214	388.87	12.23
	± 0.000090	950.0	0.12	0.0012	2.10	0.003	10.00	1.00
1200	0.001052	3141.1	9.53	0.1440	29.64	0.241	51.45	10.82
	± 0.000030	200.0	0.10	0.0015	0.60	0.003	2.00	0.80
1600	0.02124	21.8	7.71	0.265	7.35	0.301	40.21	4.78
	± 0.00150	1.2	0.10	0.004	0.18	0.005	2.00	0.30
SUM	0.00060	74188.2	9.80	0.123	109.09	0.239	175.83	27.83
	± 0.000014	970.8	0.24	0.034	2.19	0.016	15.48	1.32

* Gas amounts in 10^{-8} cc STP g^{-1}.

TABLE VII.4

NOBLE GAS ELEMENTAL COMPOSITION IN AH 77216,18

Temp. (°C)	^{4}He	^{20}Ne*	^{36}Ar*	^{132}Xe**	$^{4}He/^{36}Ar$	$^{20}Ne/^{36}Ar$	$^{132}Xe/^{36}Ar$ (10^{-4})
900	71025.3	729.75	12.23	-	5807.46	59.67	-
	± 950.0	22.9	1.0		481.16	5.23	
1200	3141.1	282.47	10.82	108.68	290.30	26.11	10.04
	± 200.0	6.44	0.8	2.2	28.32	2.02	0.77
1600	21.8	56.67	4.78	70.44	4.56	11.86	14.74
	± 1.2	1.57	0.3	1.4	0.58	0.81	0.97
SUM	74188.2	1068.89	27.83	179.12	2665.76	38.41	6.44
	± 970.8	33.85	1.32	2.6	131.16	2.19	0.32

* Gas amounts in 10^{-8} cc STP g^{-1}.

** Gas amounts in 10^{-12} cc STP g^{-1} The Xe in 900°C temperature fraction was lost. The final ratio is calculated with Xe summed up for two temperature-fractions and Ar for all these temperature fractions and hence a lower limit. The actual value can be high by about 30%.

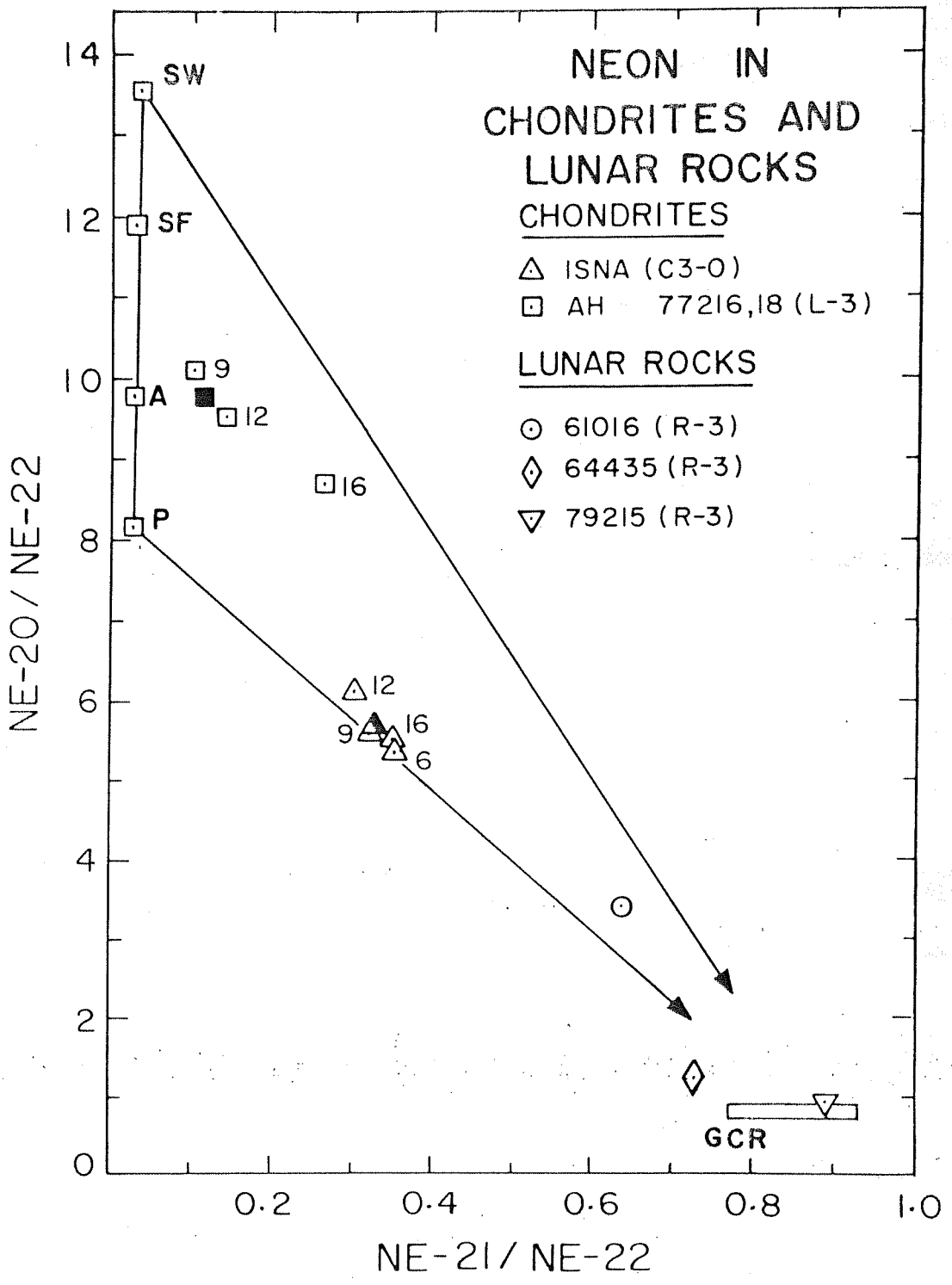
NEON IN CHONDRITES AND LUNAR ROCKS
CHONDRITES
ISNA (C3-0)
AH 77216,18 (L-3)
LUNAR ROCKS
61016 (R-3)
64435 (R-3)
79215 (R-3)
SW
SF
A
P
9
12
16
6
GCR
NE-20 / NE-22
NE-21 / NE-22
0
2
4
6
8
10
12
14
0.2
0.4
0.6
0.8
1.0

FIG. VII. 1

fraction (600^{o}) of Xe was lost. The assigned error of 30% is based on comparison with the release pattern of other gas-rich meteorites (Chapter VI).

Based on the presence of solar flare tracks and noble gas elemental pattern similar to solar wind and other gas-rich meteorites, AH-77216 can be placed in the class of gas-rich meteorites. This meteorite is a valuable addition to the inventory of the gas-rich L chondrites of which very few are known at present.

C. GCR-EXPOSURE AGES OF LUNAR ROCKS

Interior samples of three lunar anorthositic breccias 61016, 64435 and 79215 have been analysed for noble gases and results are reported. Table VII.5 shows the Ne and Ar composition of these three rocks. Being deep samples, Ne in these sample should have been purely cosmogenic but because of being beccias they may contain small amounts of trapped SW gases also. Corrections for trapped gases have been made wherever necessary, treating the observed Ne and Ar as binary mixtures. The resolved cosmogenic gas amounts; the production rates used here and the estimated GCR-exposure ages are given in the Table VII.6.

The SW corrected ^{21}Ne in rock 61016 is 0.35×10^{-8} cc STP g^{-1}. Using a composition corrected production rate of 0.077×10^{-8} cc STP g^{-1} Myr^{-1}, the GCR exposure age for

TABLE VII.5

ISOTOPIC AND ELEMENTAL COMPOSITION OF Ne AND AR

IN THE INTERIOR SAMPLES OF LUNAR ROCKS

Sample	Depth (mm)		Ne			Ar		
			20/22	21/22	22*	38/36	40/36	36*
61016(R-3)	16-18		3.41	0.647	0.540	0.847	526.19	0.520
		±	0.18	0.007	0.02	0.030	46.10	0.015
64435(R-3)	7.5-9		1.25	0.728	0.163	0.865	2734.00	0.287
		±	0.01	0.008	0.008	0.04	245.00	0.014
79215(R-3)	5-8		0.83	0.891	18.08	1.488	143.61	28.150
		±	0.01	0.009	0.90	0.05	9.5	0.850

* Gas amounts in 10^{-8} cc STP g^{-1}.

TABLE VII.6

GCR EXPOSURE AGES OF LUNAR ROCKS

Rock	Cosmogenic Gas		Production Rate		Exposure-Age (Myr)	
	^{21}Ne*	^{38}Ar*	^{21}Ne**	^{38}Ar**	^{21}Ne	^{38}Ar
61016	0.347	0.216	0.077	0.117	4.49 ± 0.51	1.85 ± 0.27
	± 0.014	0.022	0.008	0.012		
64435	0.112	0.126	0.072	0.125	1.55 ± 0.2	1.01 ± 0.16
	± 0.006	0.017	0.007	0.011		
79215	18.08	40.9	0.088	0.134	205.46 ±23	305.2 ±32.8
	± 0.82	1.9	0.009	0.013		

* Gas amounts in 10^{-8} cc STP g^{-1}.

** Errors in the production rates do not take compositional error into account.

Composition : Percentage abundance of Mg, Al, Si and Ca in 61016 are (0.018, 18.1, 20.1 and 14); in 64435 (0.1%, 17.3, 21.0 and 12.2%) and in 79215 (3.8, 14.6, 20.4 and 11.4). The Ca concentration used for 79215 is based on whole rock-composition by Bickel et al. (1978).

this rock is estimated to be 4.5 ± 0.5 Myr using production rates for 5 g cm^{-2} depth (Hohenberg et al., 1978). The cosmogenic ^{38}Ar in this sample is 0.216 x 10^{-8} cc STP g^{-1} and use of a production rate of 0.117 x 10^{-8} cc STP g^{-1} gives exposure age of 1.85 ± 0.3 Myr. This error in exposure age does not include error due to compositional uncertainty.

The Ne in the interior sample (2.5 g cm^{-2}) of rock 64435 is dominated by the cosmogenic neon and in the three isotope neon diagram, the points fall close to the GCR-end point. The cosmogenic ^{21}Ne and ^{38}Ar amounts in this sample are 0.112 and 0.126 (both in 10^{-8} cc STP g^{-1}). Using production rates of 0.072 and 0.125 (both in 10^{-8} cc STP g^{-1} Myr^{-1} units) for ^{21}Ne and ^{38}Ar respectively for the depth of this sample the exposure ages are 1.55 and 1.0 Myr respectively.

The troctolite 79215 also contains nearly pure cosmogenic neon and the trapped gas contents in very low. For this sample, the ratios are $^{20}Ne/^{22}Ne$ = 0.83 and $^{21}Ne/^{22}Ne$ = 0.89. The cosmogenic ^{21}Ne in this sample is about 16.96 x 10^{-8} cc STP g^{-1}. Using the ^{21}Ne production rate of 0.088 x 10^{-8} cc STP g^{-1}, the GCR-exposure age turns out to be 215 ± 30 Myr in agreement with the value of 170 ± 20 Myr reported by McGee et al. (1978) based on ^{37}Ar-^{39}Ar method. The $^{38}Ar/^{36}Ar$ ratio in this rock is 1.488 indicating the presence of dominant cosmogenic component. The Ar based age comes to be

too high (305 ± 30) Myr. For this rock, the production rates used are based on 200 g cm^{-2} depth for 79215 as judged from high $^{131}Xe/^{132}Xe$ in this rock.

This discordance between the Ne and Ar based ages probably arises from the uncertainty in Ca-contents which are not measured in these aliquot samples but taken from literature for bulk rock (Laul et al., 197 ; Bickel et al., 1978). For this reason the Ne-based ages are considered preferable.

CHAPTER VIII

SUMMARY AND FUTURE PERSPECTIVE

What has been the linking thread of this study is the charged particle radiations especially of the solar origin. In this chapter, a summary of the results obtained in the thesis using noble gas mass-spectrometric techniques is presented. In an interdisciplinary field like this there is always need for more observational and experimental data. Need for such information is also emphasized. Some of the results arrived at in this thesis can be put on firm footing by some new experiments. Such experiments and those to improve the findings of the thesis are proposed.

The main objectives of the study were :

(a) To investigate whether the solar energetic particles are planetary or solar in the isotopic composition of neon and in the elemental composition of the noble gases.

(b) To demonstrate the presence of SCR-produced neon in the lunar soils and to resolve it in order to determine their surface-exposure ages which can be compared with those determined by other methods. This provides a method to monitor the solar flare-activity over long time scale ($\sim$10 Myr).

(c) To decipher the records of early active Sun in gas-rich meteorites by applying the information deduced in the case of lunar soils and to estimate the ancient solar proton flux.

A. SUMMARY OF RESULTS

1. Composition of the solar energetic particles (SEP):

The problem of the SEP-composition especially of Ne-isotopic composition was taken up because of the suggestion by Dietrich and Simpson (1979) and Mewaldt et al. (1979) that the Ne-composition in the solar energetic particles (SEP) and hence the composition of the Sun is planetary. The results of this study (Chapter IV) are based on the stepwise heating mass-spectrometric analysis of the etched lunar grains of different minerals (feldspar and pyroxene) and different grain-sizes. It is concluded that the neon composition of the Sun is not planetary. It is different from but relatively closer to the solar wind composition. The agreement of the SEP-noble gas elemental composition with the SW-composition further supports this result.

In view of the large flare to flare variation it is difficult to say as to what extent averaging of a few flares can be taken to represent the long term SEP-composition. The lunar soil-based values, in contrast, represent values averaged over a few tens of Myr. Another difficulty with the

direct (CPT) measurements is that of statistics. The deduced isotopic ratios for the SEP-Ne are based on rather small number of events. The variability in the CPT-based flare-data, therefore, is not surprising. The latest available result gives $^{20}Ne/^{22}Ne$ value of 16.7(+10.3, -7.2) for 4 flares observed during 1981 (Simpson et al., 1983) which is approximately twice the value deduced earlier (Dietrich and Simpson, 1979; Mewaldt et al., 1979). Adding the 8 to 11 MeV nucleon^{-1} neon-data to their earlier data in the 11 to 26 MeV nucleon^{-1}, Mewaldt et al. (1983) have revised their value of 7.6 (+2, -1.8) to about 9.2 $\pm$ 2 which is now closer to the value of 11.8 $\pm$ 0.25 deduced in this study and that deduced by Wieler et al. (1982). Figure VIII.1 shows different values deduced by the different groups for $^{20}Ne/^{22}Ne$ ratio. The lunar and meteoritic sample-based values are distinctly higher than the directly measured values. However, the two approaches have certain basic differences and hence the difference in the values could be inherent to the techniques. The factors to which these differences can be possibly attributed are :

(a) Short term variability of flare-compositions and limited statistics in the CPT-experiments.

(b) Difference in the energy-range of the sampled solar energetic particles by the two methods.

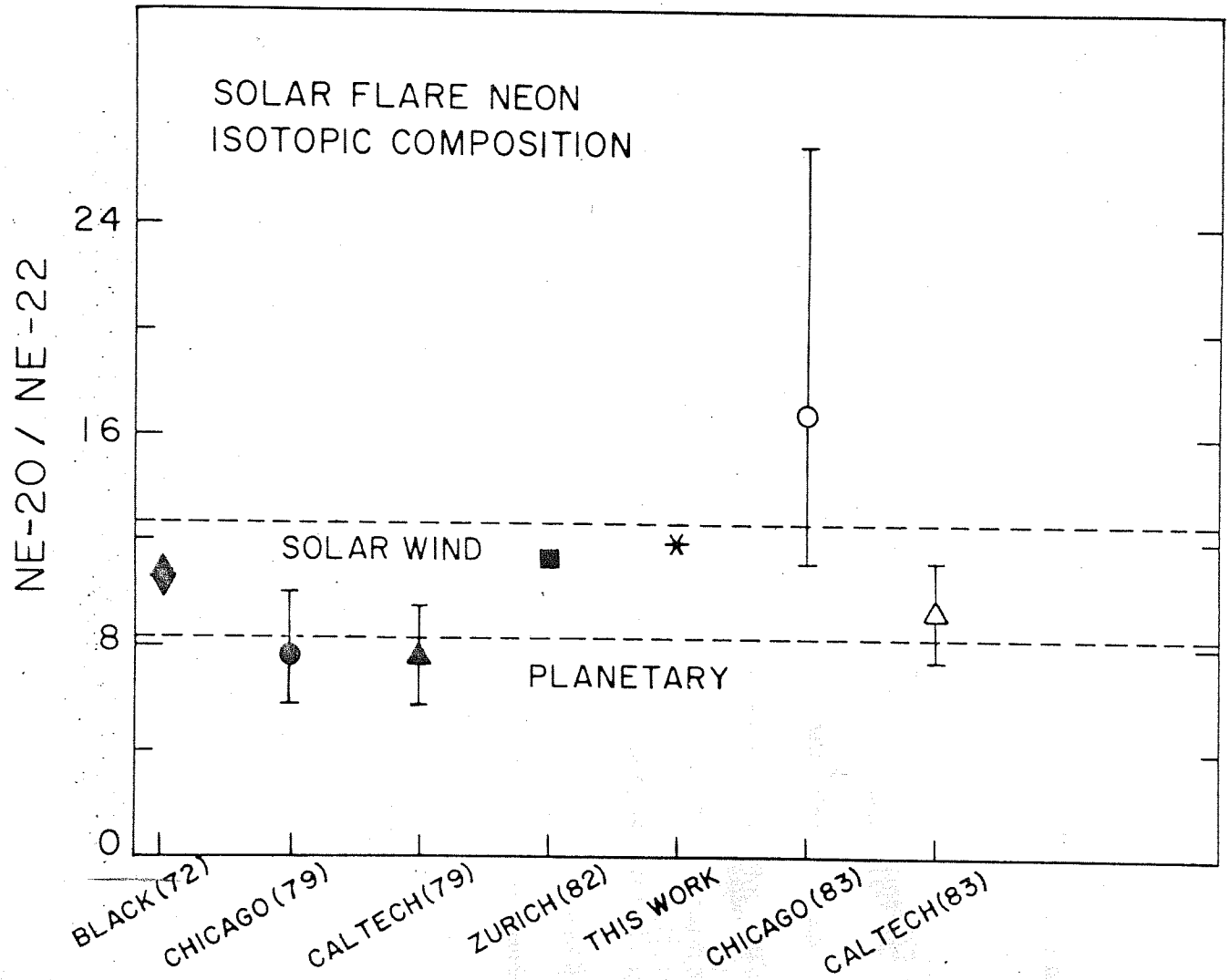

Fig. VIII.1 A summary of the $^{20}Ne/^{22}Ne$ values in the SEP and the SW determined by various groups using different technique. The normalization is with respect to the average SW-ratio deduced by Kirsten et al. (1971)

The variability of the isotopic and elemental compositions in the SEP is well known. The ratio $^{3}He/^{4}He$ has been noted to be energy dependent (Black, 1983) and therefore the dependence of $^{20}Ne/^{22}Ne$ over energy can also not be ruled out. The conclusion, therefore, is that the long term SEP-composition is not planetary either in the neon-isotopic composition or in the noble gas elemental composition. Instead it is closer to the solar wind composition. The differences in the values obtained by the two approaches are attributable to the difference in the energy-range of particles sampled and more importantly the limited statistics and short term compositional fluctuation in the flare particles. It may be important that the $^{20}Ne/^{22}Ne$ values deduced seems to be increasing with the increasing retentivity of the minerals. The feldspars give value ranging from 11.3 ± 0.2 to 11.75 ± 0.25. The pyroxenes give a value of about 11.8 ± 0.25. Limited data available on the ilmenites indicate a still higher value (Leich et al., 1975) which suggests mineral dependence of the deduced values for this ratios.

2. The Cosmogenic Effects of Solar Cosmic Ray Protons:

In this thesis, the cosmogenic effects of the SCR-protons have been demonstrated using neon as the monitor. It is shown that the etching of the lunar grain-surfaces results in relative enrichment of the SCR-proton produced Ne-component and the implanted solar flare particles. Only grain-size-suites and mineral-separates were used to keep the uncer-

tainty to a minimum. By employing stepwise heating procedures and then using three-component-analytical equations, it has been possible to resolve the SCR proton-produced neon in these samples. Based on these amounts, model calculations have been made for the SCR-exposure ages (integrated residence time in the top 2 g cm^{-2}) for samples from different lunar soils. The SCR-exposure ages so deduced, have been shown to be well correlated with the other maturity indices such as percentage of the track-rich grains and mean grain-size. The soil sample 61221, for instance, has SCR-exposure age of about 4 Myr consistent with the small percentage of track-rich grains found in it (12%) and the large mean grain size (287 microns). The mature lunar soil 69921 sample has an SCR-exposure age of about 21 Myr (lower limit) which is consistent with the fact that it contains about 90% irradiated (track-rich) grains. The deduced ages of about (130±50) Myr for the samples from the soil 14148 are, however, higher by about a factor of two than the track-based age (an upper limit of 50 Myr) and also what one would expect from regolith-models. While the deduced ages suffer from the uncertainty in the end points for the cosmogenic components , in the composition of the trapped components, the possibility of a factor of about two higher proton flux over the last hundred Myr (compared to the value of 70 protons cm^{-2} sec^{-1} deduced for last few Myr) is suggested by the present study.

3. Records of Early Active Sun : The idea of the early active sun is not new. The result reported in this thesis is consistent with the general picture of the evolution of the stars. Enough evidences exist to suggest that stars lose mass at a staggerring rate in the form of solar wind during their early stage of evolution. There are observations of the flaring stars suggesting very high particle fluxes in the high energy region also. (Worden et al. 1981; Fiegelson, 1983). The idea of highly active Sun has been invoked here to explain the observed Ne-isotopic features, in the gas-rich meteorites. The analysis has shown that a fluence of about 10^{18} protons cm^{-2} at energy of about 35 MeV is required to explain the results of the neon-analysis in the gas-rich meteorites. Two alternatives are suggested to obtain such a proton spectrum. This shape of the spectrum can be generated during the preferential trapping of the low energy particles on the ancient Sun with a higher magnetic field. Alternatively, a preferential loss of the low energy particles in the dense interplanetary medium can change a steep power law spectrum to a pulse - shaped spectrum. Recent results on individual grains of Kapoeta and Murchison also indicate the possibility of SCR-proton-irradiation of these grains (Caffee et al., 1983). It is therefore concluded that about 4.6 Gyr ago the Sun was more active and the SCR-proton flux higher by a factor of about 10^3 when the gas-rich meteorites presumably were

evolving / forming in the regolith. The conditions of the magnetic fields on the Sun and/or the denser dust-environment of the interplanetary medium is conjectured to have been responsible for the desired pulse-shaped specturm (peaking at about 35 MeV) giving rise to the low $^{21}Ne/^{22}Ne$ ratio even in the Mg-rich minerals such as pyroxene. However, the observed neon-isotopic features of the meteorites can also be explained by considering a small amount of pure (or nearly pure) ^{22}Ne to be present in the (dark portion of) meteorite. The amount required being very small ($\sim 1 \times 10^{-8}$ cc STP g^{-1}), it may be difficult to find it in the bulk sample. It is shown that such model gives GCR-exposure ages agreeing with those determined from the analysis of the light portions) which was not possible with the SCR-irradiation scenario. However, more studies should be carried out to understand these controversies.

4. Noble Gases in Meteorites and Lunar Rocks :

To study the cosmogenic and trapped noble gases, stepwise mass-spectrometric study of meteorites was carried out. Results on two of the meteorites have been reported in the thesis as they were found interesting. The carbonaceous chondrite Isna has been found to contain planetary neon. However, classification of Isna as C3(O)has been confirmed on the basis of noble gas elemental ratios. The Xe-isotopic composition has also been shown to be similar to the AVCC-

composition. The ^{21}Ne and ^{3}He based exposure ages of 0.14 ± 0.06 and 0.07 ± 0.04 Myr respectively are low and consistent with the absence of tracks in the meteorite. The study of the meteorite AH # 77216,18 a find from Antarctica, was prompted by the presence of solar flare-irradiated grains in it (Goswami, 1980). The analysis revealed high amount of trapped noble gases and a high $^{20}Ne/^{22}Ne$ ratio of about 9.8. The elemental composition of the noble gases in this meteorite has also been shown to be similar to that in the gas rich chondrite Kapoeta. This meteorite (AH #77216,18) was of L-3 class of which very few are known to be gas-rich meteorites.

The GCR-exposure ages of three lunar rocks from Apollo-16 and Apollo-17 missions have also been reported based on ^{21}Ne and ^{38}Ar in their interior samples.

B. FUTURE PERSPECTIVE

With the upward revision of the CPT-based $^{20}Ne/^{22}Ne$ value for the SEP-Ne (Mewaldt et al., 1983) there seems to be emergence of consensus over the nature of the SEP-Neon. However, considering the limited data based for the CPT-observation, and the lack of observation in the low energy region ($\sim$ 1 MeV/nucleon), need for observation of more flares cannot be over emphasized. This is necessary to remove the uncertainty arising from poor statistics. As

the neon measured by mass spectrometry in lunar soils is dominated by particles of about 1 MeV nucleon^{-1}, measurements down to this energy are critical for determining whether differences in the results by the two techniques are due to their different energies. This will also be of importance to examine if the anomalous component of the cosmic rays can affect the composition of neon deduced from lunar soils. Limited knowledge of this composition, however, prohibits any such consideration.

The status of planetary component is not clear. Massive planets such as Jupiter are expected to have retained their volatiles. The neon-isotopic measurements of Jovian-atmosphere may provide answer to this question. The noble gas elemental composition of the 'solar-component' being different from the planetary component, there is possibility of physical fractionation process in the nebula. Future planetary mission may provide vital clues to this problem.

The quantitative estimations of SCR-produced neon attempted in this thesis is dependent on the isotopic ratios of different reservoirs. The contributions of SCR-produced neon, therefore, is decided by the isotopic structure of the SCR-produced neon. The SCR-ratio used in this study are based on the results of Hohenberg et al. (1978). Several

of the cross section values being interpolated and extrapolated rather than measured, suggests that there is scope of improvement in the production rates and production ratios especially for the Mg(p, x)^{21}Ne reaction on which the partitioning critically depends. This reaction is important for the study of SCR-effects in the gas-rich meteorites also. It should be emphasised that the surface-exposure ages calculated in this work are only model ages and based on a set of certain parameters, not all of which are precisely known. With the possibility of better partitioning of components, it would be possible to stuly regolith-core samples from moon and make an attempt to infer the SCR-proton flux over different time-periods in the history of the Sun. Since track and radionuclide-based methods can not be applied to time periods beyond 10 Myr, the SCR-Ne based approach can provide a view into hitherto unravelled time window in the history of the Sun.

The problem of the high proton flux from the ancient Sun cannot still be said to have been completely resolved. There is scope for theoretical and experimental work on this problem. The trapping and subsequent loss of low energy charged particles in the Sun is not a well understood process. While the early active Sun is a viable proposition, right now the requirements to explain the anomalous isotopic structures need different kinds of spectra for different

cases. It is possible that the inter-planetary medium was different during periods when different classes of meteorites acquired their irradiation-records and therefore the proton fluxes and the spectra experienced by the grains in the regolith were different.

As a consequence of work presented in this thesis, need for the further experimental work is emphasised. These suggestions are made to extend the application of results obtained in this work and also to improve or substantiate them.

(1) More observational data for the SEP-neon with measurement down to about 1 MeV nucleon^{-1}. This will help in reducing the uncertainty associated with the results obtained from charged particle measurements which arises due to statistical fluctuation and the energy-dependence of the composition, if any.

(2) Ne-cross section measurements in Mg especially in the less than 10 MeV region and in the 50-200 MeV region are desired to improve the calculation of the production rates and production ratios of neon. This will improve the quantitative estimation of the SCR-proton-induced component in the lunar and meteoritic samples.

(3) Study of unlisturbed lunar drill core samples such as of Apollo-16. Study of the SCR-proton produced neon in these samples will permit the estimation of the solar activity at different epochs.

(4) A need emphasised by the work presented in this thesis is that of detailed work to search for ^{22}Ne-bearing phase in the dark portion of the gas-rich meteorites. Generation of pulse-shaped spectrum of SCR-protons has scope for considerable theoretical and observational work. As these two have been proposed as the plausible explanations for the problem of the gas-rich meteorites, it is hoped that it will help in solving the controversy.

REFERENCES

Alaerts L. et al. (1979). Geochim. Cosmochim. Acta 43, 1421.

Alexander C. et al. (1971). Science 172, 837.

Aller L.H. (1961). The abundance of the elements (Pub. Inter Science Pub.).

Anders E. (1964). Space Sci. Rev. 3, 583.

Anders E. (1975). Icarus 24, 363.

Anders E. (1978). In "Asteroids: An exploration assessment" (NASA conf. pub. 2053), 57.

Anders E. (1981). Geochim. Cosmochim. Acta 46, 877.

Anders E. and Ebihara M. (1982). Geochim,Cosmochim. Acta 46, 2363.

Anglin J.D. et al. (1973) in "High Energy Phenomena on the Sun" (Eds. Ramaty R. and Stone E.G.), 315.

Arnold J.R. et al. (1961). J. Geophys. Res., 3519.

Arnold J.R. (1975). Proc. Lunar Sci. conf. 6th, 2375.

Arnould M. and Norggard H. (1978). Astron. Astrophys. 64, 195.

Arrhenius G. et. al. (1971). Proc. Lunar Sci. Conf. 2nd, 2583.

Audouze J. et al. (1976). Astrophys. J. 206, L-185.

Bachall J. N. and Ulrich R.K. (1971). Astrophys. J. 170, 593.

Bart G. and Lipschutz M. E. (1979). Geochim. Cosmochim. Acta 43, 1499.

Bauer C.A. (1947). Phys. Rev. 72, 354.

Baur H. et al. (1972). Proc. Lunar Sci. Conf. 3rd, 1947.

Becker R. H. and Clayton R. N. (1977). Proc. Lunar Sci. Conf. 8th 3685.

Begeman F. and Heinzinger K. (1969). In 'Meteorite Research' (Ed. P. Millman), 87.

Behermann C. et al. (1973). Proc. Lunar Sci. Conf. 4th, 1957.

Bertch D. L. et al. (1972). Astrophys. J. 171, 169.

Bevington P. R. (1969). Data Reduction and Error Analysis for the Physical Science (McGraw Hill).

Bhai N. B. et al. (1978). Proc. Lunar Planet. Sci. Conf. 9th, 1629.

Bhandari N. et al. (1972). Proc. Lunar Sci. Conf., 3rd, 2811.

Bhandari N. et al. (1976). Proc. Lunar Sci. Conf. 7th, 513.

Bhattacharya S. K. et al. (1975). Proc. Lunar Sci. Conf. 6th, 3509.

Bibring J. P. et al. (1972). Science 175, 753.

Bickel C. E. et al. (1976). Proc. Lunar Planet. Sci. Conf. 7th, 1793.

Biswas S. and Fitchel C. E. (1965). Space Sci. Rev. 4, 709.

Biswas S. and Durgaprasad N. (1977). Please see Durgaprasad and Biswas (1977).

Black D. C. (1972 a). Geochim. Cosmochim. Acta 36, 347.

Black D. C. (1972 b). Geochim. Cosmochim. Acta 36, 377.

Black D. C. (1972 c). in "On the origin of the Solar System" (Ed. H. Reeves), 237.

Black D. C. (1983). Astrophys. J. 266, 889.

Black D. C. and Pepin R. O. (1969). Earth Planet Sci. Lett. 6, 395.

Blanchard D. R. et al. (1977). Proc. Lunar Sci. Conf. 8th, 2507.

Blanford D. E. et al. (1974). Proc. Lunar Sci. Conf. 5th, 2501.

Bogard D. (1971). EØS 52, 429.

Boeschler P. et al. (1969). In "Meteorite Research" (Ed. P. Millman), 857.

Bryant D. A. et al. (1962). I.R.E. Trans. Nucl. Sci. NS -9, 376.

Caffee M. W. et al. (1983). Lunar Planet. Sci. XIV, 86.

Cameron A.G.W. (1973). Space Sci. Rev. 15, 121.

Cameron A.G.W. (1982). In "Essays in Nuclear Astrophysics" (Ed. Barnes A., Clayton D.D., Schramm D.N.), 23.

Cartwright B.G. and Mogro-Campero A (1973). In "High Energy Phenomena on the Sun" (Eds. Ramaty R. and Stone E.G.), 393.

Chapman C. R. et al. (1975). Icarus 25, 104.

Clayton D. D. et al. (1977). Astrophys. J. 214, 300.

Clayton R. N. et al. (1973). Science 182, 485.

Clayton R. N. (1978). Ann. Rev. Astron. Astrophys. 16, 293.

Clayton R. N. et al. (1976). Science 182, 485.

Clayton R. N. et al. (1977). Astrophys. J. 214, 300.

Colgate S. A. et al. (1977). Astrophys. J. 213, 849.

Cook W. R. et al. (1980). Astrophys. J. 238, L-97.

Crawford M. J. et al. (1975). Astrophys. J. 195, 213.

Cressy P. J. and Bogard D. D. (1976). Geochim. Cosmochim. Acta 40, 749.

Crozaz G. (1977). Physics Chem. Earth 10, 197.

Crozaz G. and Walker R. M. (1971). Science 171, 1237.

Crozaz G. and Dust S. (1977). Proc. Lunar Sci. Conf. 8th, 3001.

Davis R. (1955). Phys. Rev. 97, 766.

Davis R. (1978). 'Proc. Informal Conf. Status and Future Solar Neutrinos Research' (Ed. Friedlander G.) BNL report No.50879.

Davis R. and Evans J. C. (1978). In "The New Solar Physics" (Ed. Eddy J.A.), 35.

Dietrich W.F. and Simpson J.A. (1979). Astrophys. J. 231, L-97.

Dietrich W.F. and Simpson J.A. (1979)a. Proc. International Cosmic Ray Conf. 16th 5, 85. also see Mewaldt et al. (1981).

Dorman L.I. and Miroschnichenko L.I. (1976). Solar Cosmic Rays (NASA TT F-674).

Dreibus G. and Wänke H. (1980). Abs. Book. Meteoritical Society Meeting 3rd.

Duraud J.P. et al. (1975). Proc. Lunar Sci. Conf. 6th, 2397.

Durgaprasad N. (1977). Astrophys. Sp. Science 47, 435.

Durgaprasad N. and Biswas S. (1977). Proc. Internat. Cosmic Ray Conf. 15th, 2, 103.

Durgaprasad N. et al. (1968). Astrophys. J. 154, 307.

Eberhardt P. (1974). Earth Planet Sci. Lett. 24, 182.

Eberhardt P. et al. (1965). J. Geophys. Res. 70, 4375.

Eberhardt P. et al. (1970). Proc. Apollo 11 Conf., 1037.

Eberhardt P. et al. (1979). Astrophys. J. 234, L 169.

Eberhardt P. et al. (1981). Geochim. Cosmochim. Acta 45, 1515.

Elliot H. (1973). In "High Energy Phenomena on the Sun". (Eds. Ramaty R. and Stone E. G.), 12.

Etique Ph. et. al. (1981). Lunar Planet Sci. XII, 265.

Feigelson E. D. (1982). Icarus 51, 155.

Fermi E. (1949). Phys. Rev. Lett. 75, 1169.

Fermi E. (1954). Astrophys. J. 119, 1.

Fisk L. A. (1978). Astrophys. J. 224, 1048.

Fleicher R. L. et al. (1971). Science 171, 1240.

Fleicher R. L. and Hart H. R. Jr., (1973). Lunar Sci. IV, 251.

Fleicher R. L. et al. (1973). Proc. Lunar Sci. Conf. 4th, 2307.

Fleicher R. L. et al. (1975). Nuclear Tracks in Solids (Univ. of California Press).

Fowler W. A. et al. (1962). Geophys. J. Roy. Astron. Soc. 6, 148.

Fredriksson K. and Keil K. (1963). Geochim. Cosmochim. Acta, 27, 717.

Frick U. et al. (1975). Proc. Lunar Sci. Conf. 6th, 2097.

Frier P. S. and Webber W. R. (1963). J. Geophys. Res. 68, 1605.

Garcia-Munoz M. et al. (1977). Astrophys. J. 217, 859.

Gault D. E. et al. (1974). Proc. Lunar Conf. 5th, 2365.

Geiss J. et al. (1962). Space Sci. Rev., 1, 197.

Gerling E. K. and Levskii L. K. (1956). Dokl Adad. Nauk SSCR 110, 750.

Geiss J. et al. (1972). AP-16 Proc. Sci. Rep. (NASA SP-315), 14.

Gibson E. K. and Moore G.W. (1973). Science 179, 74.

Gloeckler G. (1979). Rev. Geophys. Space Phys. 17, 569.

Goldreich P., Ward W.R. (1973). Astrophys. J. 183, 1051.

Gopalan K. and Rao M.N. (1975). Proc. International Cosmic Ray Conf. 14th, 1607.

Gopalan K. et al. (1973). TIFR Tech. Report.

Gopalan K. et al. (1977). Proc. Lunar Sci. Conf. 8th, 793

Goswami J. N. (1980). Nature 293, 124.

Goswami J.N. (1983). Personal communication.

Goswami J.N. and Nishiijumi K. (1980). Meteoritics 30, 222.

Goswami J.N. et al. (1976). Proc. Lunar Sci. Conf. 7th, 543.

Grossman L. (1980). Ann. Rev. Earth Planet. Sci. 8, 559.

Hartung J. B. (1980). In "Ancient Sun" (Eds. Pepin R.O., Eddy J.A. and Merril R.B.), 227.

Heiken G.M. (1975). Rev. Geophys. Sp. Phys. 13, 567.

Herpers U. et al. (1973). Proc. Lunar Sci. Conf. 4th, 2157.

Herpers U. et al. (1983). Earth Planet. Sci. Lett. 65, 1.

Herr W. et al. (1971). Proc. Lunar Sci. Conf. 2nd, 1797.

Heyman D. and Dziczkeniec M. (1976). Science 191, 79.

Heyman D. et al. (1975). The Moon 13, 81.

Hintenberger H. et al. (1962). Z. Naturf. 17a, 1092.

Hintenberger H. et al. (1964). Z. Naturf. 19a, 327.

Hohenberg C. M. et al. (1970); Proc. Apollo 11 Conf., 1283.

Hohenberg C. M. et al. (1978). Proc. Lunar Planet. Sci. Conf. 9th, 2311.

Hovestadt D. et al. (1973). Proc. Internat. Cosmic. Ray Conf. 13th, 2, 1498.

Hsieh K. C. and Simpson J. A. (1970). Astrophys. J. 162, L-191.

Hubbard N. J. et al. (1974). Proc. Lunar Sci. Conf. 5th, 1227.

Hudson H. S. (1978). Solar Phys. 57, 237.

Hutcheon I. D. et al. (1974). Proc. Lunar Sci. Conf. 5th, 2561.

Inoue S. and Tanaka T. (1979). Please see Tanaka and Inoue.

Kaiser T. and Wasserburg G. J. (1983). Geochim. Cosmochim. Acta 47, 43.

Kerridge J. F. and Keiffer S.W. (1977). Earth Planet. Sci. Lett. 35, 35.

Kiko J. et al. (1978). Proc. Lunar Planet Sci. Conf. 9th, 1655.

King E. A. et al. (1972). Proc. Lunar Sci. Conf. 3rd, 673.

Kirsten T. (1978). In "The Origin of the Solar System" (Ed. Dermott S.), 267.

Kirsten T. et al. (1971). Proc. Lunar Sci. Conf., 2nd, 1662.

Kirsten T. et al. (1972). Proc. Lunar Sci. Conf., 3rd, 1865.

Kirsten T. et al. (1980). Abs. Book Meteoritical Socy., Meeting 43rd.

Klecker B. et al. (1979).

Klecker B. et al. (1981). Proc. Int. Cosmic Ray Conf. 13th, 143.

Kohl C. P. et al. (1978). Proc. Lunar Planet. Sci. 9th, 2299.

Koenig H. et al. (1961). Z. Naturf. 16a, 1124.

Koenig H. et al. (1962). Z. Naturf, 17a, 357.

Koenig H. et al. (1964). Geochim. Cosmochim acta 2, 1397.

Korchak A. A. and Syrovatskii S. I. (1958). Dokl. Akad. SSSR 122, 792.

Kothari B. K. and Rajan R. S. (1982). Geochim. Cosmochim Acta 46, 1747.

Krimigis S. M. (1973). In "High Energy Phenomena on the Sun" (Ed. Ramaty R., Stone E. G.), 478.

Krimigis S. M. and Verzariu P. (1971). J. Geophys. Res. 76, 792.

Kuhi L. V. (1964). Astrophys. J. 140, 1409.

Kuroda P. K. (1960). Nature 187, 36.

Lal D. (1965). Proc. Int. Cosmic Ray Conf. 9th, 81.

Lal D. (1972). Sp. Science Rev. 14, 3.

Lal D. and Rajan R. S. (1969). Nature 223, 269.

Lambert D. (1967). Nature 215, 43.

Laul J. C. et al. (1974). Proc. Lunar Sci. Conf. 5th, 1047.

Lee T. (1979). Rev. of Geophys. Sp. Physics 17, 1591.

Lee T. et al. (1976). Geophys. Res. Lett. 3, 109.

Lee M. A. (1976). J. Geophys. Res. 81, 3207.

Leich D. A. et al. (1975). Proc. Lunar Sci. Conf. 6th, 2085.

Lewis et al. (1979). Astrophys. J. 234, L 165.

Lugmair G. W. et al., (1976). Proc. Lunar Sci. Conf. 7th, 2009.

LSPT (1971). (Lunar Sample Preliminary Examination Team) Science 173, 681.

MacDouggal, J.D. et al. (1974). Science 183, 73.

Manuel O. K. (1967). Geochim. Cosmochim Acta, 31, 2413.

Manuel O. K. and Kuroda, P.K. (1964). J. Geophys. Res. 69, 1413.

Marti K. (1967). Phys. Rev. Lett. 18, 264.

Marti K. (1969). Science 166, 1263.

Marquardt D. W. (1963). J. Soc. Ind. Appl. Math. Vol. II, 40.2, 431.

Marvin U.B. and Mosie A. B. (1980). Curatorial Branch Pub. 53 (Lyndon B. Johnson Space Centre, Houston, USA).

Mason G. M. et al. (1979). Astrophys. J. 231, L-87.

Mazor E. et al. (1970). Geochim. Cosmochim. Acta 34, 781.

Mazor E. and Anders E. (1967). Geochim. Cosmochim. Acta 31, 1441.

McDonald, F.B. and Desai U.D. (1971). J. Geophys. Res. 76, 808.

McGee J. J. et al. (1978). Proc. Lunar Planet. Sci. Conf. 9th, 743.

Mcguire R. E. et al. (1979). Proc. Int. Cosmic Ray Conf. 17th 3, 65.

Mcguire R. E. et al. (1981). Proc. Int. Cosmic Ray Conf. 17th.

McKibben R. B. et al. (1975). Proc. Int. Cosmic Ray Conf. 16th (P-2), 1512.

McKibben R. B. et al. (1979). Astrophys. J. 227, 147.

McSween H. Y. Jr. (1979). Rev. Geophys. Space Phys. 17, 1059.

McSween H. Y. Jr. et al. (1980). Proc. Lunar Planet Sci. Conf. 11th, 853.

McSween H. Y. Jr. et al. (1981). Proc. Lunar Planet Sci. Conf. 12th, 1093.

Meerson B. I. Rogacheviskii I. V. (1983). Solar Phys. 87, 337.

Methot R. L. et al. (1975). Meteoritics, 10, 121.

Mewaldt R. A. et al. (1979). Astrophys. J. 231, L.97.

Mewaldt R. A. et al. (1981). Astrophys. J. 243, L-163.

Mewaldt R. A. et al. (1983). Int. Cosmic Ray Conf. 18th (SP. 4), 42.

Meyer J. P. (1978). In "Les elements et Leurs Isotopes dans 1' Universe" 22nd Liége Internat. Astrophys. Symp. (Univ. of Liége Press), 53.

Meyer J. P. (1983). Preprint.

Mogro Campero A. and Simpson J.A. (1972). Astrophys. J. 177, L-37.

Morris R. V. (1978). Proc. Lunar Planet. Sci. Conf. 9th, 2287.

Morris R. V. (1973). Proc. Lunar Planet. Sci. Conf.

Müller O. and Zähringer J. (1966). Earth Planet Sci. Lett. 1, 25.

Ness N. F. (1968). Ann. Rev. Astron. Astrophys. 6, 79.

Newkirk G., Jr. (1973). In "High Energy Phenomena on the Sun" (Eds. Ramaty R. and Stone E. G.) NASA SP-342, 453.

Nier A.O. (1947) Rev. Sci. Instr. 18, 398.

Nier A.O. (1950) Phys. Rev. 79, 450.

Niederer F. and Eberhardt P. (1977) Meteoritics 12, 327.

Nishiizumi K. et al. (1980). Earth Planet. Sci. Lett., 50, 156.

Nyquist L. et al. (1973). Geochim. Cosmochim. Acta 37, 1655.

Padia J.T. et al. (1979). The Moon and the Planets 20, 423.

Paneth F. et al. (1972). Nature 172, 200.

Papanstassiou D. A. et al. (1974). Lunar Planet. Sci. V, 583.

Parker E. N. (1958). Phys. Rev. 109, 1328.

Parker E. N. (1963). Interplanetary Dynamical Processes.

Pellas P. and Storzer D. (1981). Phil. Trans. Roy. Soc. Lond. Ser. A, 253.

Pellas P. et al. (1969). Nature 223, 272.

Pepin R. O. (1967). Earth Planet Sci. Lett., 2, 13.

Pepin R.O. and Signer P. (1965). Science 149, 253.

Pepin R.O. et al. (1970). Proc. Apollo 11, Lunar Sci. Conf.1435.

Pestchetk H. E (1964). In AAS NASA Symposium on Physics of Solar Flares. NASA SP-50, 425.

Podosek F. A. (1978). Ann. Rev. Astron. Astrophys. 16, 293.

Poupeau G. et al (1974). Earth Planet. Sci. Lett. 24, 229.

Price P. B. et al. (1971). Phy. Rev. Lett. 26, 916.

Price P.B. and Rajan R. S. (1973). Pl. See Rajan and Price.

Price P. B. et al. (1975). Proc. Lunar Sci. Conf. 6th, P 3449.

Rajan R. S. (1974). Geochim. Cosmochim, Acta 38, 777.

Rajan R. S. and Price P. B. (1973). Nature Phys. Sci. 244, 122.

Ramaty R. et al. (1975). Space Sci. Rev. 18, 341.

Rao M. N. et al. (1971). Nature 223, 114.

Rao M. N. et al. (1979). Proc. Lunar Planet. Sci. Conf. 10th, 1547.

Rao M. N. and Venkatesan T. R. (1980). Nature 286, 788.

Reedy R. C. and Arnold J. R. (1972). J. Geophys. Res. 77, 537.

Reynolds J. H. (1956). Rev. Sci. Instr. 18, 928.

Reynolds J. H. (1960). Phy. Rev. Lett. 4, 8.

Reynolds J. H. and Turner G. (1964). J. Geophys. Res. 69, 3263.

Reynolds J. H. et al. (1978). Geochim. Cosmochim Acta 42, 1775.

Rose H. J. et al. (1973). Proc. Lunar Sci. Conf. 4th, 1149.

Rowe M. and Kuroda P. K. (1965). J. Geophys. Res. 70, 709.

Russel H. N. (1929). Astrophys. J. 70, 11.

Sabu D. D. and Manuel O. K. (1980). Meteoritics 15, 117.

Safranov V. S. (1969). 'Evolution of the proto planetary cloud and formation of the earth and planets'. (Moscow) and translated into English in 1972 by Isreal Prog. for Scientific Translations.

Schramm D. N. et al. (1971). Astrophys. Space Sci. 13, 249.

Shukla, P.N. et al. (1983). Proc. Int. Cosmic Ray Conf. 18th, OG-7, 370.

Schultz L. and Signer P. (1977). Earth Planet. Sci. Lett. 36, 363.

Schultz L. and Kruse H. (1978). Nucl. Track Det. 2, 65.

Schultz L. et al. (1972). Earth Planet. Sci. Lett. 15, 403.

Shedlovsky J. T. et al. (1970). Proc. Ap.11 Lunar Sci. Conf., 1503.

Shoemaker E. M. et al. (1970). Proc. Apollo 11 Lunar Sci. Conf. 2399.

Signer P. and Suess H.E. (1963). In "Earth Science and Mateoritic" (Ed. Goldberg E.D. and Geiss J.), 241.

Simnett G. (1971). Sol. Phys. 20, 448.

Simnett G. (1973). In 'High Energy Phenomena on the Sun' (Ed. Ramaty R. and Stone R. G.) 503.

Simpson J. A. et al. (1983). Proc. Int. Cosmic Ray Conf. 18th, Late Volume (in press).

Skunamich A. (1972). Astrophys. J. 171, 565.

Sonnerup B. U. O. (1970). J. Plasma Phys. 4, 161.

Srinivasan B. (1981). Naturwissenschaften, 66, 341.

Stettler A. et al. (1973). Proc. Lunar Sci. 4th, 1865.

Suess H. E. et al. (1964). Geochim, Cosmochim. Acta 28, 595.

Švestka Z. (1976). Solar Flares (Pub. D. Reidel Pub. Co.).

Sweet P. A. (1958). Nuovo Cimento, Suppl. 8, Ser X, 188.

Tanaka S., and Inoue T. (1979). Earth Planet, Sci. Lett. 45, 181.

Urey H. C. (1951). Geochim. Cosmochim. Acta 1, 209.

Van-Schumns, W. R. and Wood J. A. (1967). Geochim. Cosmochim Acta, 31, 747.

Walton J. R. et al. (1973). Proc. Lunar Sci. Conf. 4th, 2079.

Walton J. R. (1974). Ph. D. Thesis (Rice University, Houston U.S.A.).

Walton J. R. et al. (1976 a). J. Geophys. Res. 81, 5689.

Walton J. R. et al. (1976 b). J. Geophys. Res. 81, 5701.

Warren P. H. et al. (1983). Lunar Planet Sci. XIV 828.

Wasserburg G. J. et al. (1980). In "Early Solar System Processes and the Present Solar System" (Ed. Lal D.) Soc. Italiana di Fisica-Balogna, Italy.

Wasson, J.T. (1974). "Meteorites" (Pub. Springer-Verlag).

Wasson, J.T. et al. (1983). Lunar Planet. Sci. IVX, 828.

Webber W. R. (1967). Hand book der Phys. 46 (2), 181.

Webber W. R. et al. (1973). Proc. Internat. Cosmic Ray Conf. 13th, 2, 1516.

Webber W. R. et al. (1975). Astrophys. J. 199, 482.

Wetherill G. W. (1971). In "Physical Studies of the Minor Planets" (Ed. T. Gehrels), 447.

Wetherill G. W. (1974). Ann. Rev. Earth Planet. Sci. 3, 303.

Wetherill G. W. (1975). Ann. Rev. Earth Planet. Sci. 25, 283.

Wetherill G. W. (1976). Geochim. Cosmochim. Acta, 40, 1297.

Wetherill G. W. (1978). In "Protostar and Planets" (Ed. T. Gehrels), 565.

Wieler R. et al. (1982). Proc. Lunar Planet. Sci. Conf. 13th, A 713.

Wilkening L. L. (1971). Nininger Meteorite Award Pub. No.11, Centre for Meteorite Studies, Arizona State University U.S.A.

Wilkening L. L. (1976). Proc. Lunar Sci. Conf. 7th, 3549.

Wlotzka F. (1963). Geochim. Cosmochim. Acta 27, 419.

Worden S. P. et al. (1981). Astrophys. J. 244, 520.

Wszolek P. C. et al. (1973). Proc. Lunar Sci. Conf. 4th, 1693.

Yokoyama Y. et al. (1975). Proc. Lunar Planet Sci. Conf. 6th, 183.

York D. (1969). Earth Planet. Sci. Lett. 5, 320.

Zähringer J. and Gentner M. V. (1960). Naturforschg. 15a, 600.

Zähringer J. (1962). Geochim. Cosmochim. Acta. 26, 665.

Zimmerman P. D. and Wetheril G. W. (1973). Science 182, 51.

Zinner E. (1980). In "Ancient Sun" (Eds. Pepin R.O., Eddy J.A. and Merril R.B.) P. 201.

LIST OF PUBLICATIONS

1. Rao M.N., Venkatesan T.R., Goswami J.N. and Nautiyal C.M. (1979) Solar Cosmic ray produced neon and argon isotopes and particle tracks in Apollo 16 soils and rocks and their solar flare exposure ages (Abstract). Lunar Planet, Sci. X, 1004.

2. Rao M.N., Venkatesan T.R., Goswami J.N., Nautiyal C.M. and Padia J.T. (1979) Noble gas based solar flare exposure history of lunar rocks and soils. Proc. Lunar Planet Sci. Conf. 10th, 1547.

3. Nautiyal C.M., Padia J.T., Rao M.N. and Venkatesan T.R. (1980) Characterisation of solar and galactic cosmic ray produced noble gas components in lunar soils and rocks. Lunar Planet Sci. XI, 797.

4. Nautiyal C.M., Padia J.T., Rao M.N. and Venkatesan T.R. (1980) Cosmogenic and radiogenic noble gases in Patora and Seoni chondrites. Abstract book. National Space Science Symposium (Varanasi, India), 159.

5. Venkatesan T.R. Nautiyal C.M., Padia J.T. and Rao M.N. (1980) Solar flare cosmic ray proton fluxes in the recent past. Proc. Lunar Planet. Sci. Conf. 11th, 1271.

6. Nautiyal C.M., Padia J.T., Rao M.N., Venkatesan T.R. Englert P., Herpers U. and Herr W. (1980) (Abstract) Elemental and isotopic composition of noble gases in the Isna carbonaceous chondrite. Meteoritics 15, 252.

7. Bhandari N., Lal D, Nautiyal C.M., Padia J.T., Potdar M.B., Rao M.N. and Venkatesan T.R. (1980) Determination of pre-atomospheric sizes of meteorites. Meteoritics 15, 237.

8. Rao M.N., Nautiyal C.M. and Venkatesan T.R. (1981) Is the neon composition of our Sun, planetary or solar? Proc. Int. Cosmic Ray Conf. 17th (Paris) S H, 3.1-9, 141.

9. Nautiyal C.M., Padia J.T., Rao M.N. and Venkatesan T.R. (1981) Solar and galactic cosmic ray records of noble gases in lunar rock 79215. Lunar Planet. Sci. XI, 753.

10. Venkatesan T.R., Nautiyal C.M., Padia J.T. and Rao M.N. (1981) Compositional characterestics of solar wind and solar flare neon in the past using soils and rocks. (Abstract) Lunar Planet. Sci. XII, 1112.

11. Nautiyal C.M., Padia J.T., Rao M.N. and Venkatesan, T.R. (1981) Solar flare neon : Clues from implanted noble gases in lunar soils and rocks. Proc. Lunar Planet. Sci. 12th, 627.

12. Nautiyal C.M. and Rao M.N. (1981) Lunar and other extra-terrestrial objects : Clues to irradiation histories based on noble gas mass-spectrometry in Mass-spectrometry - Progress in Research Applications and Instrumentation. HGC-6.

13. Venkatesan T.R., Nautiyal C.M. and Rao M.N. (1981) Neon composition in solar flares. Geophys. Res. Lett. 8, 1143.

14. Nautiyal C.M., Venkatesan T.R., Padia J.T. and Rao M.N. (1982) Solar radiation effects in moon and meteorite samples : A noble gas mass-spectrometric study (Abstract) Abstract book National Space Science Symposium (Bangalore, India), 386.

15. Nautiyal C.M., Padia J.T., Rao M.N., Venketesan T.R. and Goswami J.N. (1982) Irradiation History of antarctic gas-rich meteorites. Lunar Planet. Sci. XIII, 578.

16. Rao M.N., Nautiyal C.M., Padia J.T. and Venkatesan T.R. (1981) Evolution of carbonaceous chondrite parent body. Meteoritics 31, 380.

17. Venkatesan T.R., Rao M.N., Nautiyal C.M. and Padia J.T. (1983) Solar cosmic ray proton fluxes in the last hundred million years. Paper OG-7.14. Proc. Int. Cosmic Ray Conf. 18th, 366

18. Venkatesan T.R., Nautiyal C.M., Padia J.T. and Rao M.N. (1982) SCR-proton produced xenon isotopes in Lunar rocks. Lunar Planet. Sci. XIII, 82.

19. Rao M.N., Nautiyal C.M., Padia J.T. and Venkatesan T.R. (1983) Confirmation of Solar flare neon composition using lunar pyroxenes and SCR proton flares in last hundred million years. Lunar Planet. Sci. XIV, 632.

20. Nautiyal C.M., Rao M.N. and Venkatesan T.R. (1983) Ancient solar flare neon and solar cosmic ray proton fluxes from gas rich meteorites. Lunar Planet. Sci. XIV, 544.

21. Englert P., Herpers U., Herr W., Nautiyal C.M., Padia J.T. Rao M.N. and Venkatesan T.R. (1983). Isna, an unusual, C-3(O) carbonaceous chondrite. Earth Planet. Sci. Lett. 65, 1.

22. Nautiyal C.M. and Rao M.N. (1983). Abs. Book of Workshop on "Past and present solar radiation: The Records in Meteoritic and Lunar Regolith Material", 21.